CALIFORNIA ENERGY COMMISSION

CALIFORNIA NATURAL RESOURCES AGENCY

Energy Research and Development Division

FINAL PROJECT REPORT

Optimized Natural Gas Hybrid-Electric Drayage Truck Demonstration

December 2021| CEC-500-2021-054

PREPARED BY:

Primary Authors:
Tyler Manley
Dr. Kent Johnson
Dr. J Wayne Miller

Gas Technology Institute
1700 South Mount Prospect Road
Des Plaines, IL 60018
www.gastechnology.org

Major Contributions From:
University of California, Riverside
College of Engineering - CE-CERT
1084 Columbia Avenue
Riverside, CA 92507

Contract Number: PIR-13-014

PREPARED FOR:
California Energy Commission

Pilar Magaña
Project Manager

Jonah Steinbuck, Ph.D
Office Manager
ENERGY GENERATION RESEARCH OFFICE

Laurie ten Hope
Deputy Director
ENERGY RESEARCH AND DEVELOPMENT DIVISION

Drew Bohan
Executive Director

ACKNOWLEDGEMENTS

The authors acknowledge and thank the following organizations and individuals for their valuable contributions to this project:

- The California Energy Commission for its support of this project and commitment to the research on alternative fuel vehicles.
- Southern California Gas Company for the guidance provided on this project.
- Mr. Don Pacocha, Mr. Eddie O'Neil, Mr. Mark Villa, Lauren Aycock, and Mr. Danny Gomez for performing the baseline tests and preparing the equipment for testing.
- Ms. Rachael Hirst and Grace Johnson for their analytical support for the particulate matter laboratory measurements.
- BASF, Watlow, Cummins Westport, Cummins Inc, FEV, and US Hybrid for their many helpful technical discussions.

PREFACE

The California Energy Commission's (CEC) Energy Research and Development Division manages the Natural Gas Research and Development Program, which supports energy-related research, development, and demonstration not adequately provided by competitive and regulated markets. These natural gas research investments spur innovation in energy efficiency, renewable energy and advanced clean generation, energy-related environmental protection, energy transmission and distribution and transportation.

The Energy Research and Development Division conducts this public interest natural gas-related energy research by partnering with research, development, and demonstration entities, including individuals, businesses, utilities and public and private research institutions. This program promotes greater natural gas reliability, lower costs and increases safety for Californians and is focused in these areas:

- Buildings End-Use Energy Efficiency.
- Industrial, Agriculture and Water Efficiency.
- Renewable Energy and Advanced Generation.
- Natural Gas Infrastructure Safety and Integrity.
- Energy-Related Environmental Research.
- Natural Gas-Related Transportation.

Optimized Natural Gas Hybrid-Electric Drayage Truck Demonstration is the final report for the Optimized Natural Gas Hybrid-Electric Drayage Truck Demonstration project (Contract Number PIR-13-014) conducted by the Gas Technology Institute. The information from this project contributes to the Energy Research and Development Division's Natural Gas Research and Development Program.

For more information about the Energy Research and Development Division, please visit the CEC's research website (www.energy.ca.gov/research/) or contact the CEC at ERDD@energy.ca.gov.

ABSTRACT

California's heavy-duty fleets that transport goods and freight primarily rely on diesel engines because they are robust, durable and highly efficient. With more stringent engine emission standards and the increased availability of low-cost natural gas fuel, there is increased interest in trucks powered by natural gas engines. These natural gas trucks can reduce oxides of nitrogen (NOx) emissions by 90 percent and carbon dioxide emissions by 25 percent compared to equivalent diesel trucks. Despite these advantages, natural gas truck efficiency and performance must improve to more effectively compete with incumbent diesel technology.

This project designed, integrated, and demonstrated a prototype hybrid-electric/natural gas drayage truck to achieve near-zero NOx emissions and significant greenhouse gas savings. The engine's emission control functions were modified to drive to lower NOx emissions.

The research team found that more than 80 percent of NOx emissions occur during the cold start period and major changes were required to reach near-zero levels. The project team explored multiple pathways to modify the engine control system, vehicle components, or the hybrid module. Results showed the hybrid-electric truck could easily move twice the load of the baseline nonhybrid natural gas truck with reduced emissions and with a 5 percent increase in fuel economy. In addition, the range of the hybrid truck was extended to an estimated 400 miles.

Keywords: Hybrid, Natural Gas, Optimization, Near-Zero NOx

Please use the following citation for this report:

Manley, Tyler. Kent Johnson, and Wayne Miller. 2021. *Optimized Natural Gas Hybrid-Electric Drayage Truck Demonstration.* California Energy Commission. Publication number: CEC-500-2021-054.

TABLE OF CONTENTS

LIST OF FIGURES

Page

LIST OF TABLES

Page

EXECUTIVE SUMMARY

Introduction

Heavy-duty on-road vehicles represent one of the largest sources of oxides of nitrogen (NOx) emissions, contributing roughly 26 percent of total NOx emissions in California. NOx emissions are a precursor to ozone, or smog. These vehicles are predominately diesel-fueled, with a small fraction operating on natural gas. As air pollutant and greenhouse gas emission regulations continue to tighten, advanced heavy-duty vehicle technologies are needed with improved fuel economy and lower emissions. NOx standards have dropped 90 percent for heavy-duty vehicles with the 2010 U.S. Environmental Protection Agency Heavy-Duty Engine and Vehicle Standard and Highway Diesel Fuel Sulfur Control Requirements. An additional 90 percent NOx reductions is critical in the South Coast Air Basin to meet National Ambient Air Quality Standards for ozone.

Project Purpose

While hybrid-electric vehicles are not a new concept for improving fuel economy and reducing emissions, battery electric technology combined with natural gas systems have not been fully explored as a competitive option for fleets that can benefit from hybridized natural gas vehicles. Additional research is needed to develop natural gas hybrid-electric systems that provide performance, emission, and efficiency improvements over the heavy-duty diesel vehicles available in today's commercial markets.

Gas Technology Institute, US Hybrid Corporation, and University of California, Riverside performed research and development on a natural gas engine hybrid-electric Class 8 truck through a system design approach to reduce NOx emissions and while improving fuel economy. Class 8 vehicles include most tractors used for goods movement and weigh more than 16.5 tons. This hybrid system includes a natural gas engine, an electric motor, energy storage, engine controls optimized for hybrid operation, and aftertreatment integrated onto a Class 8 truck for port drayage operations.

The researchers demonstrated successful integration of a natural gas hybrid-electric vehicle in a Class 8 vehicle for a high-volume, high fuel use platform; advancing technologies targeted at significantly reducing emissions and improving fuel economy; and resolving two market barriers to natural gas vehicles: reduced driving range and loss of load space.

The project team sought to demonstrate the commercial and economic viability of the systems to attract a commercialization partner.

Project Process

The team used a commercially available, 2010 certified, natural gas, Cummins Westport Inc. ISL G 8.9 liter engine and enhanced the system to make it characteristic of an engine meeting California Air Resources Board's (CARB) optional low-NOx "near-zero" emission standard. The commercially available, 2010 certified, Cummins Westport Inc. ISL G 8.9L and the newly certified near-zero emission engine options were reviewed and evaluated at University of California, Riverside to characterize emissions and fuel consumption results.

This engine was configured in a vehicle equipped with a liquefied natural gas fuel delivery system, a 147-diesel gallon equivalent liquefied natural gas fuel tank (400 mile range

estimated), a three-way catalyst aftertreatment system, and a throttle body fuel injection system. To reduce NOx emission spikes during transient modes, the team redesigned controls using an air-to-fuel model. Analysis reveals the key improvement in total NOx emissions was a result of lower and fewer NOx spikes from the engine's throttle control system. The reduced throttle control did not minimize engine performance.

Cold start emissions and electric stop-start technologies were considered for this project, however; they were not fully implemented but modeled for their estimated benefit. Additionally, the success of the Cummins Westport Inc. near-zero 8.9 liter engine may suggest heated catalysts are not needed and the engine's near-zero emission improvements were primarily based on engine calibration.

Project Results

In general, the hybrid-equipped natural gas engine showed 70 percent lower hot transient NOx emissions than the mandatory CARB standard of 0.2 g/bhp-hr. The hybrid system improved fuel economy by 5 percent compared to the baseline system over the cycles tested. Additional benefits could be obtained from a charge depletion mode strategy where plug-in charging and all-electric operation is prioritized over continuous engine operation. Such an approach could be applicable if ports mandate a transition to zero emission drayage trucks. Such a strategy could maximize the potential emissions and fuel economy improvements of hybridization, but at the added cost of a dual power (engine plus electric) system.

Two primary observations were identified during the review: (1) up to 90 percent of the emissions are either from rapid engine speed transients (hot start tests) or cold start emissions and (2) the impact of transient and cold start emission is more critical at the optional 90 percent lower near-zero NOx emission standard (0.02 grams per brake horsepower-hour [g/bhp-hr]) when compared to the mandatory 0.2 g/bhp-hr standard. This suggests emission differences may be significant between drivers, operation, and vehicle configurations (automatic transmissions compared to manual transmissions).

Project Benefits

Natural gas hybrid-electric Class 8 tractors with a downsized 9L engine can compete with conventional natural gas tractors by delivering 5 percent higher fuel economy and achieving or exceeding near-zero NOx emission levels. The combined power of the 9 liter engine and the electric traction motor matches or exceeds the performance of a larger 12 liter engine, addressing one of the known barriers to low-NOx engine adoption – reduced power. Incorporating this project's hybrid technology with advanced low-emission engine technology creates the potential to bring significant fuel reductions as a part of low-emission drayage activity in California's major seaports. The researchers estimate that approximately 80 percent of NOx or 2106 tons are generated by pre-2010 emission vehicles with 1.5g/bhp-hr NOx emissions. A transition of 30% of the pre-2010 vehicles (a 10% of overall heavy-duty fleet supporting the Ports of Los Angeles and Long Beach) with the compressed natural gas-hybrid powertrain could offer a reduction of approximately 600 tons of NOx, or an overall NOx reduction of 23 percent.

Technology/Knowledge Transfer/Market Adoption (Advancing the Research to Market)

University of California, Riverside, US Hybrid, and Gas Technology Inc. have coordinated with FEV, a provider of engineering design, software testing, component testing, and consulting services, and specializes in commercial electric and hybrid vehicle systems. This collaboration has resulted in identifying future research needs, and a follow-on award through the Energy Commission to translate University of California, Riverside and US Hybrid's gained knowledge into a vehicle platform that will use a Cummins Westport natural gas engine certified to near-zero NOx emission levels.

In addition to this knowledge sharing with FEV, Gas Technology Institute's Utilization Technology Development group has expressed an interest in the project and the findings will be shared with them after the project concludes. Utilization Technology Development group is a not-for-profit collaborative partnership of more than 20 natural gas distribution companies that conducts near-term applied research to develop, test and demonstrate energy-efficient, environmentally friendly, and cost-effective end-use technologies. Utilization Technology Development group's member utilities combine their interests, expertise and resources into focused research and development projects to serve their 45 million gas customers in the Americas and Europe with these advanced technologies.

CHAPTER 1:
Technical Background

Introduction

In February 2014, the California Energy Commission issued Program Opportunity Notice (PON)-#13-506 Natural Gas Engine-Hybrid Electric Research and Development. The PON recognized the importance of medium and heavy-duty vehicles to the California economy and the dilemma that they consume much of the fuel and emit most of the greenhouse gases from California fleets. Furthermore, the Energy Commission's 2011 *Integrated Energy Policy Report* anticipated that diesel consumption would grow by 22.3 percent from 2009 to 2030 due to increased use of diesel in freight.

Accordingly, as California is a leader in alternative fuel technologies, the PON was issued as an opportunity to investigate natural gas engine-hybrid vehicles as a path to simultaneously reduce criteria and GHG emission and dependency on foreign oil. While hybrid transit buses and heavy-duty trucks with diesel engines were demonstrated in the 1990s, data on hybrid electric systems with natural gas were lacking. It was expected that natural gas hybrid electric vehicles (NGHEVs) with today's hybrid technology would require less fuel storage to achieve an acceptable driving range per fill-up. Compressed Natural Gas (CNG) and liquified natural gas (LNG) cylinders are round and typically don't integrate as easily as batteries may. They are more limited in their placement by best practices for cylinder protection and maintenance. Displacing gas storage with battery storage addresses this issue in part. This combination helps resolve two of the market barriers to NGVs: reduced range and loss of load space. Also, with battery power to minimize idle and low-load engine operation, nitrogen oxide (NOx) emission can be significantly reduced in stop-and-go urban service.

For this project, the team proposed developing a novel integrated hybrid systems approach to reduce NOx emission and lower fuel consumption. System integration of the hybrid components will be the key deliverable.

Real World Fuel Economy

Fuel economy and carbon dioxide (CO2) emission are regulated in new standards for heavy-duty vehicles. Fuel economy and CO2 emission relate to the vehicle's fuel use and performance. For the heavy-duty industry, the proposed fuel economy standard is tied to gallons of fuel used per ton-mile. The CO2 emission standard is based on the mass of CO2 per unit work also called the vehicle's brake specific CO2 (bsCO2) in units of grams per brake horsepower-hour (g/bhp-hr). Since CO2 emission are being regulated for their greenhouse gas emission, and they are closely related to fuel consumption (fuel economy), one can compare between vehicles and fuels by evaluating bsCO2. Unfortunately, most literature data for in-use vehicles is reported as mi/gallon (MPG) or gCO2/mi.

To understand real world CO2 emissions for diesel and natural gas refuse vehicles, the following tables are presented to understand the baseline fuel economy for natural gas vehicles in relation to diesel vehicles. Table 1 shows the fuel economy for refuse vehicles during general in-use conditions [2] and during laboratory studies [3,4] on both a g/mi and g/bhp-hr basis. Table 2 and Table 3 show the same information, but for Class 8 vehicles over

various goods movement and certification drive cycles [2,3,4]. The data in Table 1 through Table 3 are provided from the literature and from testing conduced at UC Riverside [2, 3, 4]. The results show natural gas vehicles emit less CO2 per mile as compared to conventional diesel vehicles spanning the last three emission certification standards. On a work basis (g/bhp-hr) the CO2 emission for the natural gas are only slightly better for the TWC application and much better for the lean burn natural gas application. Although, NOx emission for the lean burn natural gas applications are considerably higher as discussed in the next section.

Table 1: Carbon Dioxide Emission Comparisons Between Refuse Vehicles and Fuels

Cycle	Units	pre 2007	2007-2009 Diesel	>2010 Diesel w/SCR	>2010 Diesel w/out SCR	Lean NG	2010 TWC NG
literature	g/mi	4369	1999				
UDDS	g/mi		2356	2822	1941	-	-
Refuse	g/mi		4888	5529	5326	1263	1435
UDDS	g/bhp-hr		558	699	656	-	-
Refuse	g/bhp-hr		588	690	769	434.8	553.6

Source: Gas Technology Institute

Table 2: Carbon Dioxide Emission Comparisons Between Class 8 Port Vehicles and Fuels (grams/mile)

Cycle	2007-2009 Diesel	>2010 Diesel w/SCR	>2010 Diesel w/out SCR	2010 TWC NG
PDT1	2800	3147	2523	
PDT2	2631	3047	2490	2142
PDT3	1982	2086	1806	
UDDS	2582	2729	2483	
UDDS_CS	2622	2936	2565	

Source: Gas Technology Institute

Table 3: Carbon Dioxide Emission Comparisons Between Port Vehicles and Fuels (grams/brake horsepower-hour)

Cycle	2007-2009 Diesel	>2010 Diesel w/SCR	>2010 Diesel w/out SCR	2010 TWC NG
PDT1	804	801	769	
PDT2	695	725	663	547.7
PDT3	565	612	548	
UDDS	579	618	562	
UDDS_CS	579	615	612	

Source: Gas Technology Institute

One of the main goals of this research project is to improve the fuel economy of a natural gas vehicle by optimizing a hybrid-electric system. Because fuel use has a direct relationship with CO2 emission, a 25 percent increase in fuel efficiency is expected to yield a 25 percent decrease in bsCO2 - a drop from 555 to 412 g/bhp-hr.

Oxides of Nitrogen Emission Standards

Final federal emission standards for the heavy-duty trucks were set in 2007 and the regulation included several programs to allow the Original Equipment Manufacturers (OEMs) to gradually introduce engines that met the final standards. The transition in emission standards over the years can be seen in Figure 1.

Figure 1: Certification Standards for NOx and PM Emissions

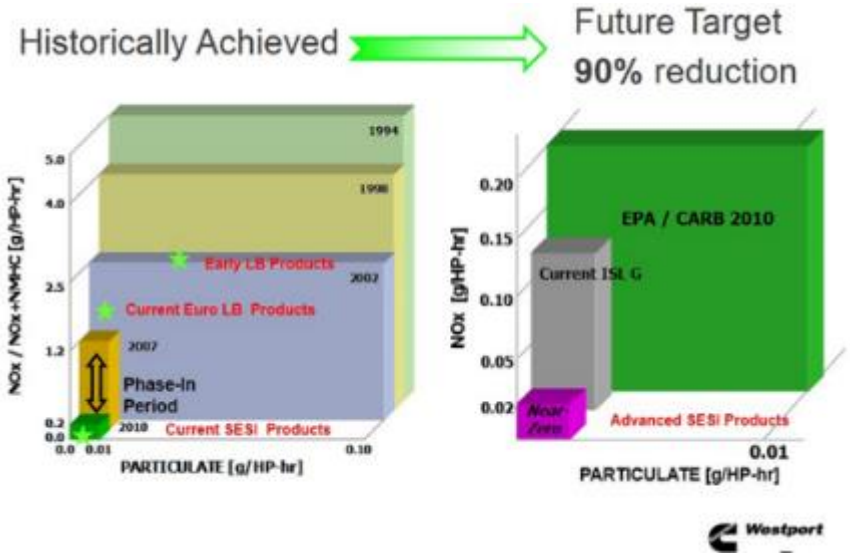

Source: CWI

Early adopters of the 2007 limits could bank excess emission reductions and use those credits in later years as they phased in new product meeting the final standard. Also shown is the voluntary target of a further 90 percent reduction in the NOx standard to 0.02 g/bhp-hr. This target value is of great interest to California and is needed to attain the federal clean air standards. Substantial financial incentives are associated with this low emission target. The California Air Resources Board (CARB) sees a value of 0.02g/bhp-hr as near zero emission and the equivalent to a 100 percent battery truck using electricity from a modern combined cycle natural gas power plant.

The definite need for a 0.02 g/bhp-hr NOx standard is evident when reviewing the Air Quality Management Plan (AQMP) from the South Coast Air Quality Management District. As part of EPA mandates, a State Implementation Plans (SIP) must be submitted every several years and the SIP includes Air Quality Management Plan (AQMP) from the Districts. On October 2, 2015 the AQMD released their White Paper for Blueprint for Clean Air [1], a document that states: "Preliminary 2016 AQMP analysis indicates approximately a 65 percent further reduction in nitrogen oxide (NOx) emission, above and beyond all currently adopted measures, to meet the 8-hour ozone standards." Note that heavy-duty trucks have the highest emission (Figure 2).

Figure 2: Estimated Emissions from Various Oxides of Nitrogen Sources in 2023

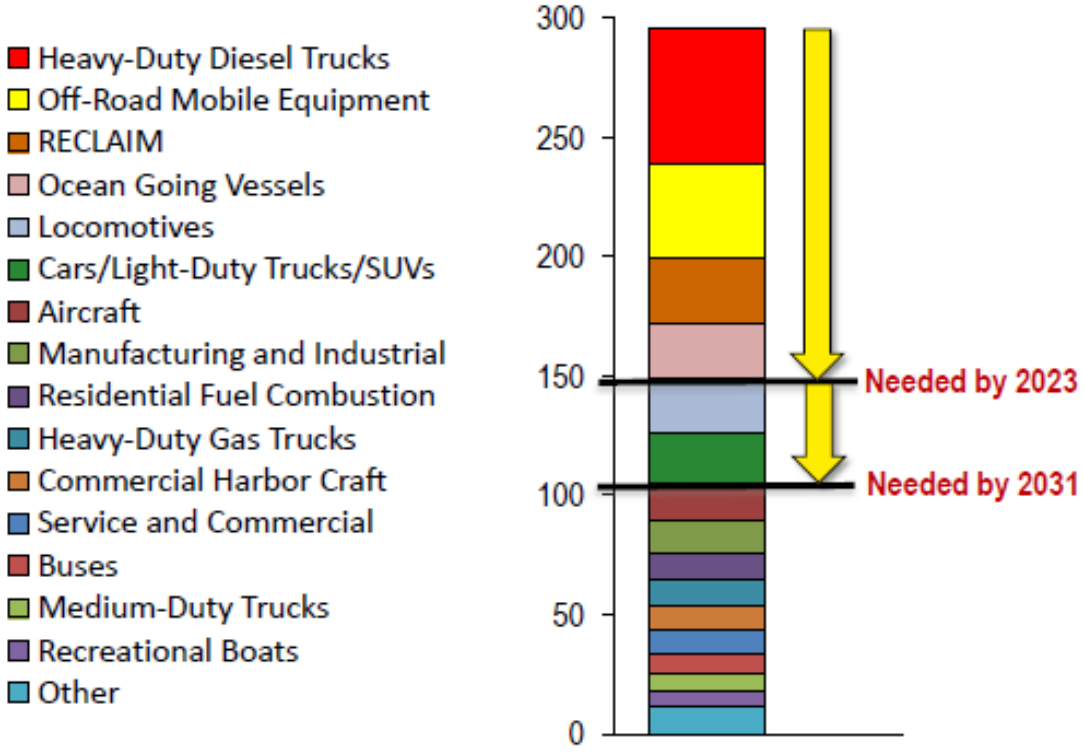

Source: Preliminary Draft 2023 Baseline Emissions Inventory, July 2015

Real World NOx Emissions

Real world emission measurements are more important that certification values. With modern portable measuring equipment, more data is being collected in real world operations and these data are showing a wide range of emission and deviations from certification values. A summary of the real-world NOx emission for refuse vehicles range from 60 to ~1 g/mi for diesel engines with/without SCR and for natural gas using a Three Way Catalyst (TWC) per Table 4 [2,3,4]. Class 8 trucks show similar results, Table 5 natural gas vehicles with the TWC showed the lowest NOx emission for port and refuse applications.

Table 4: NOx Emission Comparisons Between Refuse Vehicles and Fuels

Cycle	Units	pre 2007	2007-2009 Diesel	>2010 Diesel w/SCR	>2010 Diesel w/out SCR	Lean NG	2010 TWC NG
literature	g/mi	60-30	82.4			58.9	8.7
UDDS	g/mi		7.20	0.64	1.84	-	-
Refuse	g/mi		15.31	2.20	1.36	15.5	1.0
UDDS	gbhp-hr		1.70	0.15	0.63	-	-
Refuse	gbhp-hr		1.84	0.26	0.20	5.3	0.4

Source: Gas Technology Institute

Table 5: NOx Emission Comparisons Between Port Vehicles and Fuels (g/bhp-hr)

Cycle	2007-2009 Diesel	>2010 Diesel w/SCR	>2010 Diesel w/out SCR	2010 TWC NG
PDT1	12.12	4.20	6.26	0.320
PDT2	10.11	2.62	5.87	0.172
PDT3	6.94	0.88	3.52	0.442
UDDS	9.51	0.86	4.63	0.423
UDDS_CS	10.73	1.74	5.51	

Source: Gas Technology Institute

Although the 2010 federal and California certification standards reduced NOx emission requirements by 90 percent, to 0.20 g/bhp-hr, the NOx emission data collected for some real-world driving conditions are different from the certification values, due to low-speed operation. For example, when heavy-duty trucks are driven in urban areas with low or stop/go speeds, diesel engines operate with lower temperature aftertreatment, so emission are significantly above the standard. Furthermore, in laboratory tests with the latest NOx control technology using selective catalytic reduction (SCR), the cold-start NOx emission for the first 100 seconds were > 2.2 g/bhp-hr — ten times higher than the certification standard. These data are shown in Figure 3 [2]. Once the exhaust reaches a temperature >~225°C, the emission was 0.006 g/bhp-hr (1). Additionally, the stabilized emission of the two systems over the same time period was very similar at 0.05 g/bhp-hr (about 75 percent below the standard). The main cause for the high NOx emission is the operation of the SCR as the NOx reducing additive (urea, known as diesel exhaust fluid (DEF)) is not added until the exhaust temperature reaches ~225°C. Below that temperature, there is no urea and no NOx control.

Figure 3: Multiple Data from a Heavy-Duty Truck Operating on a Chassis Dyno in UDDS Cycle

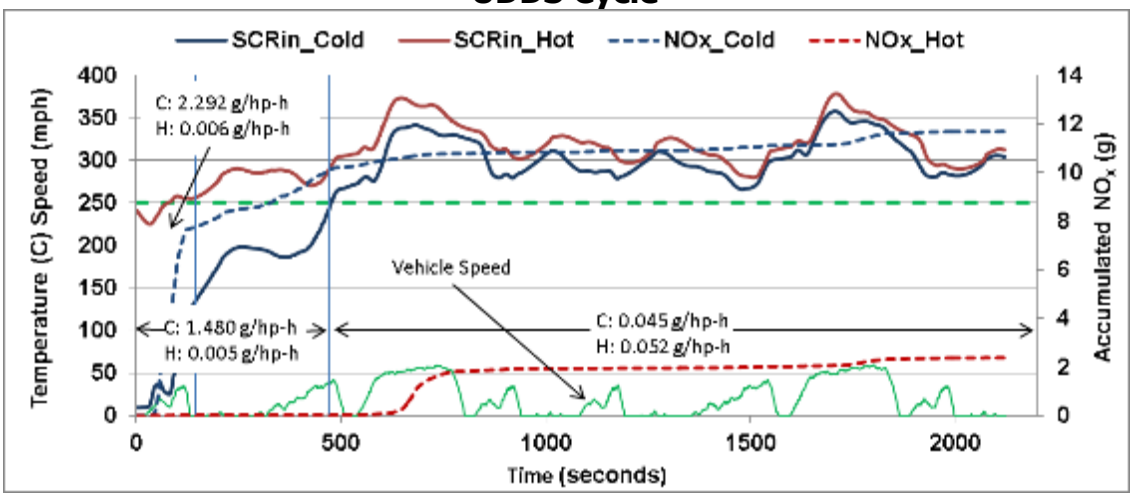

Source: Gas Technology Institute

These same trucks were tested on cycles designed to simulate port activity [5]. The port driving schedule represents near dock (2-6 miles), local (6-20 miles), and regional (20+ miles), typical of port drayage operation. The SCR was inactive for 100 percent of the near dock cycle, 95 percent of the local cycle, and 60 percent of the regional cycle. Thus, NOx emission were

on the order of 0.3 to 2 g/bhp-hr (1 to 9 g/mi) or >10 times the 2010 standard. The reason is that for exhaust temperatures <225°C no urea is injected and thus no NOx is removed. Low temperatures can come from operation at low loads and lean compression ignition combustion. Data from real world driving are show a significant difference from emission measured on the current certification cycle. While not a deliverable in this project, this research explored reducing the real-world emission when operating in city stop-and-go driving or in drayage operation. The application of hybrid-electric technology will open new opportunities for design that are not possible with current technology approaches.

CHAPTER 2:
Fuel Economy and Emission Reduction Analysis

This section describes a natural gas engine-electric hybrid design model for providing on-road driving performance, fuel efficiency, and emission control. The project proposed in this study was to start with a commercially available engine and design and demonstrate an emission control system with near-zero emission, a target value of 0.02 g/bhp-hr. The research team utilized the Cummins Westport Incorporated (CWI) 8.9 ISL-G natural gas engine and overlaid systems to improve fuel efficiency and reduce NOx emission. The main research challenges were: 1) air-to-fuel ratio control, 2) exhaust gas system, and 3) hybrid system integration of three power sources (engine, battery and electric motor).

Review

This section provides a brief introduction on fuel efficiency and emission to understand the background in current approaches for these designs and as a lead into the work performed and results expected.

Objectives

The goals of this task are to: (1) design the individual vehicle components, (2) model systems and (3) optimize component requirements and specifications. These can be summarized into the following:

- Develop and evaluate engine control (fuel/air delivery, spark timing, air-to-fuel ratio) simulation model.
- Develop and evaluate emission model for vocation specific drive cycles.
- Develop and evaluate a hybrid system control approach for vocation specific drive cycles.
- Develop and optimize the system level model integrating engine control, hybrid control, and emission control models.

Fuel economy and emission trends can be reviewed by drawing on information available for the ISL-G engine. This section is organized in three sections: 1) fuel economy 2) emission and 3) modern natural gas engines.

Fuel Economy

One of the earliest approaches for reducing exhaust NOx with uncontrolled engines was to increase the fuel consumption, as shown in **Error! Reference source not found.**Figure 4, either by adding excess fuel or by retarding the timing of fuel addition (or both). During a rich combustion process, there are hydrocarbons present that can react with and reduce the NOx emission from 0.14 to 0.02 g/bhp-hr, according to CWI reports. With a growing emphasis on greenhouse gas emission and reducing fuel consumption, this approach was replaced with exhaust control measures, such as exhaust gas recirculation (EGR) and the addition of catalytic treatment. Fuel economy based on a stoichiometrically controlled engine with EGR will have a limited fuel economy benefit without complex engine block redesigns targeting higher thermal efficiencies as suggested by Cummins Inc. Even then, fuel efficiency gains

would be limited to 5-10 percent which are important, but still significantly short of the desire for 25-50 percent reductions to meet greenhouse gasses (GHG) reduction targets in California.

Figure 4: NOx Control Using Increased Fuel Consumption

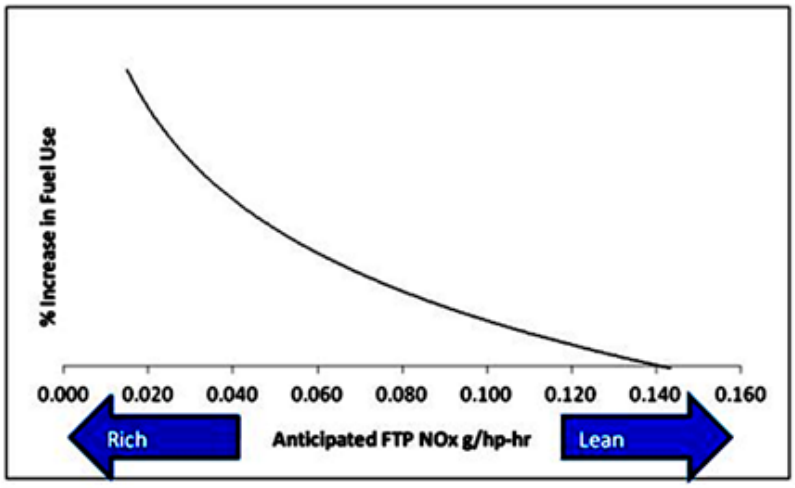

Source: CWI

One other approach is energy recovery with electric hybridization. Hybrids have the advantages of energy recovery and engine downsizing, but at the added cost of additional technologies. To overcome the added cost of these technologies, this demonstration project considers repowering existing engines where the hybrid/repower costs may be equal to or lower than the new engine cost.

In this demonstration project, the approach was to use an electric hybrid system to increase the fuel economy and reduce the GHG emission by an additional 25 percent over diesel fuel as a first step. Concept approaches, like intelligent transportation systems (ITS) using optimized fuel use route management, might offer up to a 50 percent GHG total reduction when hybrid plus ITS technologies are incorporated, but are not developed in this project.

Emissions

Regulated emission from natural gas vehicles include carbon monoxide (CO), hydrocarbon (HC) as methane and non-methane hydrocarbons, particulate matter, and NOx. Of these pollutants, NOx emission is of most concern due to ozone exceedances in industrialized regions like the South Coast Air Quality Management District (SCAQMD). Heavy-duty diesel trucks remain one of the largest contributors to NOx emission inventories as cars approach zero emission. Modern technologies exist for the efficient control of NOx emission and include exhaust gas recirculation (EGR), stoichiometric air-to-fuel ratio (AFR) control, and three-way catalyst (TWC).

EGR is the process of recirculating exhaust gases with fresh intake air to lower the oxygen concentration in the combustion process and reduce peak in-cylinder temperatures by absorbing combustion heat. NOx emissions are formed in the combustion chamber when nitrogen reacts with oxygen at high temperatures. The formation of NOx emission can be reduced by up to 30 percent. EGR is used with various fuels and combustion process and is a well-developed technology.

Natural gas engines have the option of using TWC control technology to simultaneously reduce NOx, CO, and HCs, as used in gasoline-fueled vehicles for over 30 years (Figure 5). Performance shows that TWC technology has successfully reduced HC, CO, and NOx emission by more than 90 percent, and is well developed. The function of the TWC system is to use the exhaust gas species for the oxidation of CO and THC and the reduction of NOx following the equations shown in Figure 6. However, the actual physical and chemical phenomena taking place in a TWC is quite complex. Chatterjee et al. [7] have presented a detailed analysis of the transport phenomena, adsorption/desorption processes, and surface reaction mechanisms in developing a model to simulate the TWC. Their model follows 61 reactions among 31 species.

Figure 5: Three-Way Catalytic Converter as a Cut-away

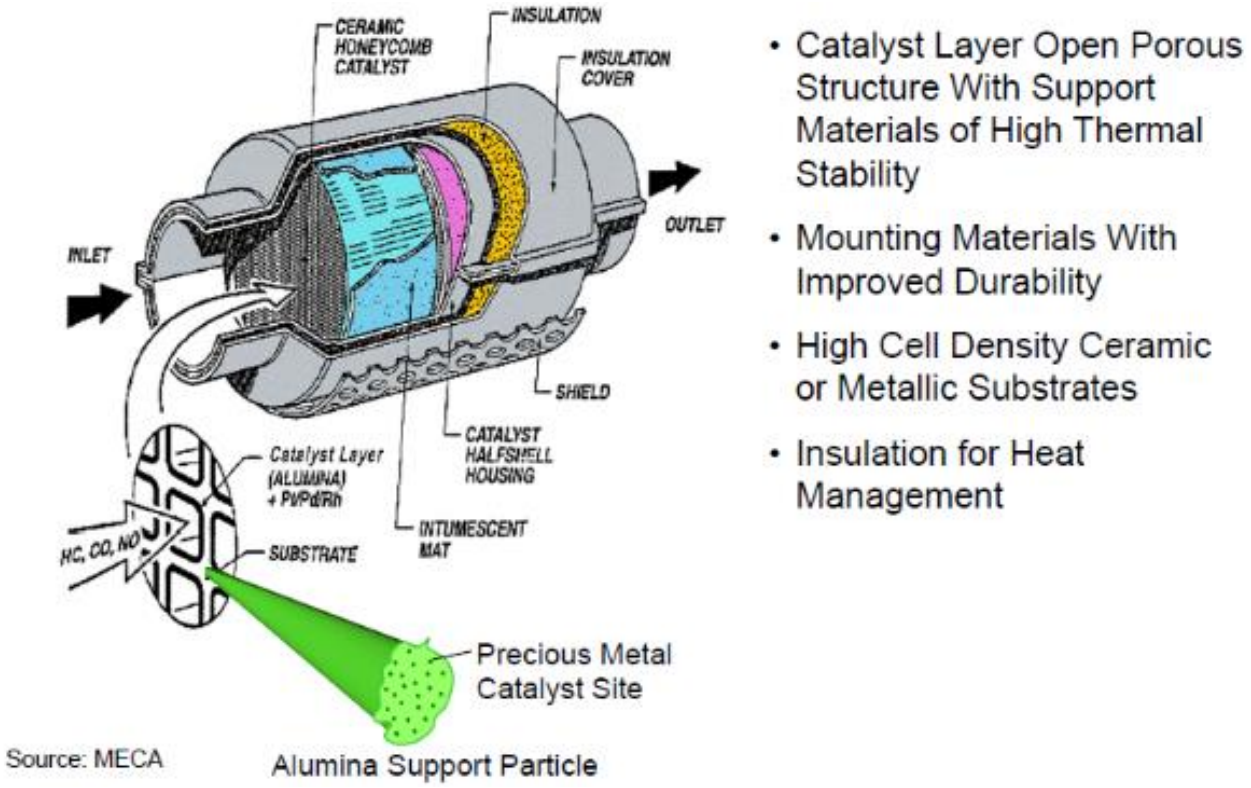

Source: MECA

Figure 6: Method of Operation of the Three-Way Catalytic Converter

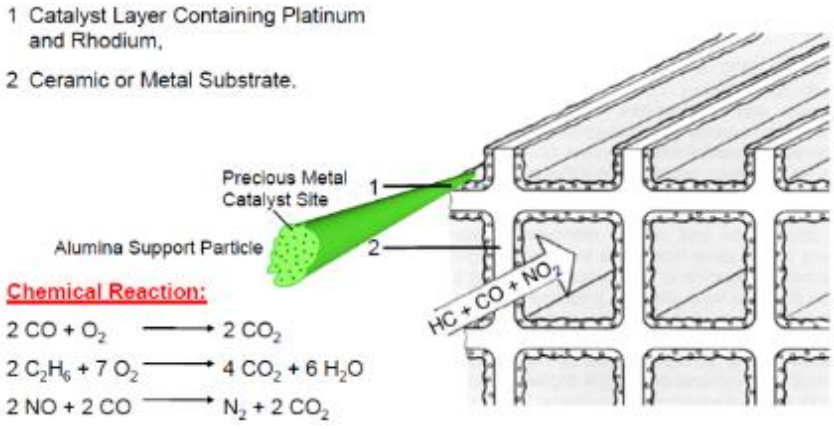

Source: MECA

The key to the emission reductions with a TWC system is an AFR management system that controls the exact balance of chemical species at the stoichiometric ratio. Figure 7 shows the importance in controlling the ARF to get maximum conversion efficiency. Controlling AFR at exactly the stoichiometric ratio is not simple due to oscillations in the AFR control modules so the intake air oscillates between rich and lean. To smooth oxygen variations, the TWC incorporates an oxygen absorbent and with exact air and fuel metering, the conversion efficiency is high. Experience shows that the designed magnitude and frequency of the oscillations about the set point leads to differences in catalyst conversion efficiencies as shown in Figure 8, the magnitude of the oscillations is reduced from ± 1.0 to ± 0.3 A/F ratio, and the sampling frequency is increased from 1.0Hz to 1.5Hz. In addition, the fuel delivery system was changed from closed-loop carburetor to multi-point fuel injectors. Because of these engineered design changes to the frequency and magnitude of the oscillations (±A/F ratio) to fuel metering control the performance of TWC was improved. In general, an AFR control problem includes knowledge of fuel injection and air intake dynamics, feedback signals, and emission results for proper design.

Figure 7: Oxidation and Reduction at Stoichiometric Mixture

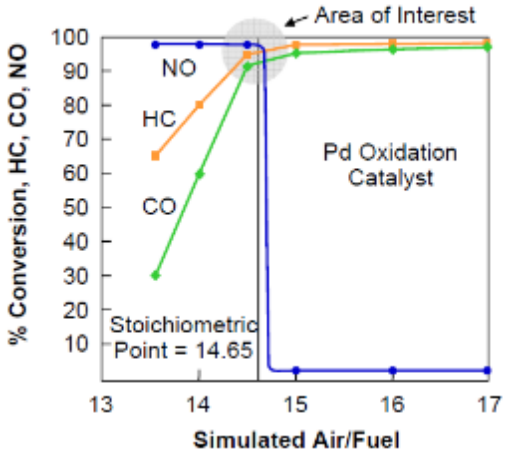

Source: Gas Technology Institute

Figure 8: Quality of Fuel Metering Control is Key to Catalyst Performance

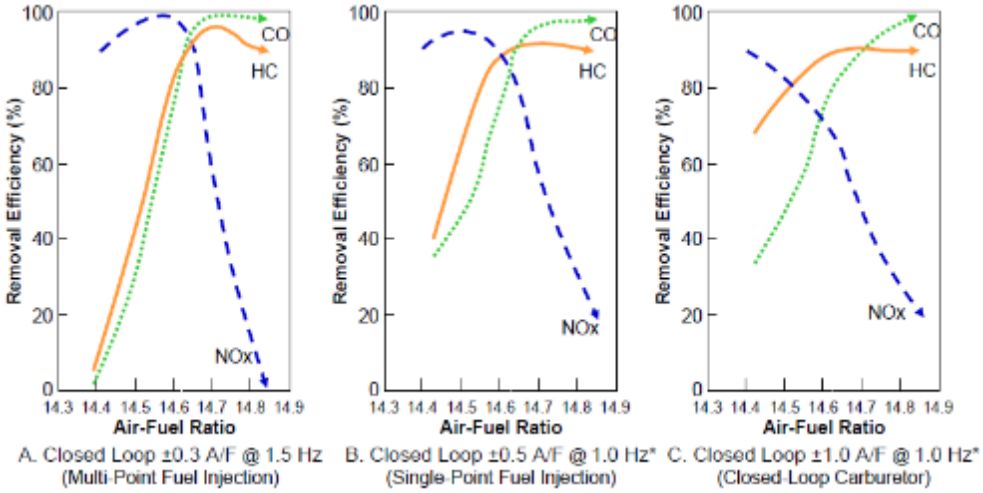

Source: Gas Technology Institute

Modern Natural Gas Engines

The CWI ISL-G natural gas engine meets the 2010 NOx emission standards of 0.2 g/bhp-hr by using several NOx control devices. As shown in Figure 9 the CWI technology includes: stoichiometric EGR (SEGR) with a TWC to control HC, CO, and NOx emission. Furthermore, CWI added cooled EGR and cooled charge air to reduce NOx formation during the combustion process.

Figure 9: Cummins Westport Inc. Technology: Spark Ignited, Stoichiometric Combustion and Cooled Exhaust Gas Recirculation

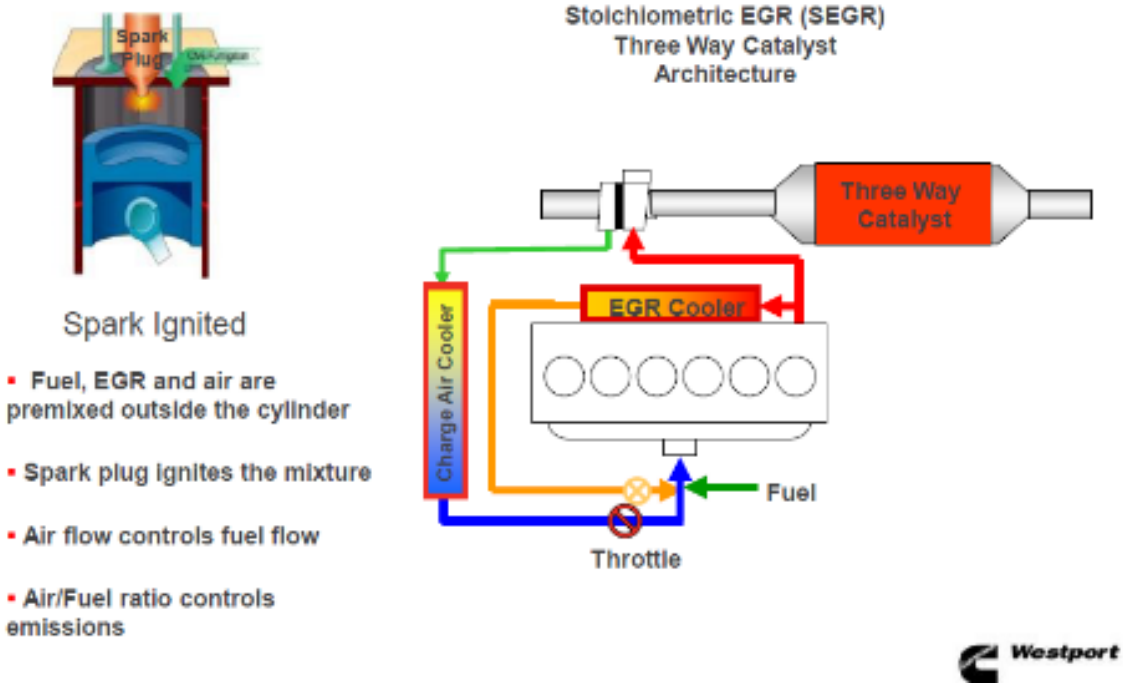

Source: CWI

In October 2016, CWI announced its availability of an even lower emission natural gas engine called the ISL-G Near-Zero engine (now L9N). This ISL-G near-zero engine is certified to NOx emission levels of 0.02 g/bhp-hr on an engine dynamometer and was tested at UCR in a vehicle on a chassis dynamometer with confirming results. The following statements were made by spokespersons for the near-zero technology and were observed in the truck with near-zero technology that was tested on UCR's chassis dynamometer so were used in planning the emission reduction portion of this research.

1. The catalyst size and composition is the same as used on the first-generation 11.9 liter engine; no special catalyst program was carried out to achieve the near-zero emission.
2. While many of the gasoline automobile manufacturers use a specially designed close-coupled catalyst to achieve faster heat-up, the CWI product does not include a close-coupled catalyst.
3. There did not seem to be a lot of added insulation between the engine outlet and the TWC.
4. The fuel delivery system was unchanged and remained as throttle body injection (TBI).

Given these observations, UCR suspected the key change needed in order to achieve the near-zero NOx emission was improved A/F sensing and fuel control so those parameters became

the focus of UCR's research. As described earlier, these parameters were key for gasoline vehicles in with TWC to reach the lowest levels.

During the proposal stage it was believed that optimizing for lowest emission and highest fuel economy was only possible with electrically heated catalysts and close coupled catalysts. While reviewing the literature and observing commercial trucks with the near-zero engine, it was learned that cold-start emission could be managed with AFR control and that the cost of an electrically heated catalyst was not needed.

ISL G Natural Gas Engine

This section discusses the basis for the engine design based on in-use testing of the ISL G 8.9 and the ISL G near-zero 8.9 liter natural gas engines.

Cold Start NOx Emissions

The cold start emissions for an 8.9 L ISLG engine represents a significant portion of the NOx emission. Figure 10 shows accumulated NOx emission as a function of time and that 85 percent of the emission were during the cold start phase. Figure 11 and Figure 12 show the same test; first on a work basis, and second, on a distance basis. In all cases the cold start NOx emission is >85 percent of the emission during the test. These high NOx emission values show the importance of controlling NOx emission during cold start.

Recent testing at UCR on CWI's near-zero NOx natural gas engine showed that >90 percent of the NOx emission were during the cold start condition. The increased percentage is a result of the much lower transient emission. These results will be presented in a report still in preparation for CWI.

The main factors controlling cold start emission is the catalyst light off time and cold https://www3.epa.gov/region1/airquality/nox.htmloperation fueling. Catalyst light off is observed when the NOx emission is abruptly reduced in the catalyst system. For the existing 8.9 L ISLG and the near-zero ultra-low NOx design show a catalyst light off temperature appear to occur at 300 °C, (Figures 10-12).

Figure 10: Real-Time Cold Start Cumulative NOx Emission: Local Port Cycle

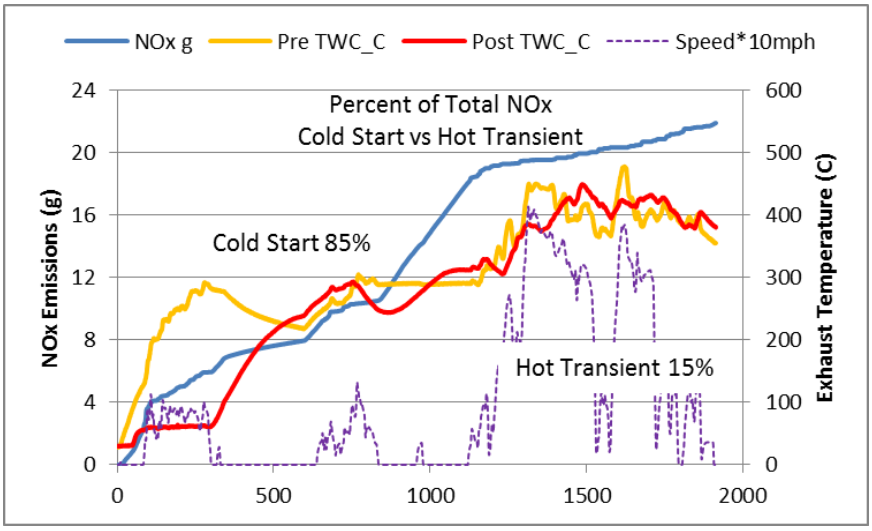

[1] **The data is from an in-use test of the ISL G 2010 Certified natural gas engine**

Source: CWI

Figure 11: Accumulated Cold Start NOx Emission on a Power Basis: Local Port Cycle

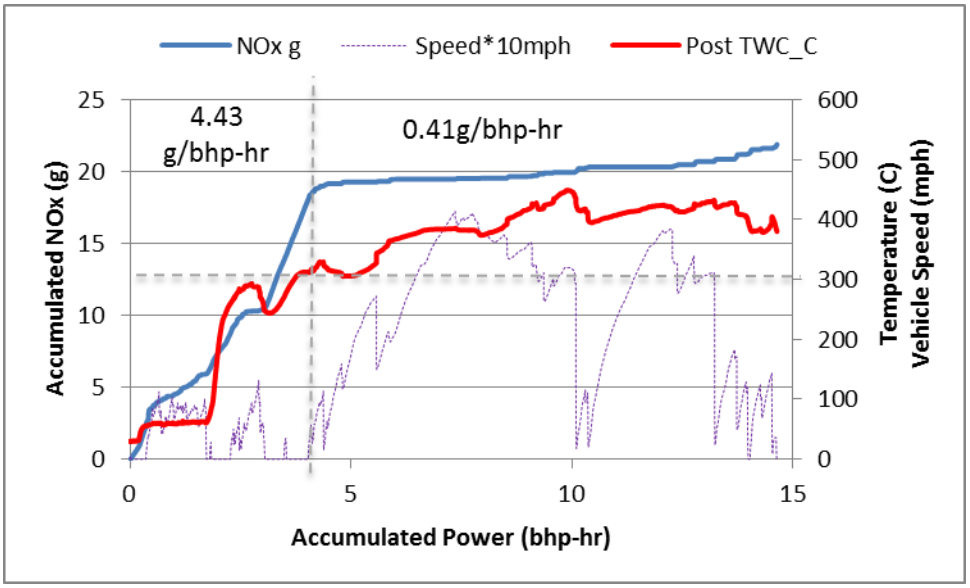

[1] The data is from an in-use test of the ISL G 2010 Certified natural gas engine

Source: CWI

Figure 12: Accumulated Cold Start NOx Emission on a Distance Basis

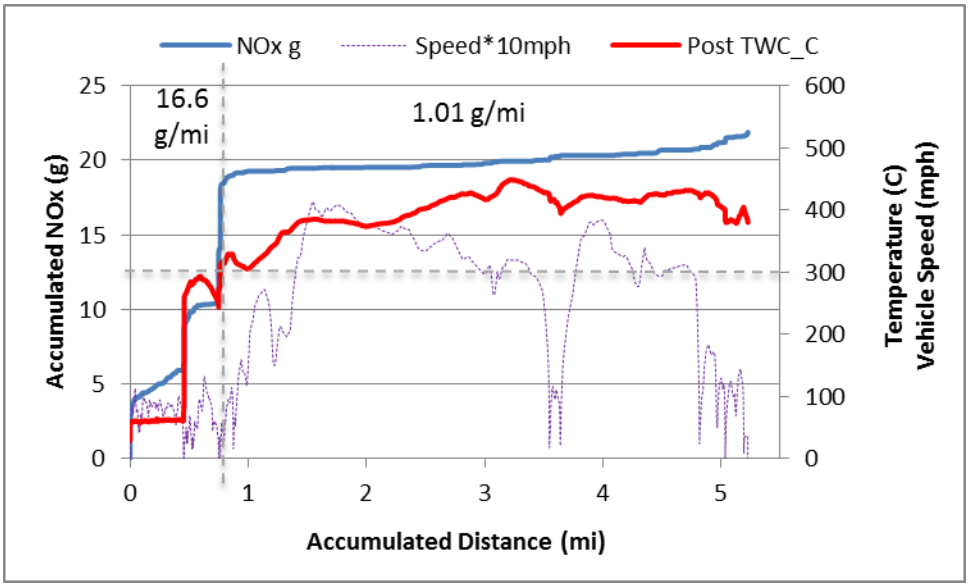

[1] The data is from an in-use test of the ISL G 2010 Certified natural gas engine

Source: CWI

During the ISL G near-zero ultra-low NOx engine testing, it was observed that the cold start NOx emission was much lower than its predecessor. This suggests an improved cold start strategy such as catalyst temperature monitoring and AFR control during warmup. Similar feedback designs will be employed to control the cold start process with the optimized engine. These strategies will be designed during the engine dyno testing.

Transient NOx Emissions

Transient NOx emission and AFR control are the source of normal engine and vehicle operating emission variation. The emission rate for transient NOx emission is 0.41 g/bhp-hr or

1.01 g/mi for the ISL-G natural gas engine tested at UCR. These emissions are higher than the certification standard for 2010 but can be reduced to meet the standard with AFR tuning. Observation of the Ultra-low NOx engine showed much lower overall emission factors at less than 0.02 g/bhp-hr and 0.06 g/mi. During these tests, it was observed that a few (1-3) NOx excursions represented 90 percent of the total emission mass, and in the case of one high NOx spike, the emission rate changed from passing the standard < 0.02 g/bhp-hr to failing the standard > 0.02 g/bhp-hr. The observation mostly occurred during rapid throttle events at idle engine speed into a loaded hill or speed/load change. The proposed AFR design will take special precautions to model this transient event and prevent the NOx spikes. Additionally, hybrid optimization can prevent the low engine speed fast transient from occurring. The presentation of these details and observations is in preparation for the report for CWI.

Fuel Economy

As discussed in the introduction, fuel economy is limited in its approach for improvements. Testing of the ISL G and ISL G near-zero showed similar fuel economy. Both engines were slightly better than the diesel comparative on a bsCO2 (g/kWhr) basis but not on a mile per gallon (diesel equivalent). Fuel economy benefits over the baseline ISL G and ISL G near-zero will be realized with the hybrid system. These details are discussed in the section on hybrid integration.

Engine Control Model

The engine control model includes the cold start, transient, catalyst, and hybrid systems in an integrated approach. These sections describe the model used for the implementation of the control strategy for the engine and later chassis testing as part of this research project.

The main control parameter for emission is an optimized AFR. AFR control design is based on three primary parameters 1) drivability, 2) emission, and 3) and fuel economy. The drivability performance of the natural gas engine relies on the stock ECM controls. The existing ECM controls were enhanced with an additional controller that optimized the fuel control elements of the vehicle for emission and the on-off control of the engine for fuel economy. The fuel control was implemented with an air-to-fuel ratio controller (AFR) and the fuel economy improvements was implemented with a hybrid energy storage and recovery system.

Cold-Start

The cold start NOx emission were managed using the engine's stock ECM controls with the following improvements: a catalyst bed temperature sensor, improved oxygen feedback sensors for proper trim, and investigation of cold start torque limitation utilizing a hybrid control design (to be optimized during chassis testing). A comprehensive cold start model was not developed as it is beyond the scope of this effort. Control approaches considered included catalyst feedback temperatures and existing cold start fuel management systems. Other approaches such as those used by Salehi et al [18] were considered.

The cold start NOx emission was expected to perform as well as the 0.02 g/bhp-hr ultra-low NOx engine as recently certified by CWI and tested at UC Riverside.

Transient

The dynamic equations that describe the four-stroke SI engine are described in this chapter. The development is limited to an understanding of some of the basic nonlinearities and dynamics for the mean value engine model (MVEM). The work here follows the research published by Sorenson [13, 14]. The model that was developed utilized a 4-cylinder engine for port and carburetor fuel injection. The equations are similar for a 6-cylinder engine, but with different coefficients. The carburetor section is important since heavy-duty NG engines utilize a single fuel injection near the throttle plate (the throttle body approach is the correct model to use and not port fuel inject model). Gasoline engines use a port fuel injection. Having both for the reader is valuable to see differences.

The detailed MVEM is out of the scope of this project. For a full description of the MVEM, see [14]. This section covers the throttle body, intake manifold, oxygen feedback, fuel injections and the four-stroke process.

The intake manifold model consists of throttle body and the intake manifold, (Figure 13) for location. The manifold is the enlarged area for air to enter from the throttle body before the air enters the port runners for each cylinder.

Figure 13: Intake Model System Showing Air Induction Model and Variable Locations

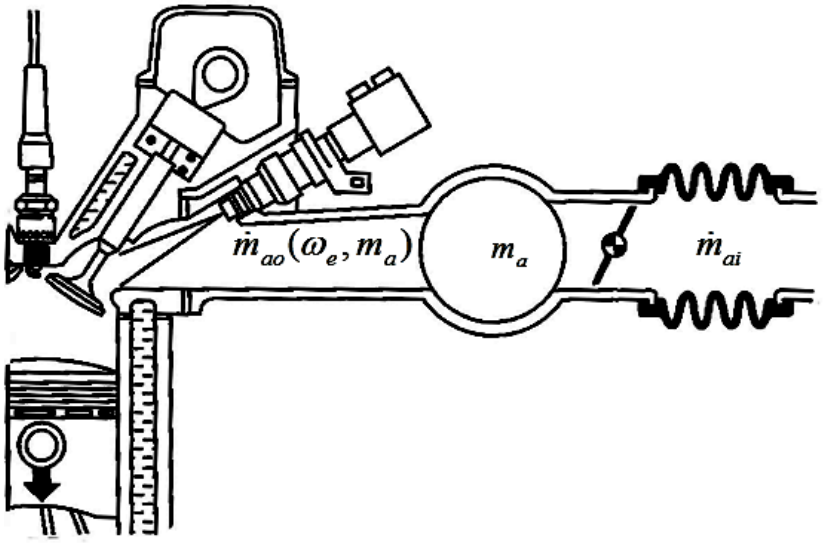

Source: CWI

The throttle body controls the airflow into the intake manifold with the throttle plate. The intake manifold volume is designed to provide an air buffer to maintain as near as possible constant air pressure to the ports during steady state and transient throttle operation. As the throttle angle increases the intake manifold pressure increases. Two inherent problems with the intake manifold are manifold air charging and signal filtering [13, 14]. The problems with the throttle are its nonlinear effect on airflow [15, 13].

Throttle Body

The airflow through the throttle body is highly nonlinear. At large throttle angles the airflow dynamics take on an entirely new set of equations [15, 13]. Fortunately, most engine designs incorporate the mass airflow (MAF) sensor that directly measures the airflow into the intake

manifold. The throttle position is still necessary for feed forward design, but not relied on for airflow measurements directly. In this project the MAF sensor is used for intake airflow therefore the dynamics of the throttle body are not explained in this project. The flow rates into the intake manifold assume one-dimensional isentropic compressible flow.

Intake Manifold

The intake manifold model includes the dynamics from the intake manifold to the intake port for each cylinder, as shown in Figure 14 for details. While this does not fully represent the CWI engine, the manipulations subsequently described show how the representativeness was improved. The model is based on the conservation of mass equation for air as follows. The reason for the model is to estimate the actual flow of air into the cylinders from the airflow measured at the throttle MAF sensor. The following equation is used to estimate the airflow into the cylinder or port airflow:

$$m_a = \dot{m}_{ai} - \dot{m}_{ao}(\omega_e, m_a)$$

Where:

m_a	mass of air in the intake manifold
$\dot{m}_{ao}$	mass flow of air out of the intake manifold and into the cylinder
$\dot{m}_{ai}$	mass flow of air into the intake manifold and through the throttle body
ω_e	engine rpm

To manipulate this equation into something more useful, the following assumptions are made [15,13]:

- The air in the intake manifold obeys the ideal gas law.
- Pressure and temperature are uniform in the manifold volume.
- The manifold air temperature is constant or changing slowly.
- The presence of fuel has no effect on the airflow.
- The amount of exhaust gas recirculation is negligible.

Ideal Gas Law: $P_m V_m = m_a R_a T_m$

Where:

P_m	intake manifold air pressure
R_a	gas constant for air
T_m	intake manifold air temperature
V_m	intake manifold air volume

Solving for m_a :... $m_a = \dfrac{P_m V_m}{R_a T_m}$

Equivalently, the Continuity Equation is now a function of manifold pressure:

$$\dot{P}_m = \frac{RT_m}{V_m}(\dot{m}_{ai} - \dot{m}_{ao})$$

The following is the equation used to estimate the airflow into the cylinder at different speeds/loads:

$$\dot{m}_{ao} = K \frac{V_m}{RT_m} \eta_v(\omega_e, m_a)\omega_e P_m$$

Where:

η_v volumetric efficiency of the motor which is a function of (ω_e, m_a)

ω_e engine speed in radians per second (rad/s)

K a constant $K = \frac{D}{4\pi N V_m}$

D cylinder displacement volume (m)

N number of cylinders

V_m intake manifold volume (m^3)

Fuel Injection

The purpose of the fuel metering system is to deliver an appropriate amount of fuel to the cylinders in proportion to the power requirement. Simultaneously, the amount of port airflow must be adjusted to maintain the stoichiometric ratio for the TWC system to work at high efficiency for conversion of NOx, CO, and hydrocarbons. It is therefore necessary to accurately know the port airflow and fuel flow into the cylinder to maintain proper AFR control.

Fuel metering has been the focus for emission reduction since the 1970's when emission concerns with light-duty gasoline passenger cars forced better control over exhaust emission. Early model vehicles used carburetors for fuel metering. Central fuel injection (CFI) control replaced the carburetor, giving the designer greater control over fuel metering using feedback from an oxygen sensor in the exhaust and electronic control of fuel injector at the throttle body (Figure 14). The successor to the CFI strategy is multi-port fuel injection (MPI) strategy. In the MPI design, the fuel is injected on the back side of the intake valve at the cylinder (Figure 15). The MPI design reduced the complexity of modeling delays that were inherent with CFI type injection, but there are still delays that make transient fuel metering non-trivial.

Figure 14: CFI Method for a 4-Cylinder Arrangement

1 Fuel, 2 Air, 3 Throttle valve, 4 Intake manifold, 5 Injector, 6 Engine.

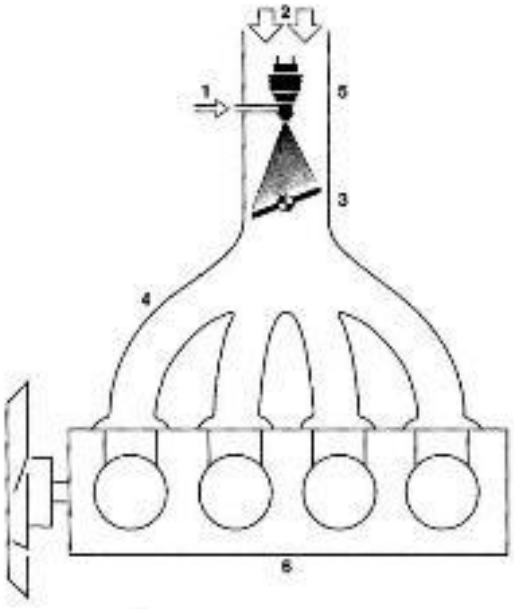

Source: CWI

Figure 15: MPI Method for a 4 Cylinder Arrangement

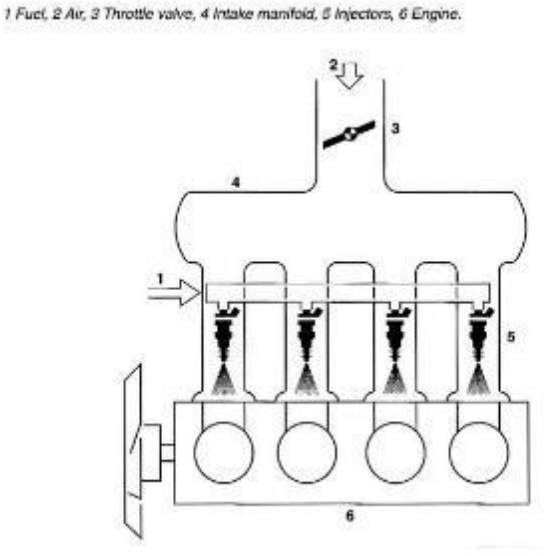

Source: CWI

Oxygen Feedback

Three significant delays contributed to the overall delay of the AFR feedback control strategy including physical delays, sensor delays, and microprocessor computation delays. The physical delays and the sensor delay are the major contributors to the low feedback bandwidth. Modern microprocessor delays are relatively insignificant here and thus not considered in this project. The following three sections describe the exhaust gas oxygen (EGO) sensor, gas transport, and four-stroke delays inherent in all SI engine control strategies.

The EGO sensor is responsible for feeding back the status of the exhaust AFR to the microprocessor during warm up, transients, and steady state operation. The EGO sensor measures the percent of oxygen in the exhaust gas stream before the three-way catalyst and just after the collector of all the exhaust runners (average engine out exhaust) (Figure 16 for location). The sensor output is designed to maintain stoichiometry by oscillating around an AFR of 14.7 $\pm$ 1 percent. Some EGO sensors operate just rich or lean of stoichiometric, but they will not be considered in this project. Figure 16 shows the sensor output for a vehicle operating at steady state. Notice the oscillating nature of the sensor. Figure 17 shows the voltage potential for the sensor as a function of oxygen percentage. Notice that the signal has magnitude 0.8 volts at low oxygen percentages and 0.2 volts at high oxygen percentages. The transition from 1.1 to 0.2 volts occurs at an oxygen percentage range from 10-11 to 10-2 which corresponds to an AFR of 14.7 (stoichiometric). This fact implies that all vehicles with EGO sensors are, by design, required to operate at stoichiometry unless the switching nature of the sensor is modified.

The EGO sensor time constant has been experimentally determined by many researchers to be $t_{ego} = 20$ ms [14, 16, 13]:

Figure 16: Steady State Switching Nature of an EGO Sensor

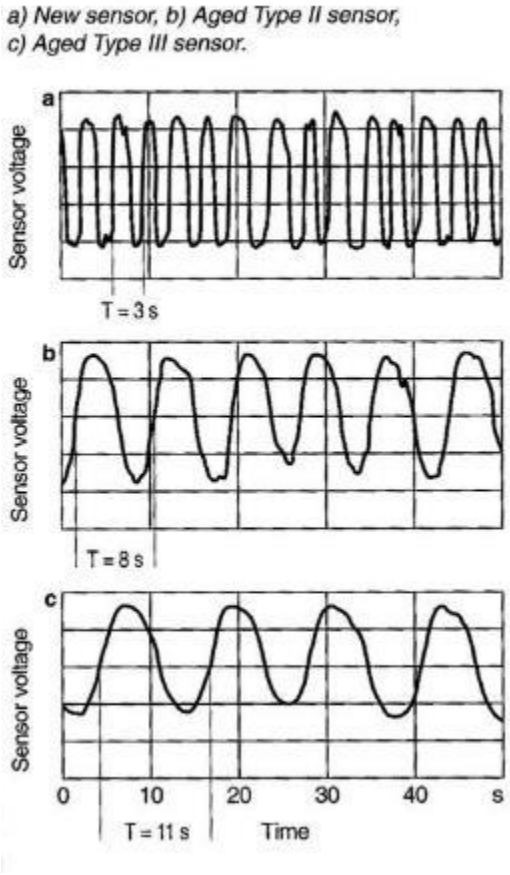

Source: CWI

Figure 17: EGO Sensor Output as a Function of Oxygen Partial Pressure

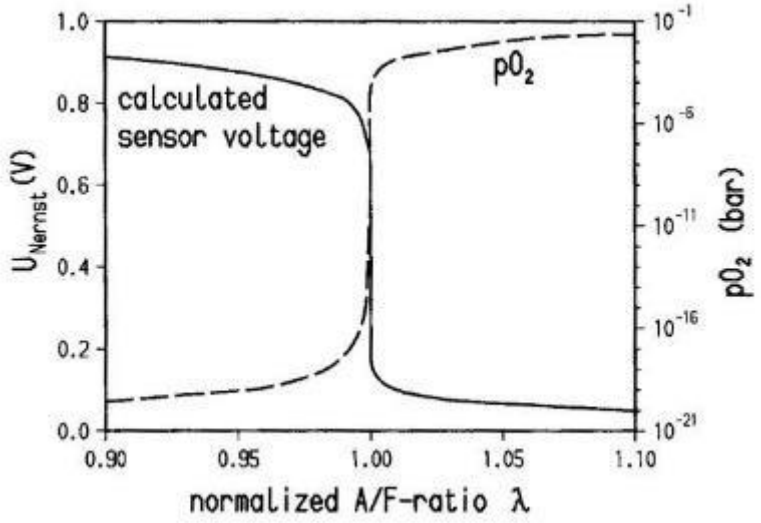

Source: CWI

Four Stroke Delays

The four-stroke delay is due to the nature of the engine design. It takes four strokes to complete a combustion event in an IC engine (Figure 18). The first stroke is the gas induction stroke. This is where the air and metered fuel are inducted into the cylinder. The next stroke is the compression stroke. In the second stroke the fuel and air have mixed thoroughly so they

are ready to combust upon command from the ignition source (spark plug timing). The third stroke is the power stroke. This stroke drives the crank shaft 180 degrees with the energy from the fuel going into heat energy and torque. The fourth stroke is the exhaust stroke where the gases exit through the exhaust valve then through the exhaust manifold to the EGO sensor then through the catalyst then out the tail pipe.

The time between fuel metering events is once per four strokes. There are two revolutions per four strokes, therefore it takes two revolutions to complete one fuel metering event. The delay is described by the following:

$$t_{pf} = \frac{2(2\pi)}{\omega_e(t)}$$

Where:

t_{pf} is the time between fuel metering events.

Note the delay is a function of engine speed ω_e (The higher the rpm the smaller the time between fuel metering events).

Figure 18: Combustion Strokes for the IC Engine

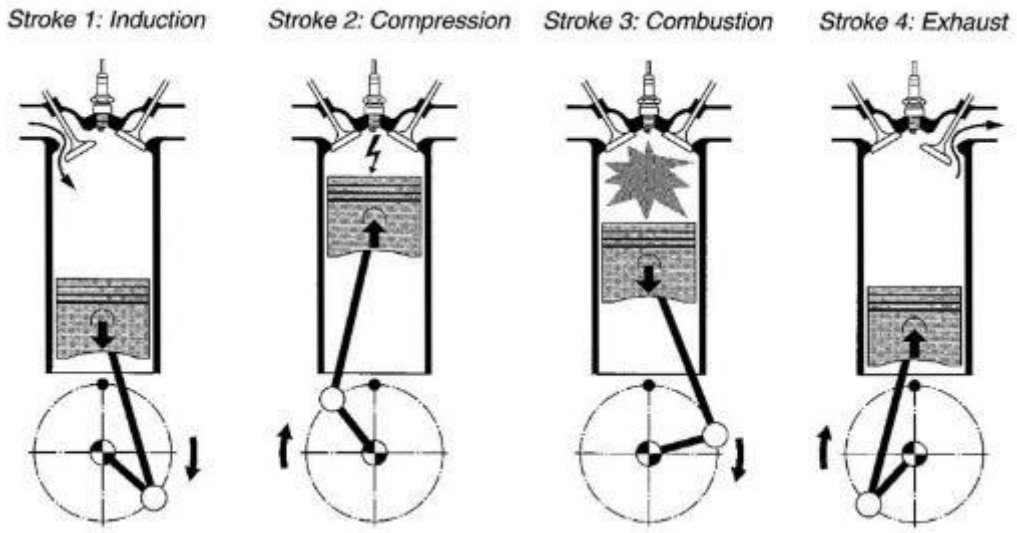

Source: CWI

Gas Transport

The physical delay from fuel injection to exhaust gas at the EGO sensor is a sum of the four stroke cycle delay and the gas transport delay. The gas transport delay is the time delay the gas takes to go from the exhaust valve to the EGO sensor. This gas transport delay is a function of engine speed and can be represented as [17]:

$$t_{pt} = 1.537\omega_e(t) + 0.0156$$

Where:

t_{pt} the time it takes a gas volume to go from the exhaust valve to EGO sensor.

Summary of Equations

The total feedback delay from fuel injection to signal recognition at the EGO sensor can be summarized by the following equations:

$$t_{delay} = t_{ego} + t_{pf} + t_{pt}$$

$$t_{delay} = 0.02 + \frac{2(2\pi)}{\omega_e(t)} + 1.537\omega_e(t) + 0.0156$$

The total AFR feedback signal delay is the sum of the sensor time constant, four stroke cycle, and the exhaust gas transport. At low engine speeds the four-stroke cycle and exhaust gas transport processes dominate the delays and at high engine speeds the sensor time constant is significant.

Simulink Model Implementation

The development of an engine simulation model was out of the scope of this project but is necessary for the evaluation of the proposed sliding mode controller and new AFR sensor. The idea behind the model is to create an environment, within Simulink, where different control techniques can be evaluated. This model should be capable of simulating engines with the main parameters available for controlling and measuring. This section covers the development of the simulation model for a mean value engine model, PI control, and sliding mode control.

Robert Weeks of Simcar.com developed a Matlab/Simulink[1] simulation model that is a commercial product [17]. The simulation was based on a nonlinear mean-torque predictive engine model developed by John J. Moskwa [15]. This model simulates a sequential port fuel injected, spark ignition engine with fuel, air and EGR dynamics. In addition, the simulation includes the process delays inherent in a four-stroke cycle engine. The model was specifically designed for the control engineer/researcher. This project uses Robert Weeks' Simulink engine model as the starting point for implementing the sliding mode controller and new AFR sensor. Modifications were necessary for the new controller.

Included in this project is a brief description of the Simulink engine model; for a more detailed description see reference [15]. The simulation includes eight main blocks (Figure 19). They are ambient conditions, external loads, throttle input, engine, sensors, controller, analysis, and actuators.

1 MATLAB and SIMULINK are trademarks of the Math Works, Inc.

Figure 19: Simulink Mean-Torque Predictive Engine Model

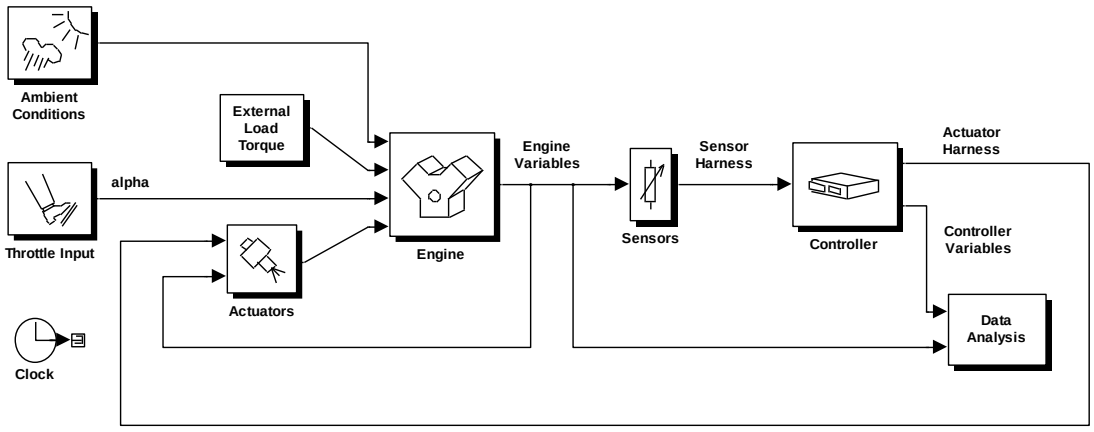

Source: Gas Technology Institute

The controller block simulates the signal conditioning, control algorithms, and output signal conditioning (Figure 20). Signal conditioning includes A/D conversion noise and saturation. The control algorithm has airflow and fuel flow estimator and includes EGR, IAC, and Spark Advance output information. The airflow estimator is based on the speed density approach and is only used in this project as a comparison to the MAF sensor. The fuel flow block simulates the fuel compensation lag and the desired commanded fuel based on PID output information from the EGO signal. The fuel flow block is where the sliding mode controller will be realized.

Figure 20: Controller Simulink Block Showing the Signal Conditioning

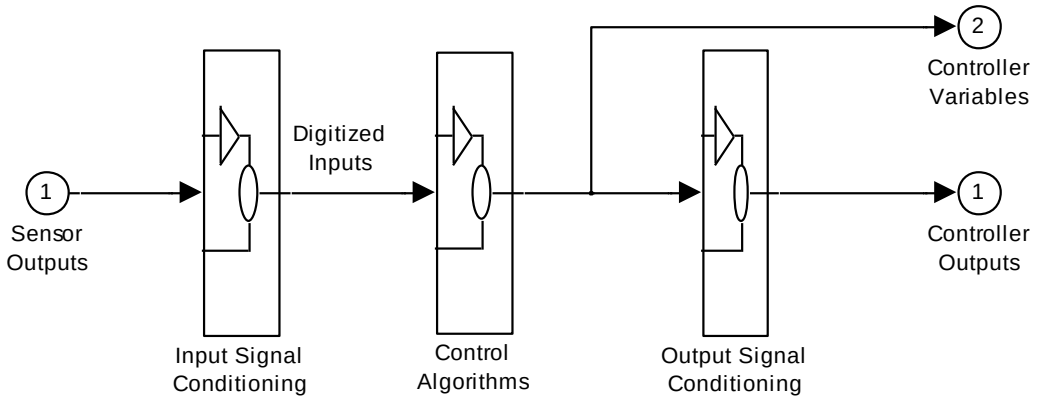

Source: Gas Technology Institute

Exhaust Gas System

The modelled exhaust gas system includes the three-way catalyst and an electrically heated section for rapid catalyst heat up for cold starts and hot restarts (during on/off hybrid control). This model helped determine that the electrically heated exhaust was unnecessary.

Three Way Catalyst (TWC) System

As discussed in an earlier section, measurements and data analysis show that near-zero NOx emission are the result of higher TWC temperatures and improved AFR control rather than

advanced catalyst designs. Recent reports on the CWI ISL G near-zero 8.9 liter engine show NOx emission below 0.02 g/bhp-hr for hot UDDS testing and only slightly higher for cold UDDS tests. Once the catalyst system is hot, the NOx emission was well below the 0.02 g/bhp-hr where cold start and transient AFR were critical to maintaining low NOx emission. As such, the TWC design approach is to use stock BASF catalyst design.

Electrically Heated Section

Cold start management with rich AFR cold operation and direct temperature feedback shows reasonably good NOx emission reductions based on recent testing at UCR on the ISL G near-zero 8.9 liter engine. As such, the electrically heated section was evaluated for its benefits to cost ratio.

Cold start NOx emission is much higher than the hot start emission. At 100 seconds into the UDDS cycle, there is a sharp reduction in NOx emission. The sharp reduction may be the result of rich air-fuel-ratio control since the catalyst temperature were still relatively low (~100-200 C) and rich conditions were observed with elevated HC emission. High HC and CO emission are an indication of rich operation. After 300 seconds into the cold start, the HC emission were sharply reduced suggesting catalyst light-off and closed loop control around the stoichiometric point.

Gasoline passenger cars with TWC systems use a catalyst closely coupled to the exhaust manifold in order to more quickly reach the light-off temperature of the underbody catalyst. For this project, the project team considered achieving the same result by adding an electrically heated pre-catalyst to reach the light-off temperature faster. System operation should include heating the catalyst at idle conditions for approximately 100-200 seconds prior to enabling the engine to provide shaft power. Additionally, the exhaust showed temperature drops from about 350 C to about 250 C when the vehicle was idling, suggesting a loss of about 1C/sec. The electrically heated catalyst can mitigate this loss for engine pre-heating on restart. As exhaust flow ranged from 30 scfm (idle) to 600 scfm (full power) for the UDDS cycle where the average for the first 10, 100, and 200 seconds was 79.9, 139, and 375 scfm. The proposed electrical heater design would handle an idle flow of 30 scfm.

Hybrid Integration

The advantage of the hybrid system is based on three primary design approaches 1) energy recovery, 2) engine stop-start, and 3) transient speed limitation. Energy recovery is where the vehicle inertial is converted from kinetic energy back into usable electrical energy. The engine stop-start control will utilize the hybrid system to operate in a fixed "charge depletion" mode, and transient speed limitation is implemented to prevent transient NOx spikes resulting from tip-in AFR excursions.

Energy Recovery

Hybrid-electric systems can recover energy from the vehicles inertia and convert his into usable electrical energy. Energy storage will be utilized to minimize fuel consumption during low power duty cycles where the engine operation is less efficient. During low power duty cycles (local DPT1) the bsCO2 emission increased from 579 to 804 g/bhp-hr (39 percent higher fuel consumption). If a hybrid-electric system is available, a portion of these losses can be eliminated. In freight movement there may also be an opportunity for advanced intelligent

transportation systems (ITS) where feed forward predictive hybrid mode operation can be integrated to even further take advantage of the hybrid system.

Stop-Start Design

Hybridization can provide significant fuel consumption benefits, especially for power duty cycles with low loads. The main benefit comes from engine stop-start operation and braking regeneration. The fuel consumption savings from engine on/off operation are estimated at up to ~60 percent with the assumption of a 1.5 kWhr and 7.5 kWhr battery storage system (Figure 21). If vehicle braking power recovery is also considered, an additional 30 percent savings can be achieved for an overall benefit of up to ~75 percent.

The low-power duty cycle seen in port operations is an ideal application for hybridization as the peak power is rarely required and the large IC engine normally used can be replaced with a smaller IC engine and electrical motor to boost overall power. If the vehicle operates beyond 20 miles from the port, the engine output at normal loads can easily be handled by the smaller IC engine with significant GHG savings. However, if a hill or condition requires more power, then the electrical motor can be activated.

Figure 21: Engine Simulation at 1.5kWhr and 7.5 kWhr Storage (No-Regeneration)

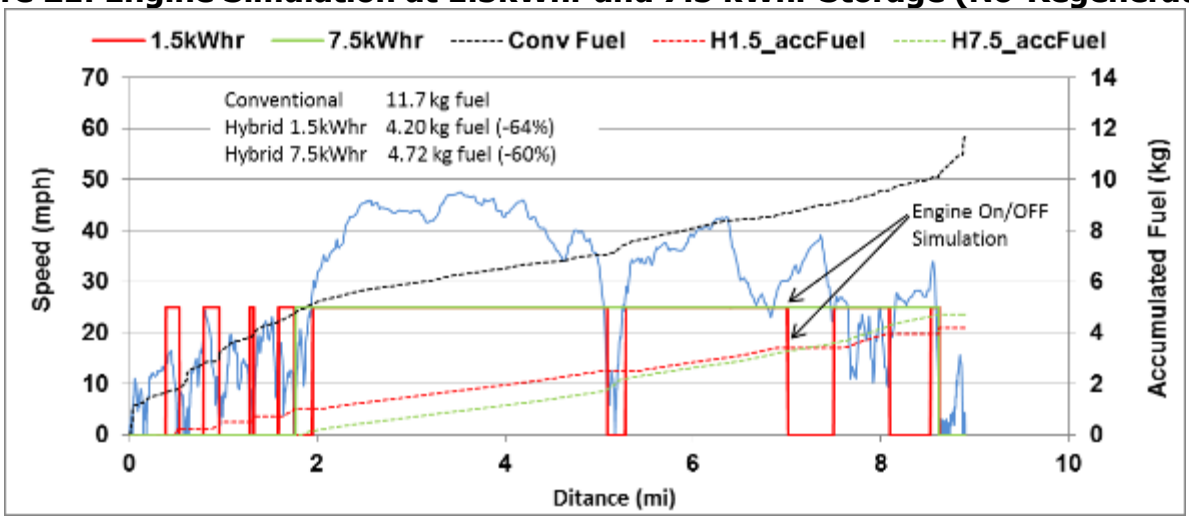

[1] **Simulated hybrid savings are based on the combined near dock and local port driving cycles. The simulation considers the a 1.5kWhr and 7.5kWhr usable battery solution. H1.5_accFuel is the accumulated fuel for the 1.5kWhr simulation, and H7.5_accFuel is the accumulated fuel for the 7.5kWhr approach. The ConvFuel is the amount of fuel consumed by a conventional heavy-duty vehicle. The engine on/off is shown by the dark red and green lines.**

Source: Gas Technology Institute

Transient Control

Dynamic or transient operations are difficult to model and include in an engine design. Consequently, engine emissions are somewhat uncontrolled during these periods and account for >50 percent of the NOx emission. For engines with NOx emission certified to <0.02 g/bhp-hr, results indicate these NOx emission spikes will reach more than 90 percent of the total NOx emission. An addition to the ECM was included in order to smooth out some of the transient emission. Chassis testing investigation shows rapid engine speed (RPM) tip-in conditions (800 rpm to 2200 rpm) result in open loop conditions. Figure 22 shows a natural gas engine system real time NOx and engine speed transition during idle tip-in. A large spike occurs immediately

after the NOx spike tip in. The rate of change of engine speed (dRPM/dt) was over 1000 rpm/second. Limiting this engine speed rate change to 300 rpm/second should eliminate the open loop NOx spike.

Figure 22: Rapid Tip-in Response for a Natural Gas Vehicle Operating on a Chassis Dyno

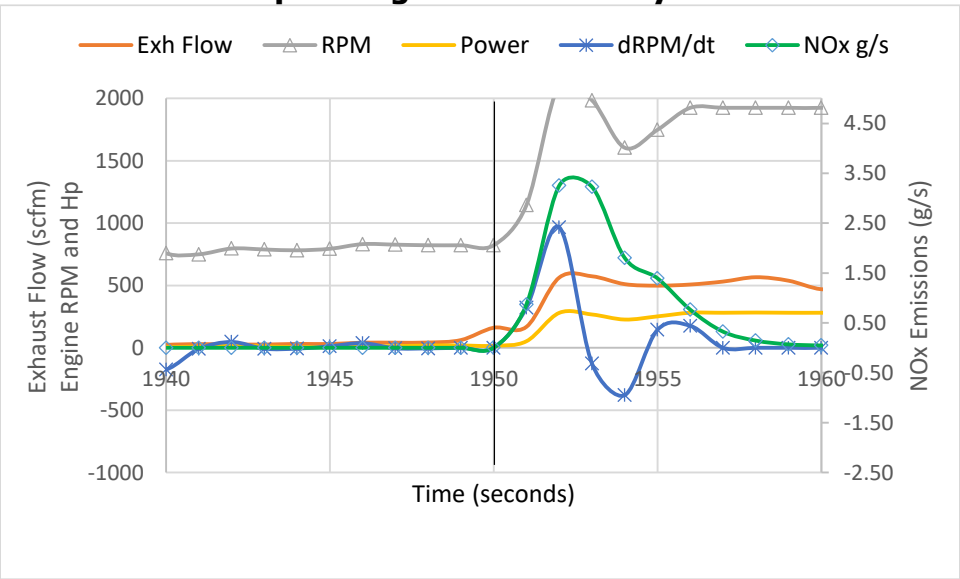

Source: Gas Technology Institute

Modeled Results

This section provides emission and fuel economy model results and a summary based on previous testing of ISL G 8.9 equipped natural gas vehicles and the recent testing of the ISL G near-zero 8.9 engine.

Emissions

Figure 23 shows a rapid engine transient model for the AFR controller. The results show that the AFR control is maintained within a 2-3 second tip-in throttle transient. The ability of the model to maintain AFR control within 2-3 seconds is consistent with results presented in earlier sections when fast engine speed tip-ins resulted in NOx spikes. Combining the proposed AFR model and limiting engine speed transients to 300 rpm/sec will minimize NOx emission. It is predicted NOx emission will be well below 0.02 g/bhp-hr and may be consistently below 0.010 g/bhp-hr during hot transient tests with hot restarts.

Cold start emission can be managed with rich AFR control (as will be evaluated) or by usage of an electrically heated pre-catalyst section. If the catalyst is pre-heated, the cold start NOx emission is designed to be less than 0.02 g/bhp-hr and will be lower than the recently introduced ISL G near-zero engine.

Figure 23: AFR Control Simulation with Rapid Tip-in Throttle Command

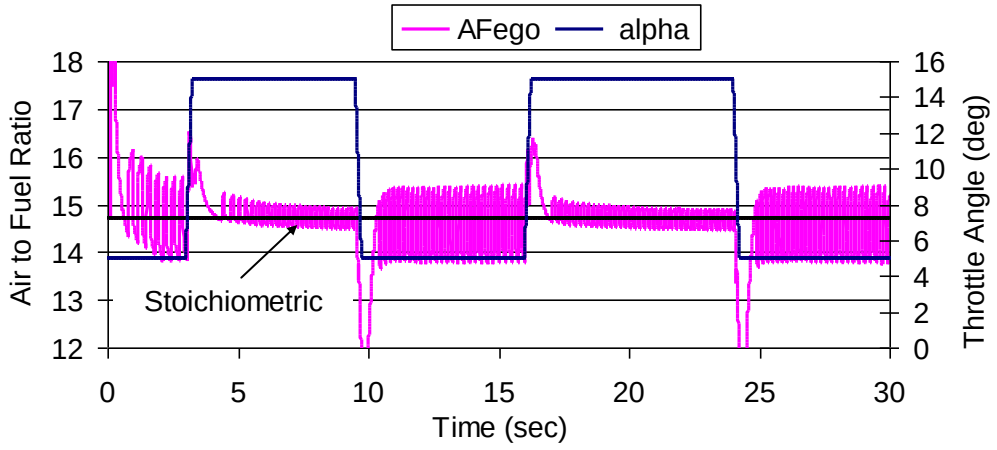

Source: Gas Technology Institute

Fuel Economy

Engine on/off control, energy recovery, and transient speed control are estimated to improve the bsCO2 from 550 g/bhp-hr to 412 g/bhp-hr (reduction of 25 percent). The benefit will be greatest for the more transient low duty cycle tests where the hybrid has a larger advantage over its conventional natural gas equivalent.

CHAPTER 3:
Component and Sub-System Requirements and Specifications

This section describes the component selection for the engine dynamometer testing. Additional component specifications needed to describe the fully integrated hybrid truck that was tested on a chassis dynamometer. This section is organized into five sections: 1) engine, 2) controller, 3) AFR model, 4) aftertreatment, and 5) sensor sections.

Natural Gas Engine

The natural gas engine section includes information on the engine, fuel system, catalyst and integrated systems for engine dyno testing.

Engine

The test engine for the engine dynamometer was a commercial CWI Model ISL G natural gas engine, certified to 2010 standards (Figure 24). The engine represents an FTP emission certification of 0.2 g/bhp-hr NOx and 0.01 g/bhp-hr PM. The lug curve used to load the engine on the dynamometer is provided in Figure 25. California pipeline fuel was used in this study as it meets Cummins specification methane number and is representative of natural gas available in California. The engine dynamometer laboratory is a fully controlled laboratory for intake air, fuel, coolant, and engine back pressure specifications as per CFR 1065.

Figure 24: 2007 ISL G Cummins Westport Inc. (CWI) Natural Gas Engine

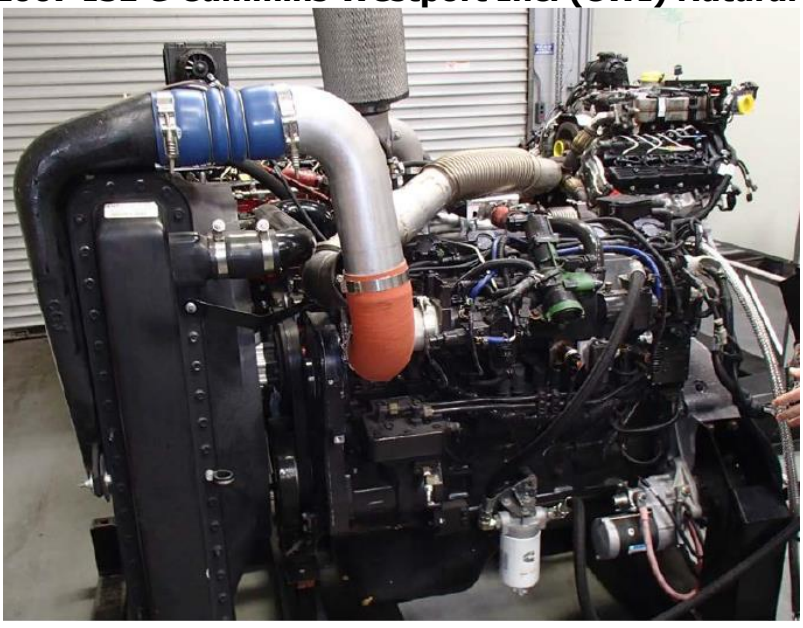

Source: Gas Technology Institute

Table 6: Summary of Selected Main Engine Specifications

fg.	Model	Year	Eng. Family	Rated Power (hp @ rpm)	Disp. (liters)	NOx Std g/bhp-h	PM Std. g/bhp-h
CWI	ISL-G	2009	7CEXH0540LBH	320 @ 2000	8.9	0.2	0.01

Source: Gas Technology Institute

Figure 25: Published ISLG 8.9 Natural Gas Engine Power Curve

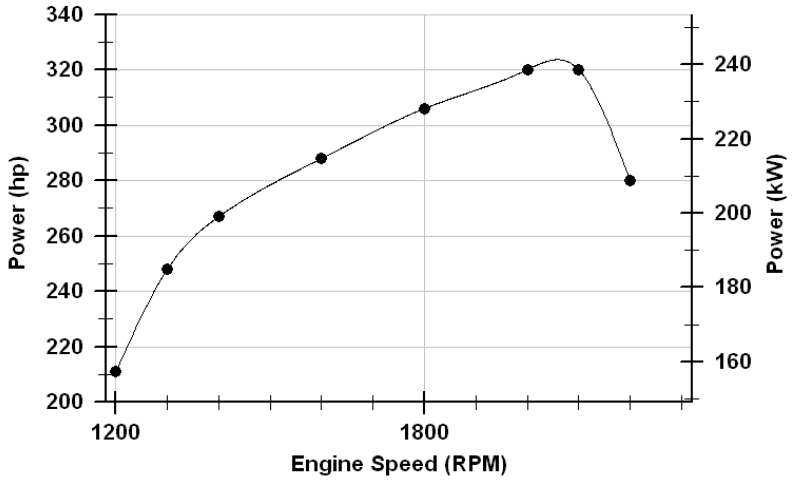

Source: Gas Technology Institute

Fuel System

The fuel system planned for the engine testing utilizes compressed natural gas (Figure 26). The fuel supply system is capable of providing enough fuel for a single day of testing. Local pipeline fuel was used for the engine and chassis testing.

Figure 26: Natural Gas Fuel System

Source: Gas Technology Institute

Engine Control System

The add-on engine control system focused primarily on AFR, catalyst warm up, and hybrid management. For the engine testing the focus of the effort will be on AFR and catalyst warm up control. This section describes the integration and specifications of the add-on engine controller

Description

The add-on controller selected for the project was a dSPACE microautobox system. A schematic showing a typical integration for AFR engine control is shown in Figure 27. The dSPACE controller is an add-on engine controller in parallel to the OEM-supplied ECM, thus, the signals still enter the OEM controller but the actual control was performed by the dSPACE system.

Internal to the dSPACE system is the Simulink model for AFR control (as discussed in Chapter 2) where the model-based controller and feedback models implemented for a closed loop feedback system.

Figure 27: dSPACE Schematic Layout

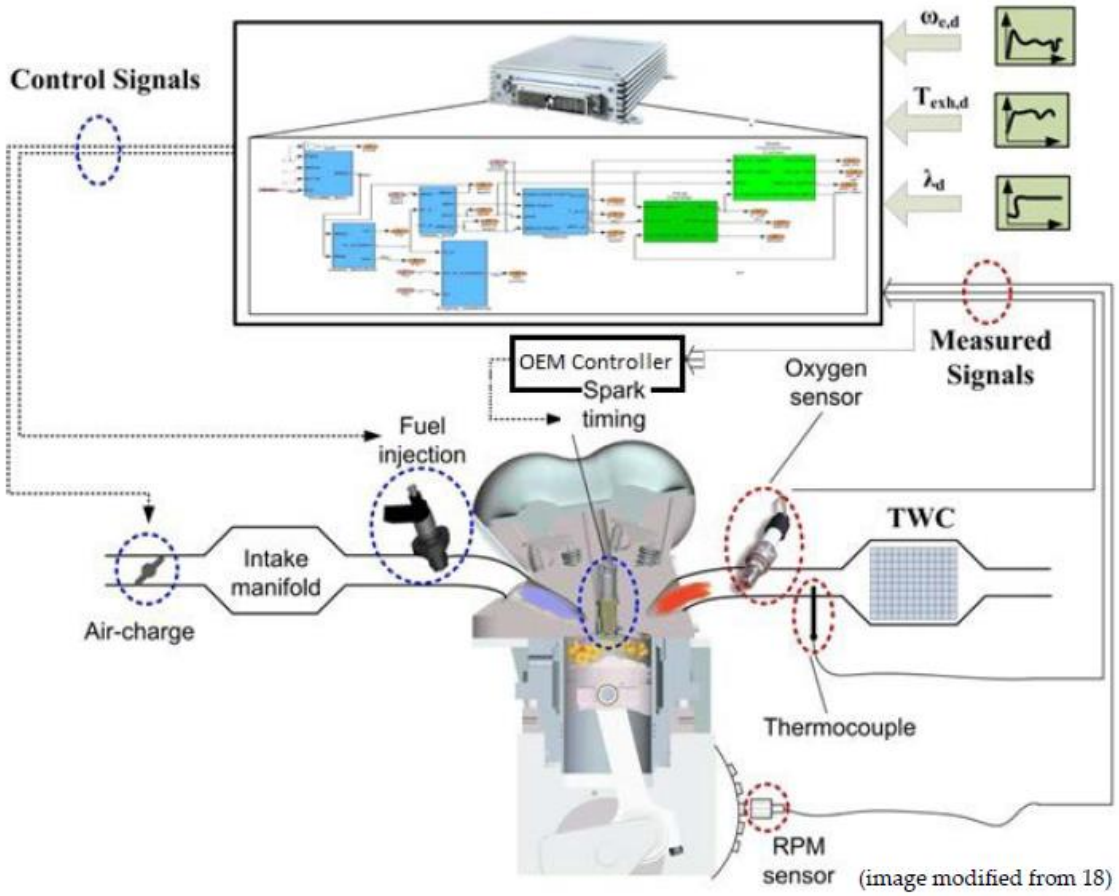

Source: Gas Technology Institute

Specifications

Following is a summary of the dSPACE part numbers and items selected for the embedded engine control system:

- ACE_MABXII ACE_MABXII_1512/1513 15,780.00: Advanced Control Education Kit MicroAutobox II consisting of MicroAutoBox with DS1401 PowerPC 750GL 900 MHz processor board, Ethernet I/O interface, Lemo/RJ45 ethernet cable, and DS1512 & DS1513 I/O board, CDP Control Development Software Package and Microtec C Cross Compiler with USB dongle, crimping tool
- RapidPro Power Unit stack version for an electronically connected RapidPro stack-system
- Crankshaft/Camshaft Sensor Input Module 9 DS1647 DS1647 Digital Out Module - 8 channels SC-DO8/2 (8ch digital out with push-pull functionality)
- Sensors: Lambda Module 11 DS1638 DS1638 8-channel thermocouple sensor input module 12 DS1664 DS1664
- Direct Injection Module - 2 channels 13 DS1662 DS1662_M 2 PS low side driver - 6 channels

Simulink AFR Model

The Simulink embedded control model integrated into the dSPACE management system was used to predict proper controlled fuel and air management prior to injecting the fuel. Fuel trim was performed with the oxygen lambda sensors integrated into the measurement system of dSPACE. The Simulink model performed the AFR control, catalyst warmup, and hybrid integration signal. For the engine dyno testing, the hybrid integration signal was inactive, as there is no way to integrate energy recovery during engine testing.

Air Flow Model

The intake manifold block consists of three sub blocks: air dynamics, fuel dynamics, and EGR dynamics (Figure 28). The air dynamics calculates the port airflow, which includes manifold filling dynamics, experimentally determined volumetric efficiency, and air density corrections. The EGR flow rate is subtracted from the port flow rate. The fuel dynamics include start of injection delays and fuel film fractions χ and γ (see fuel sub model for explanation of film factors).

Figure 28: Intake Manifold Simulink Dynamic Block

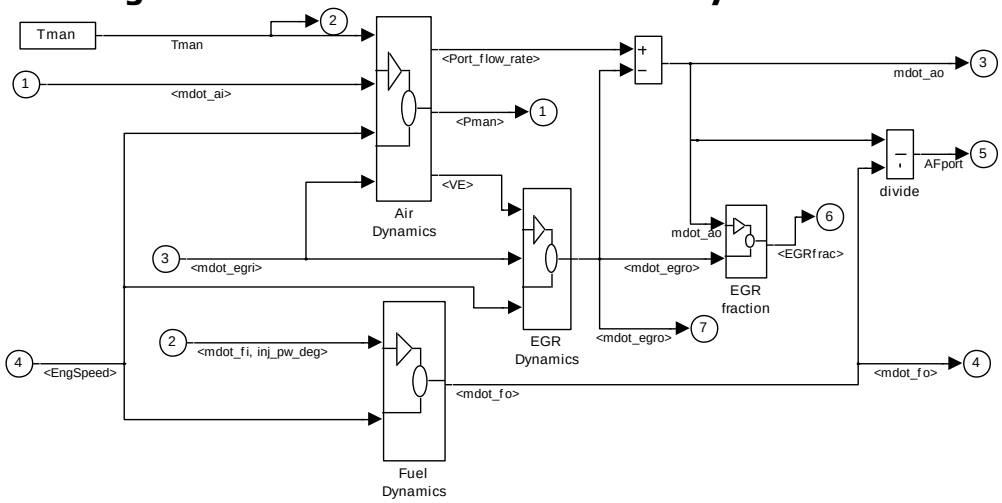

Source: Gas Technology Institute

The engine block has three sub blocks: torque production, intake to exhaust delay, and manifold pressure as shown in Figure 29. The torque production includes pumping friction, cylinder air charge, air fuel influence, intake valve close to spark torque delay, spark influence, and spark to torque delay. Each of these blocks are experimentally determined and used to estimate torque production as a function of dynamic engine conditions. The intake to exhaust delay is a time varying delay that is a function of engine speed and airflow into the port. The exhaust pressure is a delay block based on the time varying engine speed and port pressure. These blocks are used to estimate conditions at the exhaust manifold.

Figure 29: Engine Block and the Three Sub-Systems

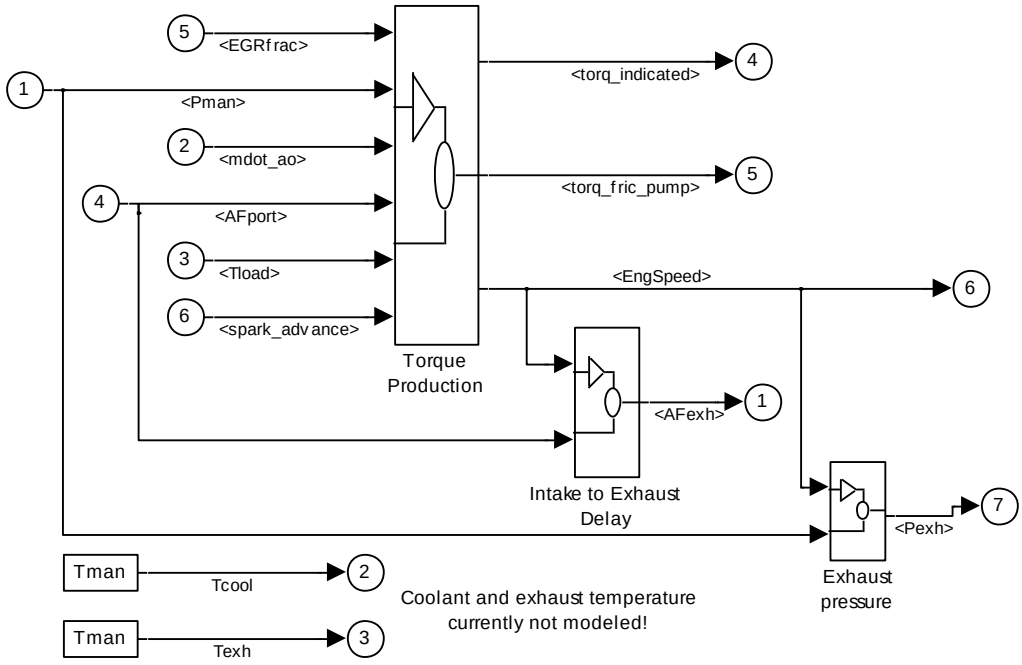

Source: Gas Technology Institute

The exhaust manifold block (Figure 30) contains the time varying delays in the AFR at the EGO sensor. The AFR delay is a function of engine speed exhaust airflow and EGO sensor dynamics.

Figure 30: Exhaust Manifold Block and its Sub Systems.

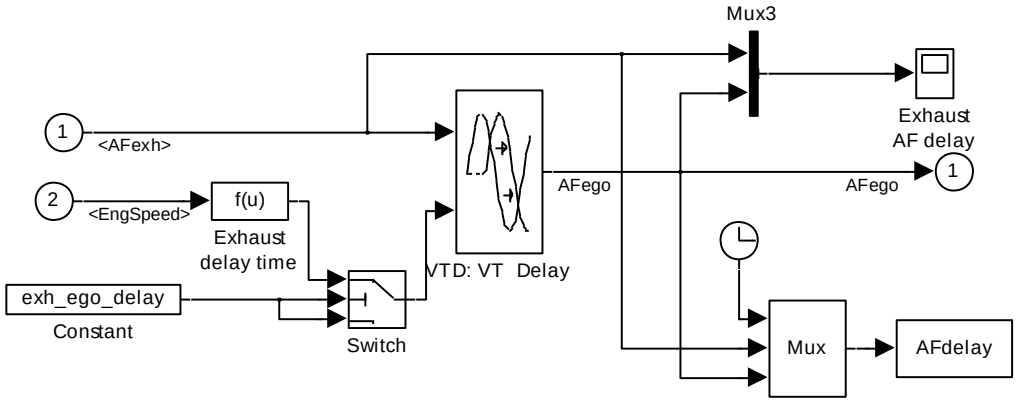

Source: Gas Technology Institute

The next main block at the top of the model is the sensor block. The sensor block is where each sensor's dynamics can be modeled. For example, the first order time lags for the EGO sensor, binary switching behavior of the EGO sensor, and air mass sensor response time to the rate of change in airflow into the intake manifold (Figure 31).

Figure 31: EGO Simple First Order Lag Dynamics and Simple Relay Output Signals

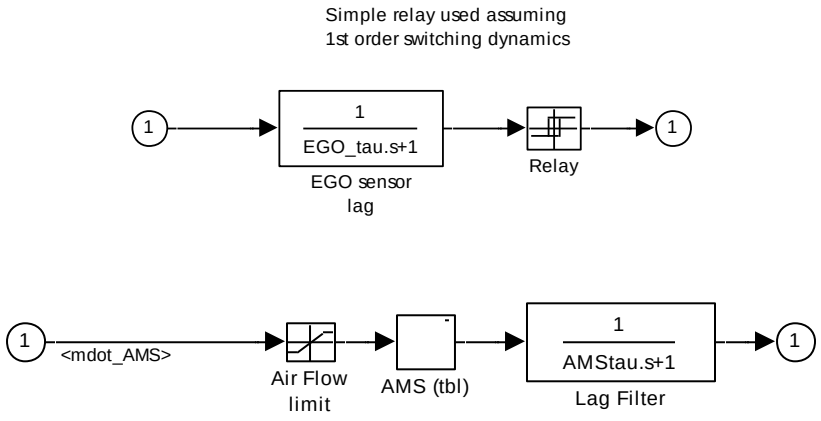

Source: Gas Technology Institute

PID Feedback Model

The controller block simulates the signal conditioning, control algorithms, and output signal conditioning (Figure 32). Signal conditioning includes A/D conversion noise and saturation. The control algorithm has airflow and fuel flow estimator and includes EGR, IAC, and Spark Advance output information. The airflow estimator is based on the speed density approach and is only used in this project as a comparison to the MAF sensor. The fuel flow block simulates the fuel compensation lag and the desired commanded fuel based on PID output information from the EGO signal (Figure 33). The fuel flow block is where the sliding mode controller will be realized (see Section 3.1 for development and implementation of sliding mode control).

Figure 32: Controller Simulink Block Showing Conditioning and Algorithms

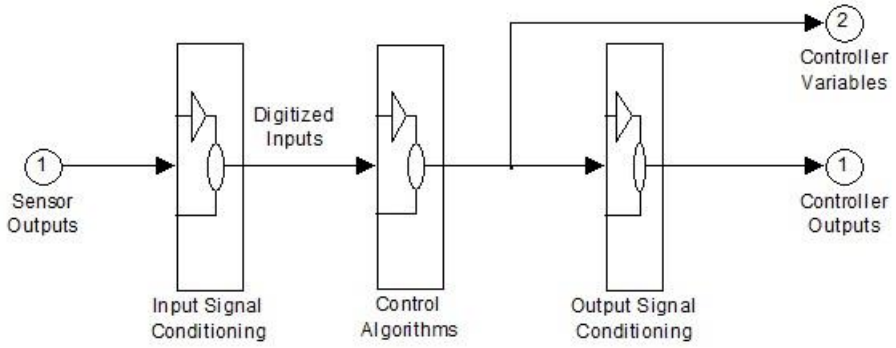

Source: Gas Technology Institute

Figure 33: Controller Fuel Subsystem Block Showing the PID Controller

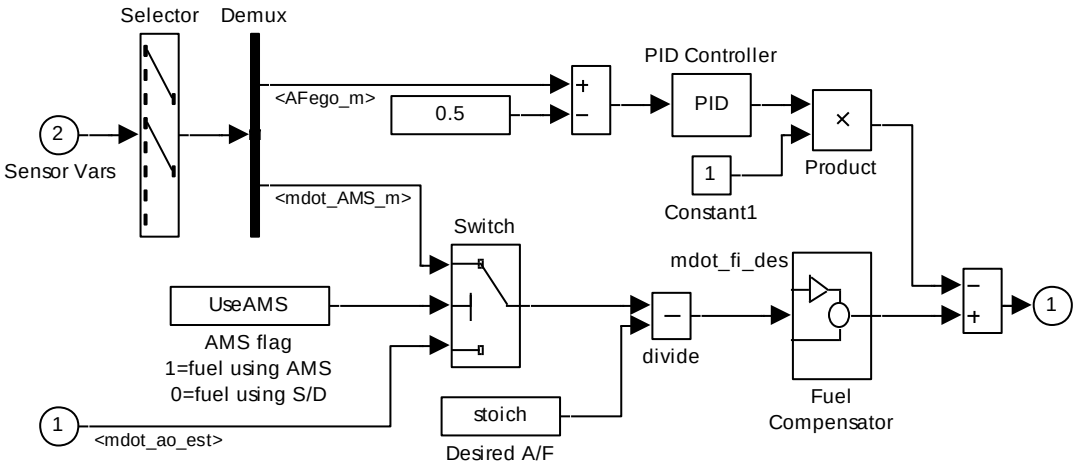

Source: Gas Technology Institute

Aftertreatment System

The exhaust aftertreatment system, as originally planned, included two components: 1) the electrically heated pre-catalyst section and 2) the three way catalyst. In order to minimize recertification costs, the electrically heated pre-catalyst was evaluated for its benefit to cost ratio.

Electrically Heated Pre-Catalyst

In general, the electrical TWC heater design is focused on heating for idle conditions. The heater will heat 30 scfm of exhaust from 20°C to approximately 300°C during cold start conditions and other times when the exhaust has cooled below the set point. The following discussion provides details for the other systems and how they will integrate with this design (Figure 34).

Figure 34: Exhaust Heating Section From Watlow

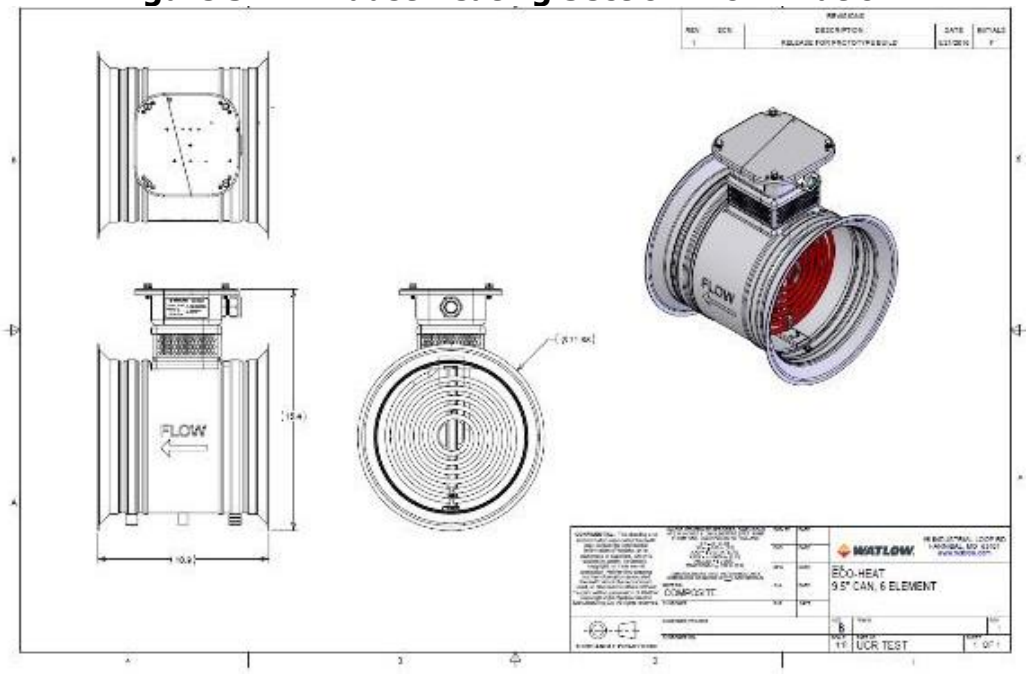

Source: Gas Technology Institute

Cold Start

Because cold-start generates >85 percent of the NOx emission during a typical driving schedule, UCR suggested operating with a rich AFR and adding a catalyst heater for approximately 100 seconds to pre-heat the TWC at idle conditions. During cold- and warm-start, the vehicle will be powered by batteries until the TWC design temperature is reached. Once the TWC has reached the design operating temperature, the electric heaters will be turned off and the natural gas engine will power the drive and breaking mechanisms and the electrical system.

During cold start operation the engine fueling is operated slightly rich to minimize cold start NOx. As the TWC heats, the AFR control is adjusted continuously to minimize THC emission in parallel with controlling NOx emission. Engine dyno testing identified actual settings with TWC temperature monitors and air-to-fuel ratio measurements. At an exhaust flow of 30 scfm during idle, electrical heating may be useful, although the commercial near-zero trucks seem to be hitting the targets without a pre-heater.

Hot Restart

To optimize the range of the vehicle, engine shut down is planned where TWC temperature management is needed for engine restart. Engine restart designs include an option to restart the engine with the electrical heater and disconnect the heater once a minimum temperature is obtained in the TWC. The minimum temperature would have been be determined during analysis of engine and chassis testing. It is expected that the rate of engine heating and cooling would include electrical heating at an exhaust flow of 30 scfm during idle.

Three Way Catalyst System

The TWC catalyst is representative of that used commercially in the near-zero 8.9L engine in order to achieve the NOx control as reviewed earlier (Figure 35). However, the overall TWC system was upgraded by changing the pre and post catalyst lambda sensors in order to better control the AFR. Furthermore, the exhaust and TWC will be wrapped with insulation for additional thermal management and rapid light off during cold start/hot re-start conditions. A feedback thermocouple will be installed near the catalyst bed for AFR cold start feedback control.

Figure 35: Catalyst Aftertreatment System

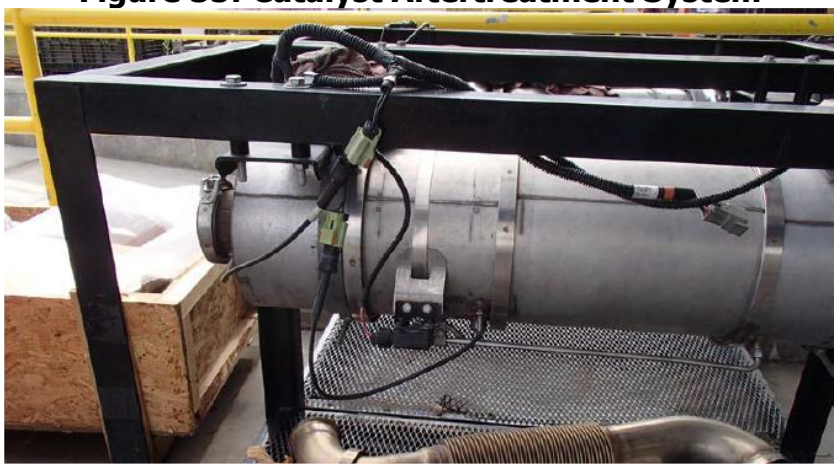

Source: Gas Technology Institute

AFR Feedback Sensors

The initial plan was to use wide band oxygen (AFR lambda) feedback sensors with the new model-based control system. As it turns out, advanced switching sensors were designed, but a fixed AFR performed better. Improved switching O2 sensors were installed in a similar location as with the technology used with passenger cars and light trucks: two sensors were used; one before and the other after the TWC (Figure 36). This pair of sensors allows one to determine if the oxygen storage capacity (OSC) for the catalyst is meeting design. Otherwise, a malfunction light will illuminate. The part numbers were discussed previously in the Engine Control Section and described here in detail as sensors are a critical element to the AFR control system.

The oxygen sensor continually detects the oxygen content in the exhaust gas, both before and after the catalyst. A switching heated oxygen sensor measures the transition between a targeted AFR and controls to that point by dithering around this AFR for precise, but fixed control.

In addition to the traditional measurement approach discussed in the next section, UCR also used a high speed advanced 100 Hz high speed NOx/O2 real time prototype measurement system provided by NTK Sparkplugs. This system resulted in similar NOx information as with the MEL and is discussed during the engine testing.

Figure 36: Upgraded AFR Feedback Sensors

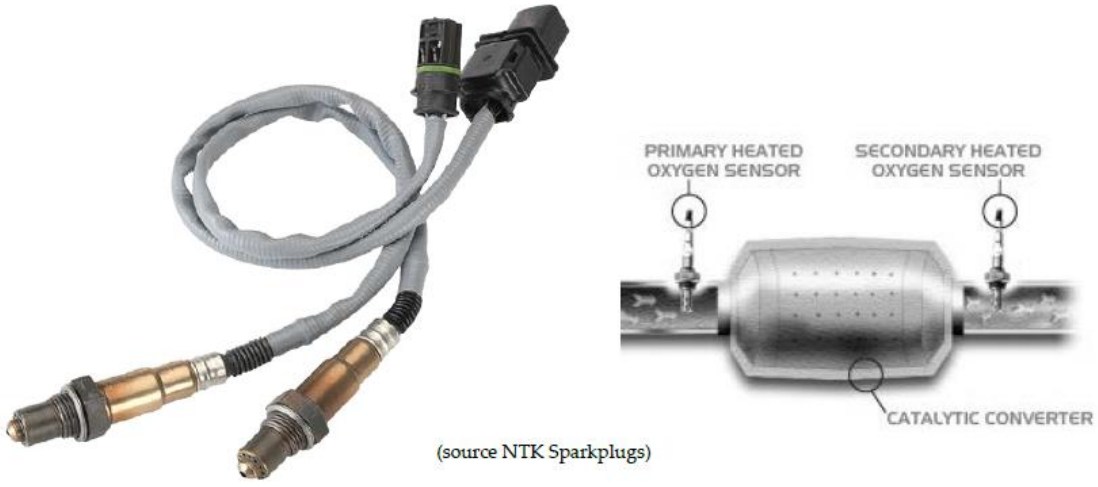

Source: NTK Sparkplugs

CHAPTER 4:
Component and Sub-System Specification

This section provides an overview of and depicts the major components and sub-systems designed and integrated into the vehicle by US Hybrid (USH).

US Hybrid's integration of engine components included a Cummins ISL-G coupled with an auto clutch, a 240 kW electric motor, 80 kWh battery storage, and finally an automatic transmission. USH has provided system definitions for the lithium ion battery, controller, charger, and associated battery management system. USH has sourced several electrical auxiliaries; a 300 Amp DC-DC converter, direct drive power steering, direct drive air conditioning, and an air compressor. The electrification of these auxiliary components will provide 100 percent redundancy.

The Plug-in Hybrid Electric LNG Truck (PHET) keeps the original Cummins ISL-G engine and Allison Transmission, but adds a drive motor/generator in-line between the engine and transmission with Auto Clutch and, all electric air, hydraulic and HVAC system with 12V and 24V batteries, DC-DC converter powering the auxiliary systems, and a high voltage Lithium-ion battery.

The existing Cummins ISL-G engine runs on LNG and remains in the vehicle to provide propulsion when needed. A 240kW electric motor was installed between the engine and the existing Allison automatic transmission. An electronically controlled pneumatic-driven clutch allows the electric motor to be decoupled from the engine, and permits electric-only operation. All electric auxiliary systems, power steering, air compressor, and air conditioning, were installed in parallel with the engine driven systems. In this context, "parallel" indicates that auxiliary systems were installed at the same time as other engine driven systems. It may also indicate that they can operate while in traditional, LNG-only mode or in electric-only mode. This gives the vehicle all the capabilities of the original when in electric only mode.

Two major enclosures have been added to the vehicle to permit electric and hybrid operation. The behind the cab enclosure houses the air compressor, the 12V batteries, and an additional twelve fuses and relays. The passenger side enclosure houses the battery, high voltage distribution, drive motor inverters, DC/DC converters, auxiliary motor drive, and the battery charger. They have all been integrated into one unit with two distinct sections that separate the battery and high voltage distribution from the rest of the electronics.

An additional coolant system has been added to support the cooling of the electronics and the drive motor. A radiator and two pumps have been added to the middle section of the vehicle, just behind the fifth wheel connection. One coolant pump circulates water to the drive motor, while a second coolant pump circulates water to the electronics, such as the two drive inverters, the DC-DC converter, the auxiliary motor inverter, and the battery charger. To control and monitor the hybrid drive system and execute the user's commands, a CAN data bus interconnects all the electronic equipment and displays the status on a dash mounted LCD user display touch screen. Three LED lights (Green, Red, Amber) on the dash are also used to indicate vehicle status during hybrid mode and charge mode.

Transitioning between pure electric mode and hybrid mode is an automated transparent function that is controlled by the vehicle control unit and requires no input from the driver. The vehicle Hybrid Controller Unit (HCU) can sense when there is a heavy load on the vehicle and will automatically start the LNG engine to accommodate. The engine may also turn on if the high voltage battery has reached its minimum charge level and needs to be recharged by the drive motor acting as a generator. The vehicle is equipped with an onboard charger that allows it to be plugged in when not in service, providing a full battery at the beginning of every shift.

The use of an air-actuated clutch between the engine and electric motor allowed for the different modes. Timing of actuation was key so that the engine would not be choked if already on, or inadvertently cranked when transitioning to hybrid mode. The electric motor was controlled to simulate its operation as an engine (idle control), since it is connected to the input of the transmission. Properly balancing the torque request (performance) from the driver and sustaining the battery state of charge (battery life and fuel economy) required a lot of testing. It was first evaluated at US Hybrid facility, then tuned further and validated during the chassis dynamometer testing.

Drivetrain, Motors, and Controllers

System Description

The electric traction motor shown in Figure 37 was placed in-line with the engine and transmission. In battery mode, the engine is shut off, and the motor drives the truck (Figure 38). While operating in hybrid mode, the motor assists the engine to enhance its torque and power and increase fuel economy. The controllers also reduce transient emission

Figure 37: Motors and Controllers

Source: Gas Technology Institute

Figure 38: Drivetrain

Source: Gas Technology Institute

Dual Traction Motor Specification, Design and Integration:

The overall development of the traction motor, located in the drivetrain, was refocused when a detailed engineering review was performed. Market use survey information and drive cycle studies showed the need for a higher continuous power rating and increased torque at lower speed. For US Hybrid to meet these requirements, a dual motor system with integrated clutches was implemented (Figure 39).

Detailed engineering, design, serviceability review, integration review and cost review were completed for the individual motors, shafts, engine side clutch spline interface, connecting adapter plates, flywheel housing, clutch housing, clutch/flywheel interface, motor spline interface, and clutch pull reaction bearing. The cable routing, protection and connection to the inverters were established. The cooling line connection and routing was integrated.

Figure 39: 240 kW Dual Motor System

a) Power Interfaces b) Cooling Loop inlets/outlets c) rotor d) dual motor sections e) clutch and f) ring adapter attachment location

Source: Gas Technology Institute

The clutch housing connecting the dual motor system to the engine was integrated. The clutch size and specification were generated. All parameters and components of the clutch, clutch actuation, and flywheel for the transmission connection were also integrated (Figure 40).

Figure 40: System Design

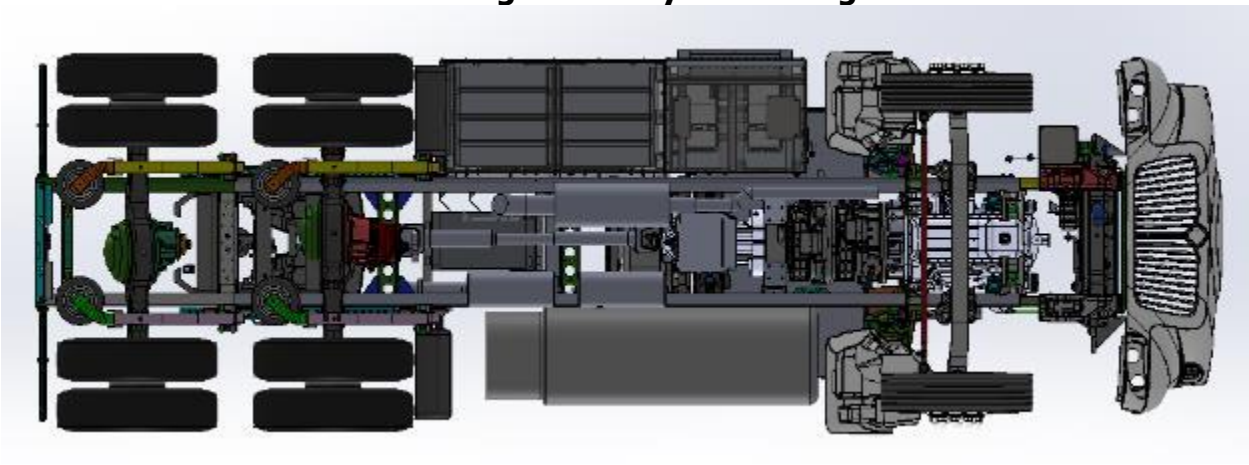

Source: Gas Technology Institute

The energy storage system in Figure 41 is an 80 kWh lithium ion battery with a safety disconnect and fusing protection system.

Figure 41: Energy Storage System

Source: Gas Technology Institute

US Hybrid engineers designed the packaging of A123 Modules and battery management systems (BMS) into a custom-designed battery enclosure (Figure 42). Battery pack capacity is 80kWh with a maximum power capability of 240 kW.

Figure 42: Battery, Controller, Charger and Auxiliary Drive Housing

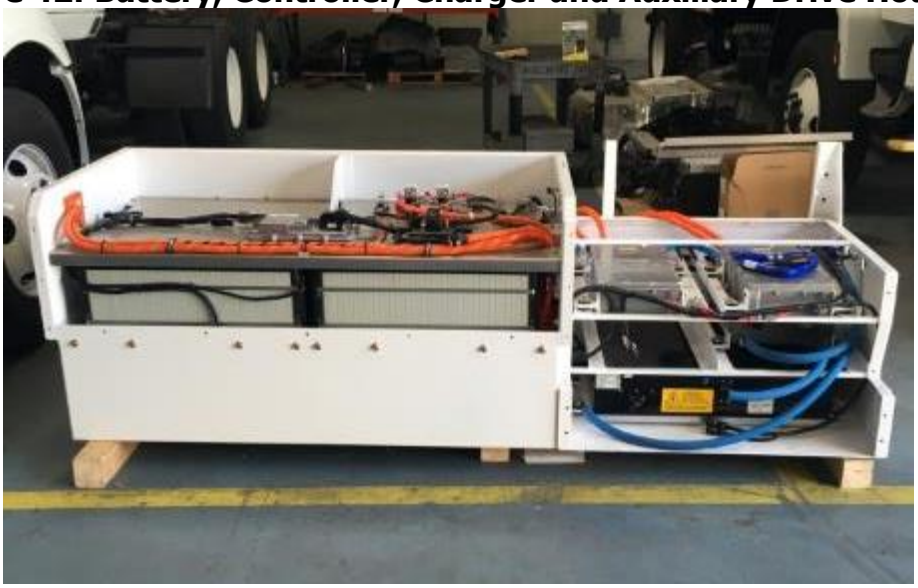

Source: Gas Technology Institute

The wiring harness shown in Figure 43 is composed of the high voltage electric traction and battery system wiring. The control wiring system includes the driver interface and control signals.

Figure 43: Power/ HV Cables and Wiring Harness

Source: Gas Technology Institute

The power steering in Figure 44 and Figure 45 is an electro-hydraulic system that allows full assisted steering during battery operation. During Hybrid operation, the steering is provided by the engine-driven hydraulic system. The transition between the two is invisible to the driver.

Figure 44: Electro-Hydraulic Pump

Source: Gas Technology Institute

Figure 45: Electro-Hydraulic Pump

Source: Gas Technology Institute

The A/C compressor (Figure 46) provides the electric driven air conditioning system during battery electric operation.

Figure 46: A/C Compressor

Source: Gas Technology Institute

The air compressor shown in Figure 47 is an electric driven compressor system powering the vehicle air system (Figure 48) during battery operation. During hybrid operation, the air system is provided by the engine-driven air compressor. The transition between the two is invisible to the driver.

Figure 47: Air Compressor

Source: Gas Technology Institute

Figure 48: Truck Air System

Source: Gas Technology Institute

Vehicle charging is provided by an on board 20 kW hi-frequency galvanically-isolated unity power factor and high efficiency charger system as shown in Figure 49. The battery energy management and the vehicle control manage the charging system. The charger is compatible with the electric vehicle supply equipment (EVSE) charging infrastructure and interface protocol at the Total Transportation Services, Inc. (TTSI) facility.

Figure 49: Charger

Source: Gas Technology Institute

Figure 50: Charging Port

Source: Gas Technology Institute

Vehicle Description

Legends for Figure 51 and Figure 52:

- RED: Electric Drive Motor and Transmission
- ORANGE: High Voltage Power Electronics
- BLUE: High Voltage Battery
- GREEN: Electric Auxiliary Systems

Figure 51: System Configuration (Side View)

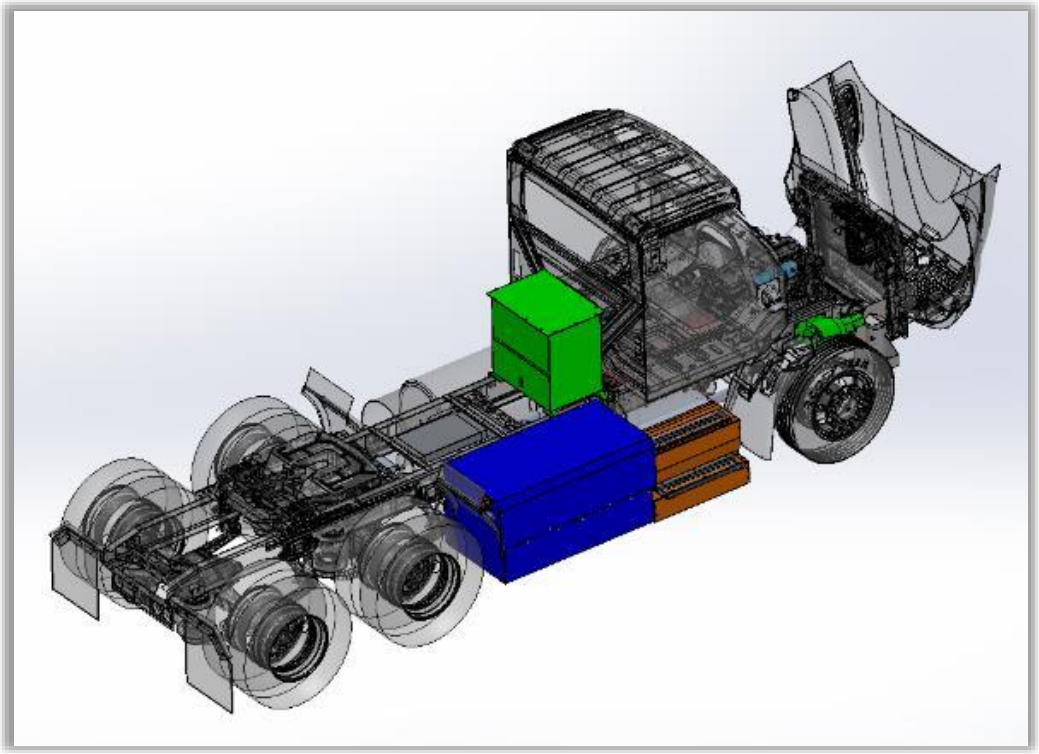

Source: Gas Technology Institute

Figure 52: System Configuration (Top View)

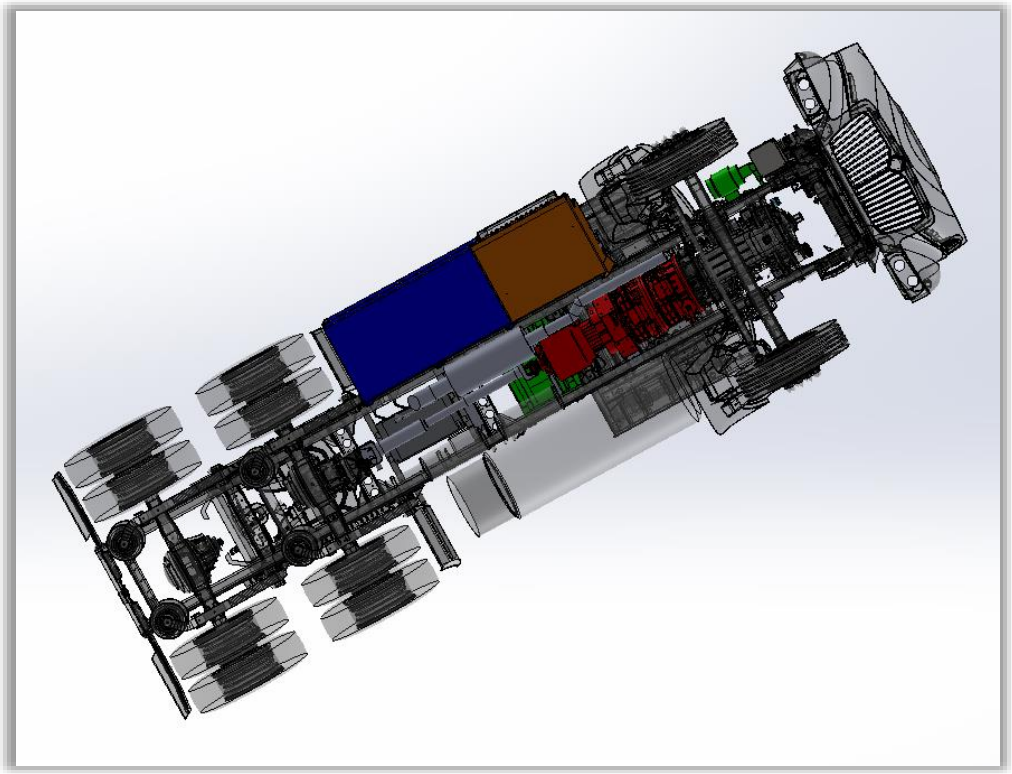

Source: Gas Technology Institute

CHAPTER 5:
Component Test Data and Emission and Performance Benefits

Approach

This section describes the methods for testing the integrated components and emission measurements on engine and chassis dynamometers. It also describes the test cycles for the evaluation of the demonstration project. A significant project effort was needed to prepare for the first ever measurements of a near-zero natural gas engine with NOx emission near ambient levels. As no solution existed for this challenge, the project had to explore several approaches to be able to measure the emission from the near-zero engine.

Engine Dynamometer Laboratory

Engine dynamometer laboratories are expensive and complex facilities but provide data of high accuracy and precision since the engine operation is tightly controlled while following prescribed drive cycles. The dynamometer test laboratory used in this project has five major systems: a 600 horsepower (hp) General Electric DC electric engine dynamometer (Figure 53), a fuel handling system, an air conditioning system to adjust temperature and humidity of the intake air, a cooling water system with a radiator to handle reject heat, an electric system to either add or carry power away from the dyno, and finally, a computer control module to enable the system to run following selected operating cycles. The dynamometer is capable of performing either transient cycles, such as the certification federal test procedure (FTP), or steady state cycles as needed. Temperature and humidity are controlled to specifications in 40 CFR Part 1065 in order to qualify an engine's emission results.

Figure 53: UCR's Heavy Duty Engine Eddy Current Transient Dynamometer

Source: Gas Technology Institute

Installation of an engine onto a dynamometer is a rigorous sequence of events starting with fork lifting the engine into the dyno laboratory (Figure 54 - Left) and following with making strong and properly balanced customized mounts for the engine frame support structure (Figure 54 - Right). Once the engine was installed, the final connections were made to the natural gas fuel tank, TWC system, fuel lines, charger are support, cooling fluids, intake air conditioning system, and many other electrical and sensor related details (Figure 55).

Figure 54: Fork Lifting Engine into Test Cell and Installing Customized Mounts

Source: Gas Technology Institute

Figure 55: Engine Setup with Connections to Laboratory Services and Aftertreatment

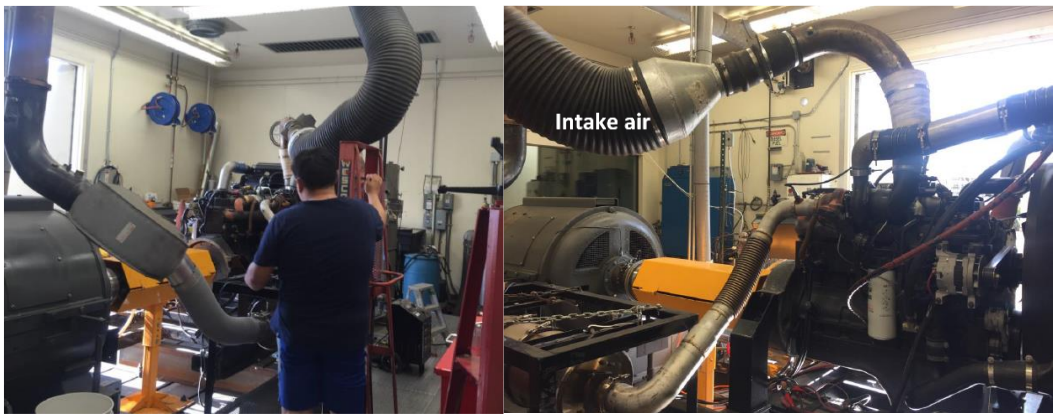

Source: Gas Technology Institute

Dilute Measurements

The near-zero NOx level of 0.02 g/bhp-hr presents significant measurement problems as the levels of NOx in the dilution tunnel are approaching detection limits following the traditional dilute CVS federal reference method. This section discusses the traditional and inventive methods that were employed in order to measure NOx for the near-zero engine. This section also provides the new calculations and measurements needed (ie. trace analyzers and exhaust flow) and a comparison between the traditional and proposed new methods for near-zero testing. In addition to the traditional methods, UCR added a second raw measurement using a tailpipe sensing system developed by NTK Sparkplugs with details in the next section. This section discussions some upgraded steps that were essential in order to make near-zero NOx measurements.

Traditional Measurement Methods

Normally UCR measures emission from an engine by connecting the engine exhaust to UCR's heavy-duty mobile emission lab (MEL). The details for sampling and measurement methods of mass emission rates from heavy-duty diesel engines are specified in Code of Federal Regulations (CFR): Protection of the Environment, Section 40, Part 1065. UCR's unique heavy-duty diesel mobile emission laboratory (MEL) is designed and operated to meet those stringent specifications. MEL is a complex laboratory and a schematic of the major operating subsystems for MEL are shown in Figure 58. The accuracy of MEL's measurements was checked/verified against ARB's and Southwest Research Institute's heavy-duty diesel laboratories (9, 10, 11, 12, and 13). MEL routinely measures Total Hydrocarbons (THC), Methane, Carbon Monoxide, Carbon Dioxide, Nitrogen Oxides, and Particulate Matter (PM) emission from diesel engines. In addition to measuring regulated emission, the laboratory can add special instruments to measure: particle size distribution (PSD) with TSI's Engine Exhaust Particle Sizer 3090 (EEPS), particle number (PN) with a TSI 3776 condensation particle counter (CPC), soot PM mass with AVL's Micro Soot Sensors (MSS 483), NH3 emission with an integrated real-time tunable diode laser (TDL), and batched low level nitrogen dioxide (NO2) emission with a Fourier Transform Infrared Spectrometer (FTIR). Samples can be collected for off-line analyses such as hydrocarbon speciation, carbonyl emission, polynuclear aromatic hydrocarbons, etc. The complete design capabilities of MEL for measuring regulated and non-regulated emission are described in Cocker et al (8).

Traditionally NOx concentration in the exhaust is measured with a heated chemiluminescent detector (HCLD) that is setup to sample continuously from the Constant Volume Dilution System (CVS) during engine operation. The NOx analyzer is also set up to sample and measure ambient and dilute bag concentrations following automated routines of the MEL laboratory. The samples collected from the CVS dilute tunnel are passed through an acid-treated filter to prevent measurement interferences from ammonia (NH3) concentrations. The acid-treated filters are replaced daily.

Figure 56: Major Systems Within UCR's Mobile Emission Lab (MEL)

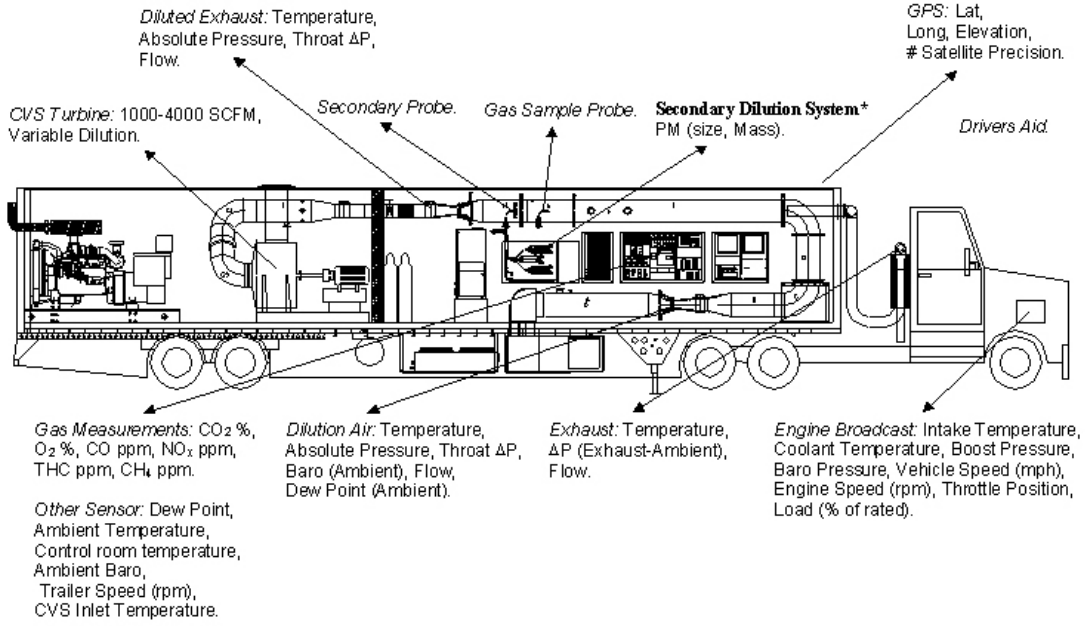

Source: Gas Technology Institute

NOx Measurement Solutions for the Near-Zero Engine

Three new approaches were considered for measuring near-zero NOx emission. These included 1) real-time raw sampling and exhaust flow measurements, 2) real-time ambient second by second corrections, and 3) advanced trace type analyzer bag measurements. The new measurement methods required instrumentation upgrades which are discussed below.

Raw NOx Measurements

The raw NOx measurements utilized a fast responding analog 300 HCLD CAI analyzer that sampled raw exhaust through a low volume heated filer and heated sample line. The low volume design improved the response time of the analyzer with the exhaust flow measurement. The heated filter was acid treated to minimize NH3 interference with the NOx measurement. A real-time, high-speed exhaust flow meter (100 Hz model EFM-HS Sensors Inc) was used to align NOx concentration with real time exhaust flow measurements. The EFM-HS was correlated with UCR dual CVS system prior to testing to improve the accuracy between the raw and dilute CVS methods and eliminate exhaust flow biases from propagating through the comparison.

Trace Level NOx Analyzer

An ambient/trace level chemiluminescence NO-NO2-NOx analyzer Modal 42C Thermo Environmental Instrument Inc (TECO) was used for the real-time ambient measurements and the low concentrations of NOx in the sampling bag. This analyzer was calibrated and integrated specially for this ultra-low NOx project. The span on the instrument was set to 600 ppb and showed a signal to noise ratio about an order in magnitude lower than the traditional (600 HCLD) analyzer. The signal averaging was reduced from 30 seconds to 1 second and showed a T10-90 and a T90-10 just over 10 seconds (slightly higher than the specifications of 40 CFR Part 1065). The slightly slower time constant should not impact the gradual transients expected during real-time ambient measurements or bag concentrations. Although the trace TECO analyzer falls short of the requirements of 1065, it would provide an accurate and

improved assessment of NOx emission below 1 ppm as compared with the nominal 1065 instruments.

Calculation Upgrades

The calculation approaches for the traditional and improved methods are presented in Table 7. While the improved measurement method uses calculation methods that comply with 40 CFR Part 1065, this section outlines the observation differences without the details of working in molar flow rates as per 40 CFR Part 1065.

Table 7: NOx Measurement Methods-Traditional and Upgraded

Type	Analyzer	Meth. ID	Description
Traditional	600 HCLD dil 600 HCLD amb	M1	Modal NOx with ambient bag correction
Traditional	600 HCLD dil 600 HCLD amb	M2	Dilute bag NOx with ambient bag correction
Upgrade	300 HCLD raw	M3	Raw NOx no ambient bag correction
Upgrade	600 HCLD dil TECO amb	M4	Modal dilute NOx with ambient real time correction
Upgrade	TECO dil TECO amb	M5	Trace analyzer dilute bag with trace ambient bag correction

Source: Gas Technology Institute

Traditional Methods:

The traditional NOx measurement methods are described in the next two equations. The first equation is the real-time modal measurement corrected for the ambient bag concentration and real time dilution factor, Method 1 (M1). The second traditional equation (M2) is based on dilute bag and ambient bag concentrations and an integrated dilution factor over the cycle.

$$NO_{x\_m1} = \sum_{i=1}^{n} (Q_{cvs_i} * \Delta t_{\_i}) * \rho_{NO_x} * \left(C_{m\_i} - C_a * \left(1 - \frac{1}{DF_i} \right) \right)$$

Where:

$NOx_{\_m1}$	the Method 1 NOx measurement method (g/cycle)
Q_{cvs_i}	is the instantaneous CVS flow
ρ_{NOx}	is the density of NOx from 40 CFR Part 1065
C_{m_i}	is the instantaneous NOx concentration measured with the dilute NOx 600 HCLD CAI analyzer
C_a	is the ambient bag NOx concentration measured by the 600 HCLD CAI analyzer
DF_i	instantaneous dilution factor

$$NO_{x\_m2} = (Q_{cvs\_ave} * \Delta t) * \rho_{NO_x} * \left(C_d - C_a * \left(1 - \frac{1}{DF_{\_ave}} \right) \right)$$

Where:

$NOx_{\_m2}$	the Method 2 NOx measurement method (g/cycle)
Q_{cvs_ave}	is the average CVS flow
ρ_{NOx}	is the density of NOx from 40 CFR Part 1065
C_d	is the dilute bag NOx concentration measured with the dilute NOx 600 HCLD CAI analyzer
C_a	is the ambient bag NOx concentration measured by the 600 HCLD CAI analyzer
DF_{ave}	average dilution factor

Upgraded Methods

The upgraded NOx measurement methods are presented in the next three equations. These upgrades included new analyzers, sample lines, sample filters, and exhaust flow measurement systems. For Method 3 (M3) there is no ambient correction. For Method 4 (M4) the real time dilute NOx is corrected for ambient real time NOx on a second by second basis. For Method 5 (M5) the trace NOx analyzer is used to measure the dilute bag and ambient bags (similar to Method 2).

$$NO_{x\_m3} = \sum_{i=1}^{n} (Q_{exh_i} * \Delta t_{\_i}) * \rho_{NO_x} * (C_{m\_i})$$

Where:

$NOx_{\_m3}$	the Method 3 NOx measurement method (g/cycle)
Q_{exh_i}	is the instantaneous exhaust flow measured in the tail pipe
ρ_{NOx}	is the density of NOx from 40 CFR Part 1065
C_{m_i}	is the dilute bag NOx concentration measured with the dilute NOx 300 HCLD CAI analyzer

$$NO_{x\_m4} = \sum_{i=1}^{n} (Q_{cvs_i} * \Delta t_{\_i}) * \rho_{NO_x} * \left(C_{m\_i} - C_{a\_adv\_i} * \left(1 - \frac{1}{DF_i}\right)\right)$$

Where:

$NOx_{\_m4}$	the Method 4 NOx measurement method (g/cycle)
Q_{cvs_i}	is the instantaneous CVS flow
ρ_{NOx}	is the density of NOx from 40 CFR Part 1065
C_{m_i}	is the dilute bag NOx concentration measured with the dilute NOx 600 HCLD CAI analyzer
C_{a_adv}	is the trace ambient bag NOx concentration measured by the TECO trace NOx analyzer
DF_i	instantaneous dilution factor

$$NO_{x\_m5} = (Q_{cvs\_ave} * \Delta t) * \rho_{NO_x} * \left(C_{d\_adv} - C_{a\_adv} * \left(1 - \frac{1}{DF_{\_ave}}\right)\right)$$

Where:

$NOx_{\_m5}$	the Method 5 NOx measurement method (g/cycle)
Q_{cvs_ave}	is the average CVS flow
ρ_{NOx}	is the density of NOx from 40 CFR Part 1065

C_{d_adv} is the dilute bag NOx concentration measured by the TECO trace NOx analyzer

C_{a_adv} is the ambient bag NOx concentration measured by the TECO trace NOx analyzer

DF_{ave} average dilution factor

Statistical Evaluation of Various Methods for Near-Zero Engines

The traditional CVS sampling system dilutes its sample prior to measurement where the magnitude of the ambient concentration is at the level of sample measurement. UCR evaluated its upgraded measurement system for near-zero NOx during recent testing of a near-zero heavy-duty vehicle where the bsNOx emission ranged from 0.003 to 0.05 g/bhp-hr.

Table 8 lists the cycle average for the raw, dilute and ambient NOx concentrations for the 10th, 50th, and 90th percentile as determined from histograms. The 50th percentile raw, dilute, and ambient NOx concentration were 0.55 ppm, 0.17 ppm, and 0.07 ppm respectively. If the cold start tests were removed, the 10th percentile dilute and raw concentrations would be reduced to 0.326 and 2.11 ppm, respectively.

Notwithstanding the need for new methods to calculate the NOx emission from a near-zero engine, there was also the realization that a few NOx spikes of ~25 times the average value will set the final emission rate. It is critical to capture all excursions, especially spikes of high NOx concentrations as these will impact the M1, M3, and M4 measurements. Those approaches use real-time signals where M2 and M5 are integrated with bag signals.

Table 8: Cycle Averaged Raw, Dilute, and Ambient Concentrations (ppm)

Percentile	Amb	Dilute [1]	Raw [1]	C_{a_cor}/Dil percent
10th	0.234	0.632	6.533	105 percent
50th	0.070	0.168	0.554	54 percent
90th	0.021	0.033	0.070	10 percent

[1] With the cold starts removed, the 10th, 50th, and 90th would be 0.326, 0.146, and 0.031 ppm for the dilute concentration and 2.11, 0.450, and 0.069 ppm for the raw concentration, respectively.

Source: Gas Technology Institute

As discussed in the calculation section, the ambient concentration is subtracted from the dilute concentration prior to calculating the mass-based emission. For normal emission standards, the subtraction is typically a small number subtracted from a large number. However, at the 0.02 g/bhp-hr emission level, the measured ambient concentration is now about the same as the dilute value. The ambient corrected NOx concentration (Ca_cor) used in the dilution measurements is the product of ambient NOx concentration and an inverse ratio of the dilution factor. If the Ca_cor is divided by the dilute NOx measured a factor that is representative of the ambient correction divided by the measured dilute NOx signal. This factor shows the magnitude of the ambient concentration in comparison the measured signal and gives the reader a perspective of the weight that the ambient has at and below 0.02 g/bhp-hr NOx emission. Figure 57 shows the 10th, 50th, and 90th percentile statistics for the Ca_cor/NOx ratio in percent and Figure 58 shows the distribution of the ratio.

The results show a 10th, 50th and 90th percentile (Ca_cor/Cd) ratio of 10 percent, 54 percent and 105 percent, respectively. This suggest more than ½ of the measurements were sampled

where the dilute concertation was 50 percent of the ambient corrected (Ca_cor) concentration. The low concentrations measured by dilute methods will impact all the methods except the M3 that uses the raw sampling approach where no dilution correction is needed.

Figure 57: Raw, Dilute, and Ambient Measured NOx Concentration Distributions

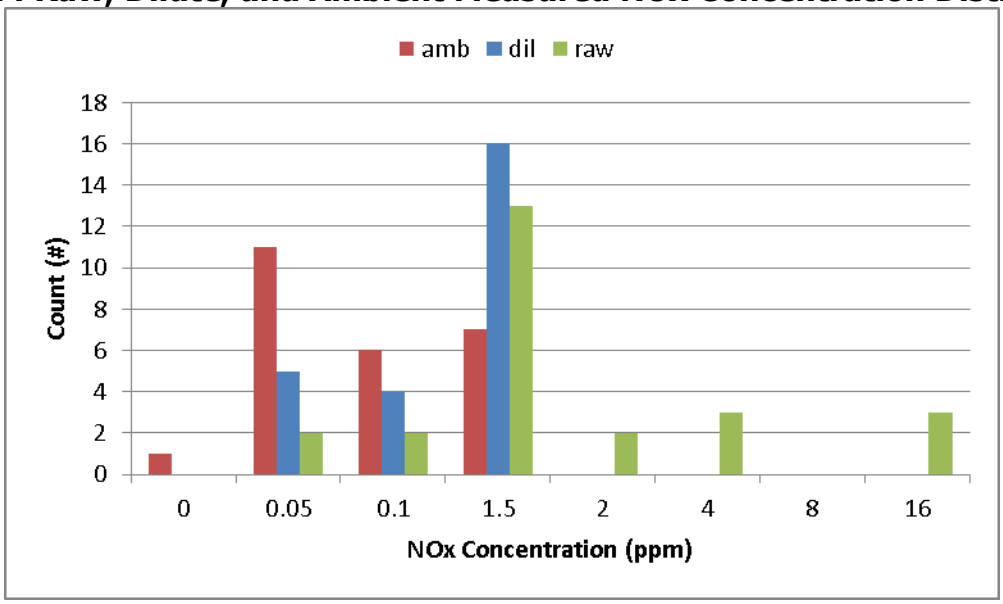

Source: Gas Technology Institute

$$C_{a\_cor} = C_a * \left(1 - \frac{1}{DF_{\_ave}}\right)$$

Where:

C_{a_cor}	is the ambient NOx concentration factor corrected for the dilution term
C_a	is the ambient bag NOx concentration
DF_{ave}	cycle average dilution factor (typically 20-30)
$\left(1 - \frac{1}{DF_{\_ave}}\right)$	dilution factor term (varied from 0.95 to 0.98 in this study)

Figure 58: Ambient Fraction of Dilute NOx Concentration Distribution

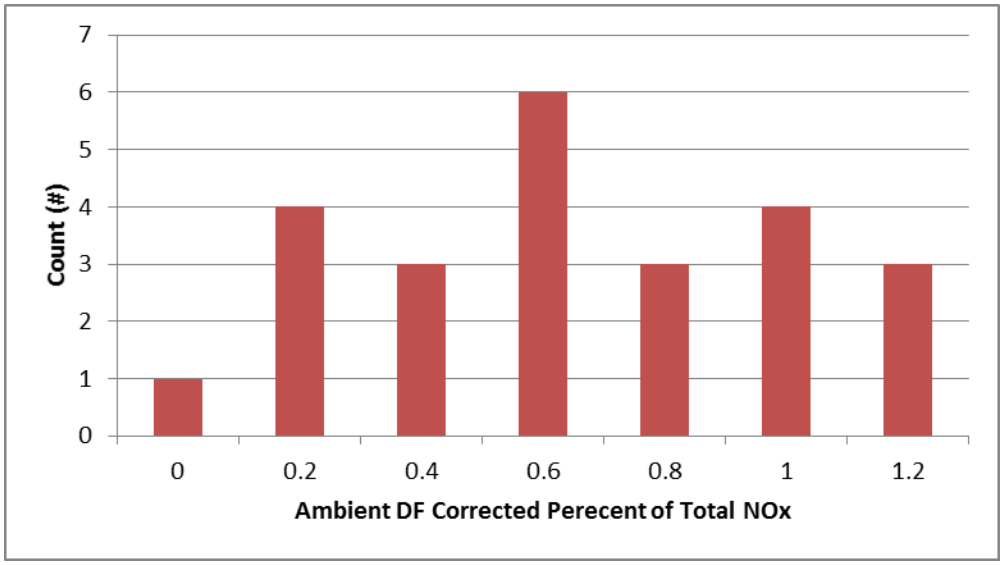

Source: Gas Technology Institute

With dilution air concentration approaching measured tunnel values, a question was raised about the confidence in the calculated emission factors. A comparison of the various methods is shown in Table 9 with M1, the reference method. For M2, the average NOx emission was within 5 percent of M1 values; however, M2 values varied widely about the average from cycle to cycle. On average, M3 values were ~18 percent lower than M1, except for the CBD tests. Further investigation of the CBD tests showed one of the M1 tests had a negative emission rate due a high ambient bag concentration compared to the modal dilute concentration. The M4 average NOx emission rate was higher and relatively more variable than observed with M1. The M5 average value was significantly lower for all tests compared to the M1.

Table 9: NOx Emission Average Percent Difference From Method 1

Trace	M2	M3	M4	M5
UDDS1x	-17 percent	-40 percent	96 percent	-87 percent
DPT1	31 percent	-42 percent	-8 percent	-99 percent
UDDS2x	7 percent	-13 percent	21 percent	-70 percent
RTC	4 percent	-21 percent	111 percent	-7 percent
DPT1	-21 percent	-11 percent	25 percent	-14 percent
DPT2	3 percent	-20 percent	25 percent	-61 percent
DPT3	12 percent	-22 percent	27 percent	-72 percent
CBD	19 percent	23 percent	32 percent	16 percent
Ave	5 percent	-18 percent	41 percent	-49 percent
Stdev	17 percent	20 percent	40 percent	42 percent

Source: Gas Technology Institute

Looking deeper into the data, the M4 method uses continuous ambient concentrations for real time correction of the background calculation. The trace analyzer shows some short-term drift that doesn't appear to be related to ambient concentration changes. Additional investigation is needed but was outside the scope of this project. The research suggests the M4 method will have more variability and less confidence in the calculated values. The M5 utilized the trace NOx analyzer for bag measurements. Surprisingly the M5 method showed a much lower mean value. Investigations of analyzer drift or stability problems were carried out and no issues were found during the deeper analysis.

A comparison of the statistical significance between the traditional M1 and other methods is provided. The two tailed paired t-test and f-test results suggest the two traditional methods do not have statistically different means or different variances at 95 percent confidence, Table 10 (M2 p-value >> 0.05 for both). The upgraded methods showed a different result that varies. The M3 (raw exhaust flow approach) mean difference is not statistically significant at 95 percent confidence (M3 p-value > 0.06) but is at the 90 percent confidence. The M4 (RT ambient correction) and M5 (trace bag evaluation) upgraded methods both have statistically different means (p-value < 0.05 for both).

Table 10: Statistical Comparison to Method 1 Values

Method	ttest/pvalue	ftest/pvalue
M2	0.521	0.998
M3	0.060	0.152
M4	0.021	0.141
M5	0.001	0.104

Source: Gas Technology Institute

Each of the added methods (M3, M4, and M5) while promising on paper, need more data and analysis in order to evaluate confidence limits of the calculated emission factors. The M3 measurement showed good alignment between the measured NOx signal and the exhaust flow signal. Examination of the data shows that >80 percent of the NOx emission come from a few very large spikes. A closer inspection shows that the NOx concentration and exhaust flow spike occur simultaneously and are usually a result of a rapid acceleration from idle. Driving is a key parameter that adds variability to the data that is independent of the measurement method.

With the M4 approach of continuous ambient NOx ambient correction, a deeper analysis shows the analyzer had a slight zero stability issue over the 20-40 minute test cycle not found during the three minute bag analysis. This drift may be the cause of the poor M4 method comparison. From limited trials, the M5 method with an ambient-air NOx analyzer appears as the preferred approach due to high accuracy of the ambient and dilute bag measurements. The drift issue found for the M4 measurement didn't appear to be a factor during the short bag analysis, but additional tests should be performed to evaluate.

In summary, the M1, M2, and M3 appear to be the most reliable where the M3 results are more consistent at the extremely low concentrations measured. For the testing reported in this study the M2 method was used since the emission levels were closer to 0.1 than 0.002 g/bhp-hr as evaluated for CWI's ISL G 8.9L near-zero engine.

Tailpipe Measurements

The tailpipe high speed NOx system called NTK Compact Emission Meter (NCEM®) includes measurements of NOx, PM mass, PN, oxygen (O2), and air/fuel ratio (Figure 59). While the Air/fuel ratio is available in the latest generation NCEM, this feature was not available during this project. The NCEM uses direct measurement sensors of the raw exhaust gas rather than dilution sampling. As the result, there is no delay time and measurements can be performed in near, real-time, thus providing an independent measure of the NOx and other emission.

Figure 59: High-Speed Tailpipe Measurement System NCEM NTK-Sparkplugs

Source: Gas Technology Institute

The NOx sensor is one of a family of sensors based on solid state technology that are widely used by many OEMs for controlling the AFR and for monitoring NOx in SCR aftertreatment devices. The sensor detects NOx by measuring O2 ions created by the dissociation of NOx into N2 and O2 in the detection chamber shown in Figure 60. The design used for this specific sensor converts NO2 to NO and O2 in a trap layer before the gases reach the detection portion of the element. Therefore, the sensitivity to NO and NO2 is essentially the same. Only under conditions where there is a very high gas flow rate or very cold gas that the element heater cannot overcome, would the ratio start to diverge from 1:1. In those cases the sensitivity to NO2 could be slightly lower than the sensitivity to NO.

The Particle Mass/Particle Number (PM/PN) sensor is based on the Pegasor PPS-M technology, where particles are charged in a corona discharge with the total measured charge proportional to the particle surface area, as shown in Figure 61. PM/PN can then be determined via calibrations that are used to establish calibration constants. To determine PM, the signal is calibrated against an AVL MSS 483, which is in turn calibrated against a gravimetric filter where the filter face temperature is not controlled to the 47°C±5°C specifications in 40 CFR 1065. To determine PN, the sensor is calibrated against a TSI scanning mobility particle sizer (SMPS). Both the PM and PN calibrations are performed with a soot generator that provides soot particles with a unimodal distribution with peak concentration around 75 nm. The calibration does have some sensitivity to the particle size distribution, which has been discussed in detail elsewhere.

Simulations using a range of possible diesel particle size distributions, however, have shown that the maximum theoretical error is 23 percent when using surface area as a proxy for number and 39 percent when using surface area as a proxy for soot mass, although the actual error is expected to be much less than these values (Ntziachristos et al., 2012). For the test vehicle itself, internal data indicates that its size distribution is bimodal with a minor peak at 15 nm and a larger peak at 75 nm, which should be relatively well represented by the distribution used for the calibration. Also, since the sensor measures PM in the raw exhaust, with only a

small amount of dilution, the total PM and total PN measured by the NCEM is primarily solid PM.

Figure 60: NOx Principle of Operation From NCEM

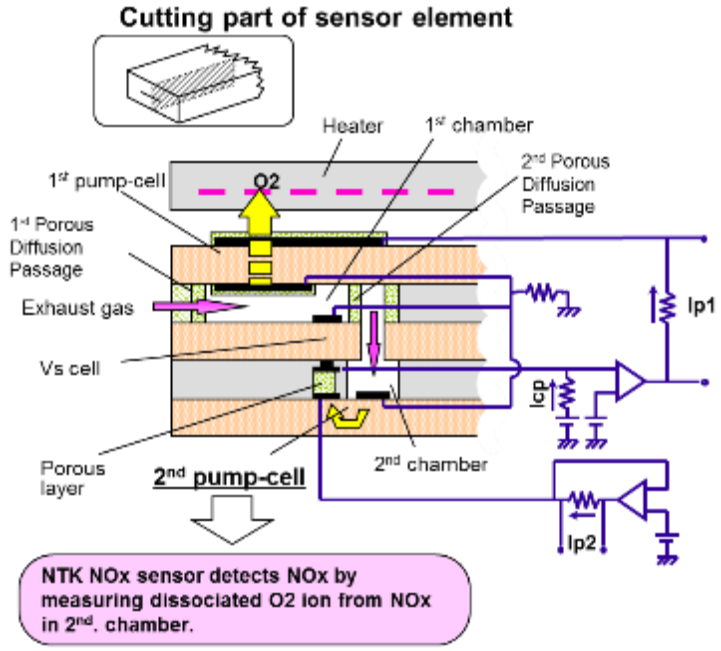

Source: Gas Technology Institute

Figure 61: PM Principle of Operation From NCEM

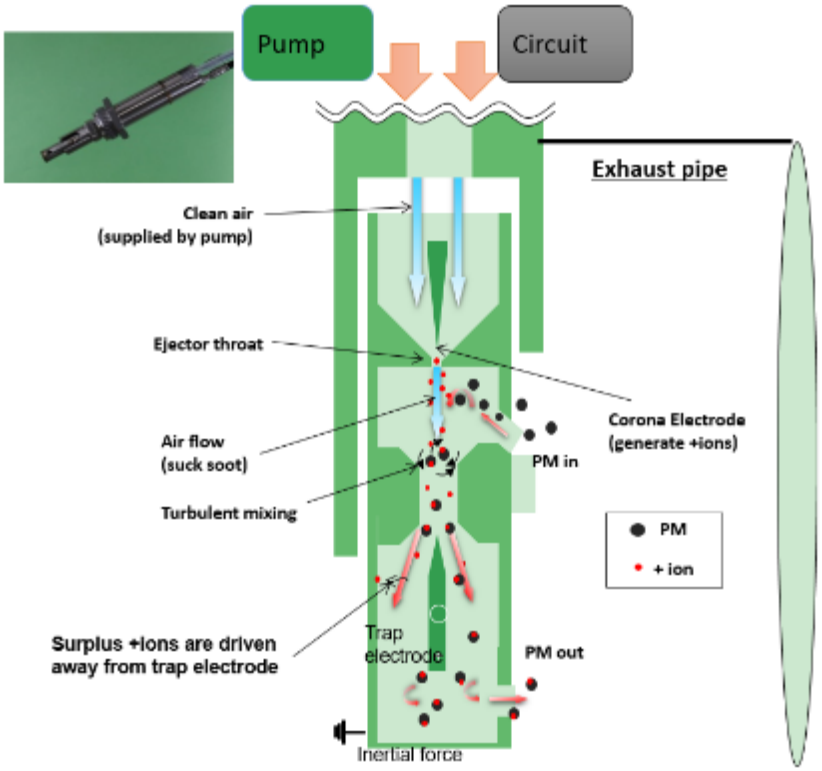

Source: Gas Technology Institute

Test Cycles

Four engine test cycles were considered for this project: 1) Federal Test Procedure (FTP), 2) hybrid simulation "stop/start" approach, 3) excess load during FTP testing with electric charging, and 4) a steady state ramp modal cycle (RMC) (Figure 62). These test cycles represent typical engine certification, simulated hybrid operation emission, and fuel mapping cycles from heavy duty engines.

Figure 62: Ramp Modal Engine Test Cycle

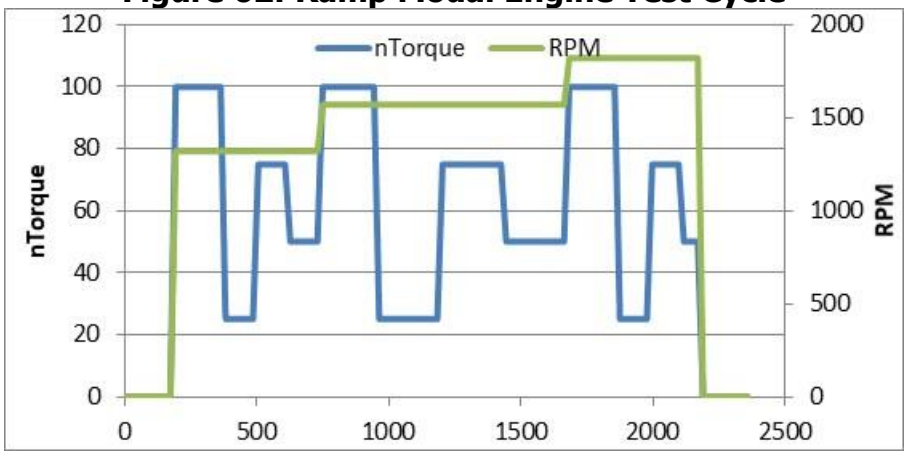

Source: Gas Technology Institute

Test Engine for Dyno

The engine tested in this project was the ISL G 280 Cummins Westport Inc. (CWI) Natural Gas engine. The engine was initially certified as a 0.2 g/bhp-hr NOx and 0.01 g/bhp-hr PM based on the family number ECEXH0540LBH found on the engine label. CWI further developed this engine as an ultra-low NOx engine where the NOx emissions were reduced by 90 percent from the standard to 0.02 g/bhp-hr. A recently released EO for the near-zero design with engine family GCEXH0540BH, also on the CARB website shows the lower NOx standard is 0.02 g/bhp-hr and the actual certified test value was 0.01 g/bhp-hr. This project compared the NOx emission of the hybrid-electric vehicle relative to the 0.02 g/bhp-hr engine certification level over representative drive cycles.

Selected specification and properties of the test engine are provided in Table 11. While the engine rating was earlier stated at 320 hp, the actual rating was 280hp as will be shown in the engine map measured on the dynamometer. This is not surprising as CWI offers a series of ratings for this engine ranging from the ISL G-320 to -300 to -280 to – 260 and to – 250.

Table 11: Summary of Selected Main Engine Specifications

Mfg	Model	Year	Eng. SN	Rated Power (hp @ rpm)	Disp. (liters)	Adv NOx Std g/bhp-h [1]	PM Std. g/bhp-h
CWI	ISL G 8.9	2007	46738468	320 @ 2000	8.9	0.2	0.01

Source: Gas Technology Institute

Test Fuel

Pipeline natural gas fuel found in Southern California pipeline was used for this study as it is representative of the natural gas generally available in California and it meets the CWI fuel specification, as indicated in Table 12. Vehicle re-fueling was performed at the LNG station at Agua Mansa, Riverside California.

Table 12: Selected Fuel Properties for Local CNG Test Fuel

Property	Molar percent	Property	Molar percent
Methane	94.65	Pentane	0.01
Ethane	3.87	Carbon dioxide	0.35
Propane	0.41	Oxygen	0.00
Butane	0.08	Nitrogen	0.63

1 Based on these fuel properties the HHV is 1,042.5 BTU/ft3 and the LHV is 939.9 BTU/ft3 with a H/C ratio of 3.905, a MON of 132.39 and a carbon weight fraction of 0.745 and a SG = 0.58. Note these results meets the US EPA 40 CFR Part 1065.715 fuel specification for natural gas fueled vehicles.

Source: Gas Technology Institute

Results

Performance

The first step in testing the emission of an engine is determining the lug curve or relationship between the engine power and torque as a function of engine RPM. As shown earlier, several steps were needed to get the engine mounted onto the dyno and to get specially designed connectors to link the engine with the dynamometer. After the engine was suitably and safely mounted, the engine map was measured with results show in Figure 63. Note the maximum power is at about 280 horsepower and the maximum torque is about 950 ft-lbs at 1400RPM. While the torque is somewhat higher than the OEM curves, the engine was clearly an ISL G-280 and not a -320. The peak torque is at 1400RPM like the OEM curve.

Figure 63: ISL G 280 Hp Natural Gas Engine Lug Curve During Engine Dyno Testing

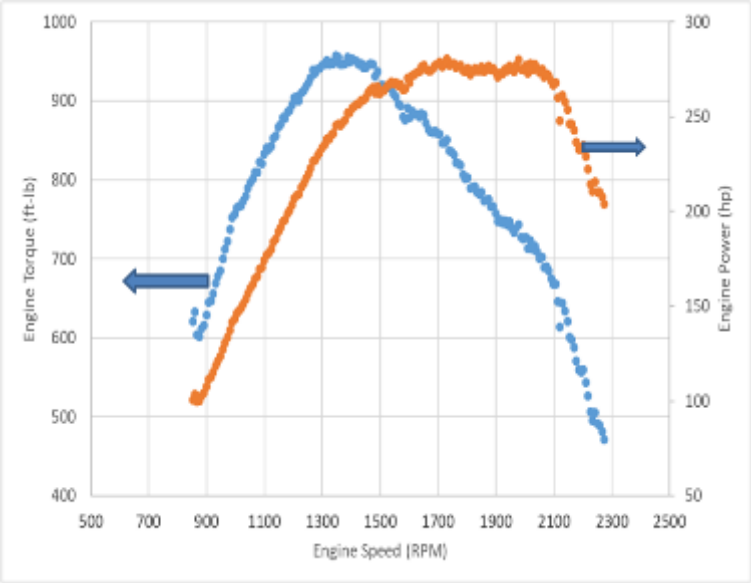

Source: Gas Technology Institute

Emissions

This section discusses the integrated, real time and simulated hybrid emission profile for the engine dyno stage.

Integrated Emission for Various Cycles

The overall emissions are shown in Table 13. The continuous NOx measurements with the NTK Compact Emission Meter (NCEM®) are used and while values are like values from MEL, the NTK values are reported in this summary. Notwithstanding; the NTK measurements offer an independent and real time assessment of MEL emission and issues with engine calibration. The emission from the federal reference cycle, FTP, and the Ramp Modal Cycle, RMC, emission are based on these tradition cycles. The "hyb" and "estFTP_Hyb" data points are the actual and simulated emission from the hybrid drive conditions.

Following the FTP certification cycle on the dynamometer, the emission factor was 0.18 g/bhp-hr, a value below the NOx 2010 certification limit of 0.2 g/bhp-hr. Ammonia emission were on the high side as compared with diesel and averaged between 93 and 214 ppm. The CH4 emission were also higher than an average diesel engine, which is common for natural gas engines. The PM mass was a little higher than expected at 6.5 mg/bhp-hr.

Table 13: Emission Summary for Engine Dyno Testing

				Engine		Ave Modal Emission Factor (g/bhp-hr)							PM (mg/bhp-hr)			Conc. ppm
Trace	Case	Weight	sec	bhp	bhp-hr	THC	CH4	NMHC	CO	NOx	CO2	NH3	PM mg	eBC	cor_eBC	NH3
FTP	baseline	29,000	1200	57.6	19	2.56	2.40	0.17	8.3	0.180	610	0.4	6.55	-	-	93.6
RMC	baseline	29,000	2400	120.6	80	1.93	1.78	0.15	6.6	0.133	491	0.4	1.74	-	-	214.7
Hyb	baseline	29,000	454	36.4	5	2.12	1.97	0.15	6.1	0.154	612	0.1	-	-	-	25.9
estFTP_Hyb	baseline	29,000	1200	57.6	19	0.51	0.47	0.04	1.5	0.037	0	0.0	-	-	-	0.0

Source: Gas Technology Institute

Real-Time NOx Emissions

Closed loop steady state calibration issues for an existing engine can be evaluated on the RMC cycle. For this evaluation the fast-response, NTK Compact Emission Meter (NCEM®) instrument was used. Results in Figure 64**Error! Reference source not found.** show the rapid response of the NTK device as the AFR was dithering. Further even with a TWC at a high temperature, there are significant NOx emission for part of the cycle.

Figure 64: Real-Time NOx Assessment of the RMC Cycle

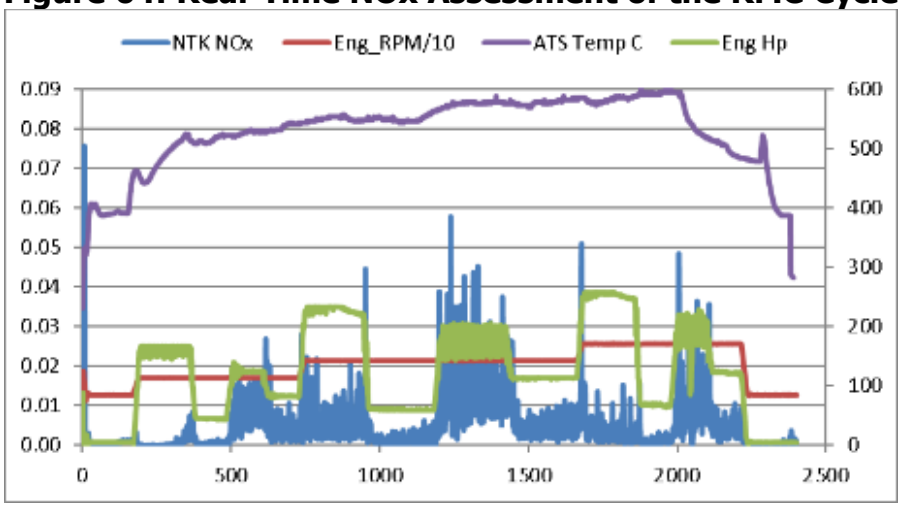

Source: Gas Technology Institute

Further detail of the operation of the existing natural gas engine with the TWC system for control of emission can be seen in Figure 65 and Figure 66. Note that the outlet oxygen concentration is highly variable, a state that is not seen with passenger cars as the oxygen sorption material used in the catalyst formulation will trap oxygen and keep the system near the stoichiometric levels so that both NOx and hydrocarbons will be converted. A catalyst ingredient, therefore, serves to either store or release oxygen depending on the deviation from the target AFR.

Figure 65: Engine Oxygen Switching Sensor Performance

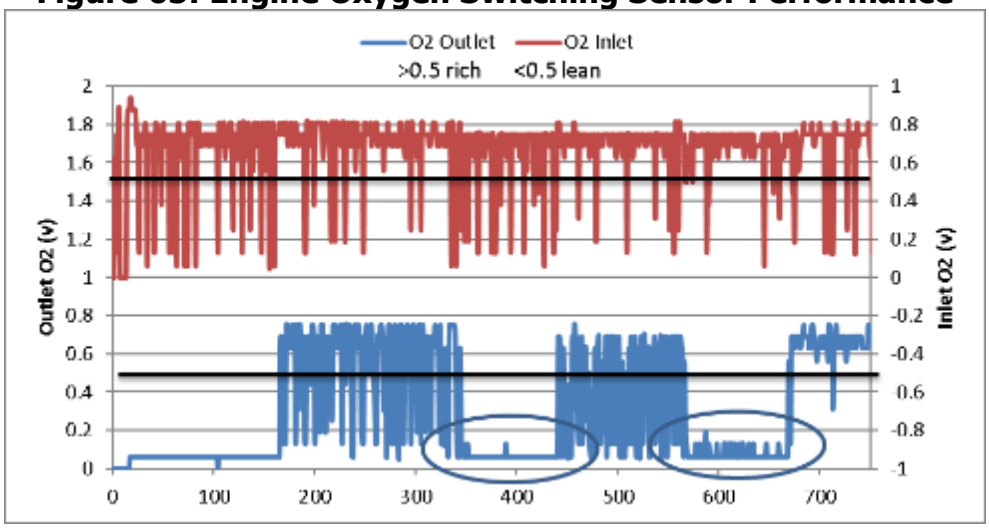

Source: Gas Technology Institute

Figure 66: Fuel Regulator and ATS Oxygen Compensation Percent

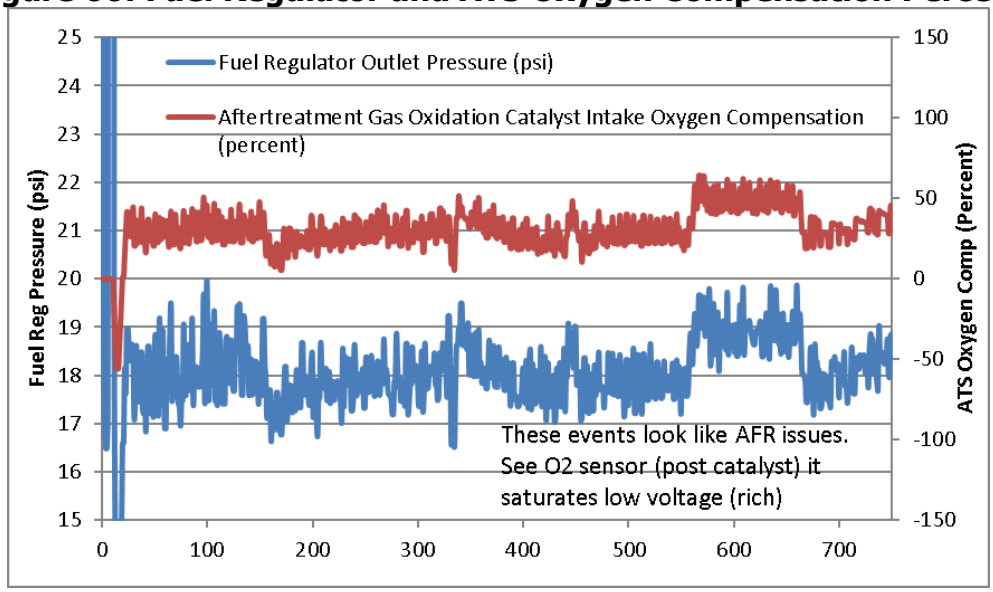

Source: Gas Technology Institute

Simulated Hybrid "Start/Stop"

Hybrid stop/start capabilities are possible with battery powered systems. In this section a test is performed to consider the emission that would be present if for three parts of the FTP the engine is in engine mode and the other sections it is in all electric mode.

The hybrid simulation test cycle used three parts of the FTP test cycle (Figure 67). For the other part of the test cycle the electric drive system is assumed to be operating where no emission are produced, but work was still being performed. The normal FTP accumulated NOx emission is presented in Figure 68 and shows that the hot start NOx emission are fairly constant at around 0.1 g/bhp-hr. This would suggest start/stop technology could work for a natural gas engine if the catalyst stays hot between intervals. Others have found that adding better insulation or an internal burner might be needed for thermal management in cold climates.

The NOx emission from the hybrid cycle was 0.15 g/bhp-hr emitted only over a portion of the cycle. During this portion only a fraction of the work was used which can be visualized by results in Figure 69 which shows the areas of the accumulated NOx emission that add up to the 0.15 g/bhp-hr where for the rest of the time the emission are zero in electric mode. If the full work is considered, the emission of NOx would be reduced to 0.037 g/bhp-hr or close to the near zero NOx level. In calculating real world emission, it is likely that emission from cranking and for charging the batteries would need to be included. These emissions will be considered during the chassis emission evaluation.

Figure 67: Hybrid Simulation Cycle: FTP

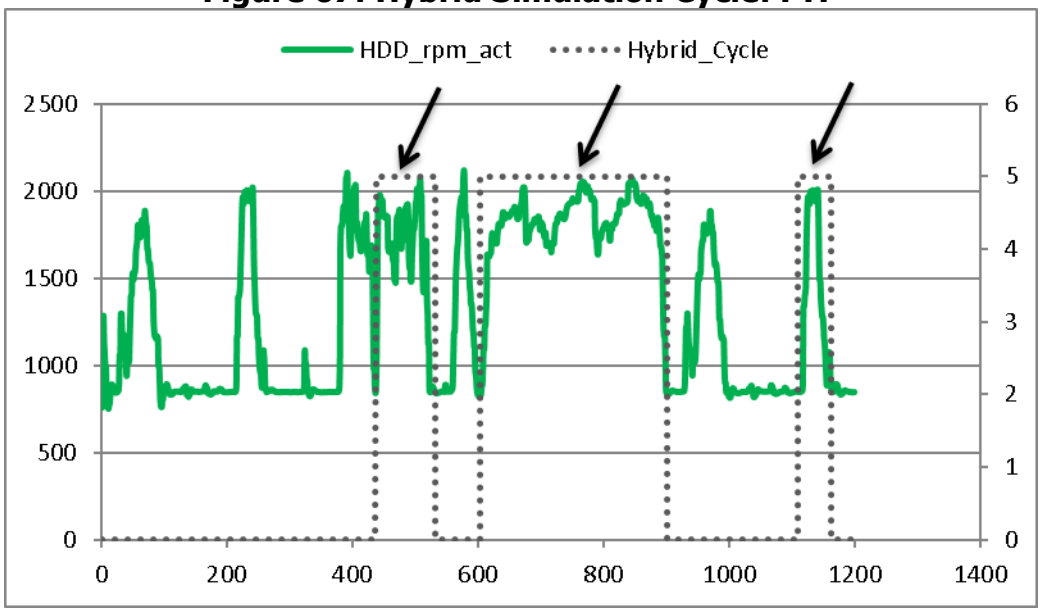

Source: Gas Technology Institute

Figure 68: Real-Time NOx Accumulation as a Function of Work-FTP

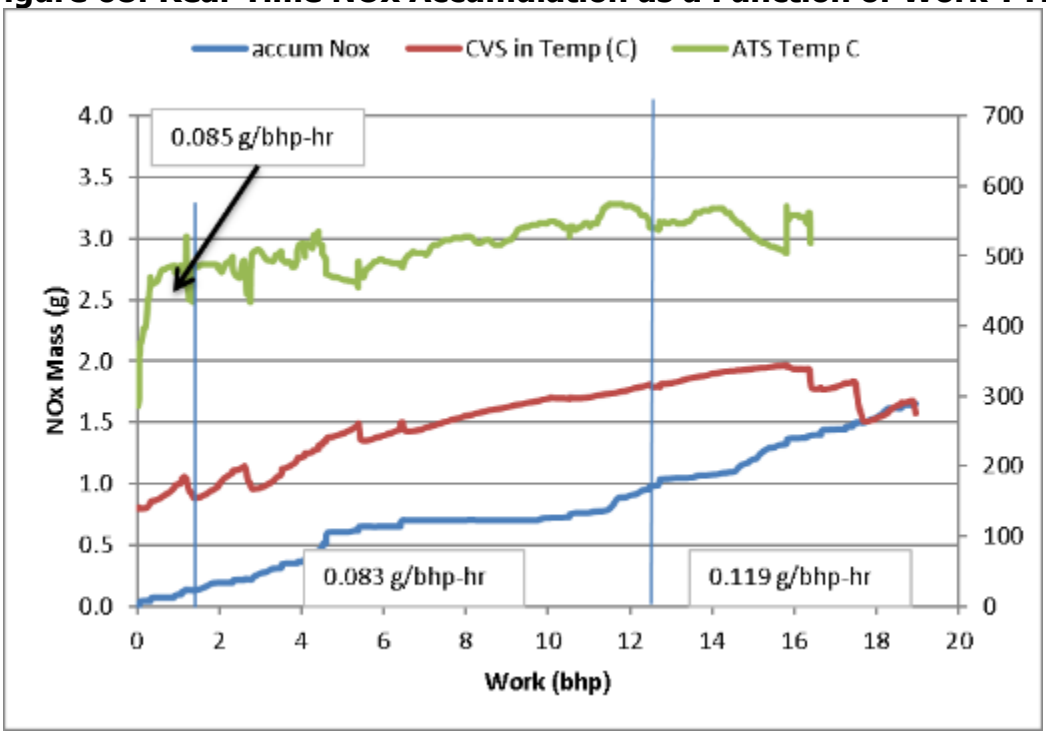

Source: Gas Technology Institute

Figure 69: Simulated Hybrid Cycle With Accumulated NOx-FTP

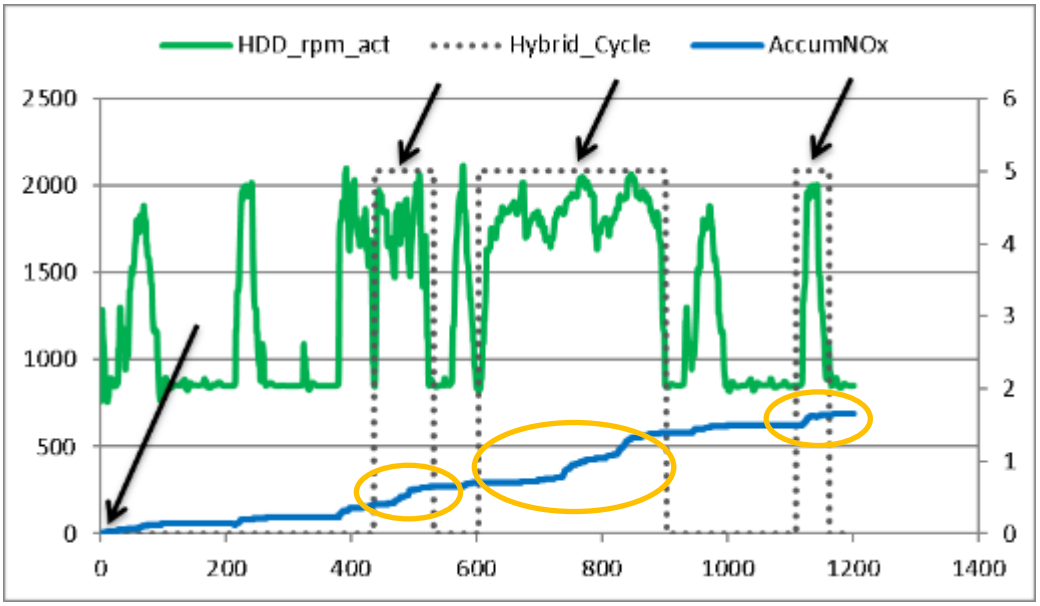

Source: Gas Technology Institute

Fuel Economy

The project considered fuel economy and greenhouse gas emission given the importance of these two factors in the California climate change plans. For this engine, the FTP CO2 emission were slightly higher than the 555 g/bhp-hr FTP value for the near zero version. However, that technology made some modifications to better comply with the Tier 2 GHG standards on the horizon.

Global Warming Potential

Black carbon was not measured during the testing on the engine dynamometer; however, several climate forcing gases, CO2, CH4, and estimated N2O, were measured and results are in Table 14. These measurements provide a window towards estimating the global impact of the new near-zero engine.

Table 14: MEL Summary GWP HDD Testing

Trace	Case	Weight	CO_2	CH_4	est N_2O	GWP ($CO_{2\ eq}$)	CO2/GWP	eBC mg	eBC/$PM_{2.5}$
FTP	baseline	29,000	610.0	2.40	0.047	723.7	0.84	-	-
RMC	baseline	29,000	491.3	1.78	0.047	540.8	0.91	-	-
Hyb_01	baseline	29,000	146.4	0.47	0.047	163.2	0.90	-	-

Source: Gas Technology Institute

Cold Start Optimization

Some thought and effort went into reducing the very high cold-start NOx emission by heating a section of the exhaust pipe to preheat the catalyst prior to engine ignition. Towards that goal, Watlow provided an exhaust catalyst-heater prior to UCR's engine testing (Figure 70). To integrate the heater section, supplemental power from UCRs engine grid/battery systems was needed. Figure 71 through Figure 73 show the complex layout and connections that would have been needed to operate the heater outside of the vehicle. These are provided for informational purposes. Modeling showed diminishing marginal returns for installing the engine. Due to this, the complex power system integration, and schedule impacts, the Watlow system was not installed or evaluated on the engine dynamometer.

Figure 70: Heater Section Supplied by Watlow for Cold Start Improvement

Source: Gas Technology Institute

Figure 71: Schematic for Setting Up the Electrically Heated Catalyst Section

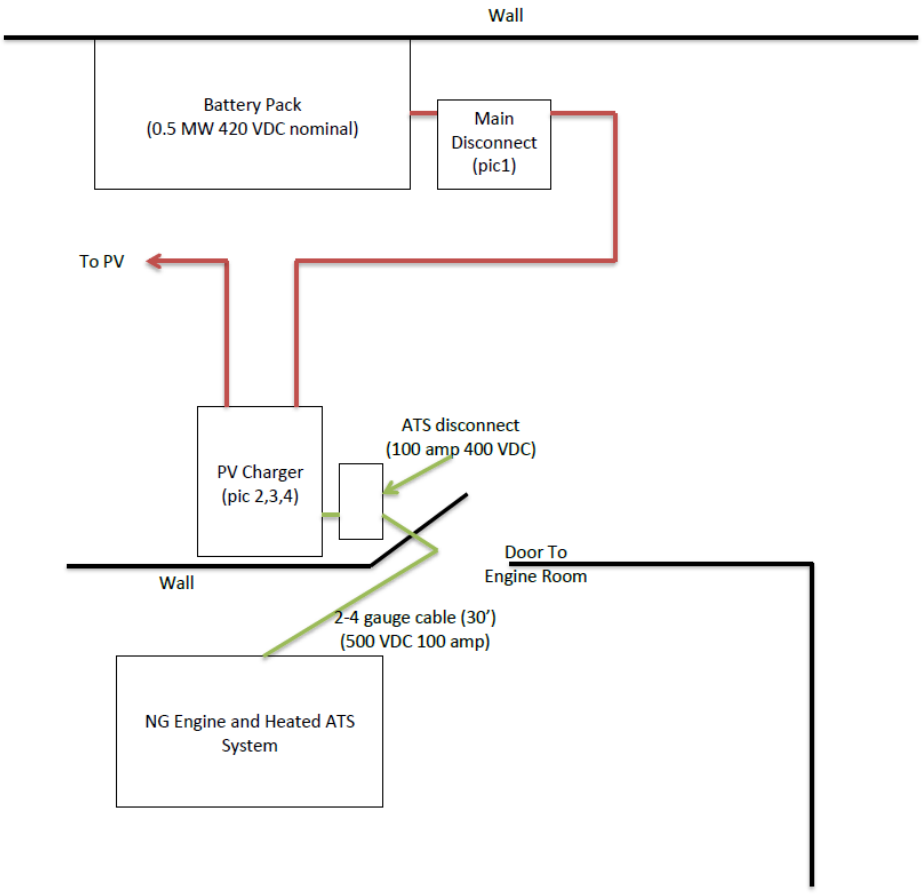

Source: Gas Technology Institute

Figure 72: Main Power Cabinets, Batteries and Controls Near the Engine Dyno

Source: Gas Technology Institute

Figure 73: Main Power Electrical Connection for Electric Heater

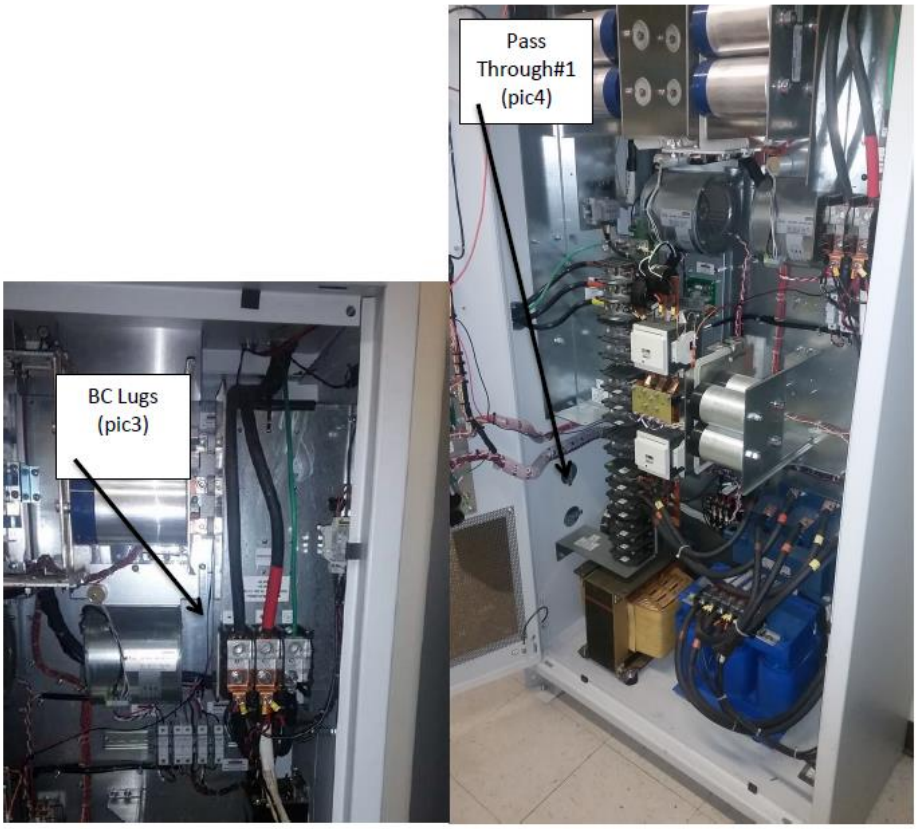

Source: Gas Technology Institute

CHAPTER 6:
Chassis Dynamometer Demonstration

UCR is equipped with several laboratories for accurate real-world emission evaluation of heavy duty and light duty vehicles. This section describes the chassis dynamometer demonstration for the integrated hybrid natural gas truck.

Approach

The approach for the chassis dynamometer is similar to the engine dynamometer for emission measurements since the MEL is used as the measurement tool for both laboratories. This section describes the setup and approach for the chassis dynamometer testing.

Chassis Dynamometer

UCR's chassis dynamometer is an electric AC type design that can simulate inertia loads from 10,000 lb to 80,000 lb which covers a broad range of in-use medium and heavy-duty vehicles (Figure 74). The design incorporates 48" rolls, axial loading to prevent tire slippage, 45,000 lb base inertial plus two large AC drive for achieving a range of inertias. The dyno has the capability to absorb accelerations and decelerations up to 6 mph/sec and handle wheel loads up to 600 horsepower at 70 mph. This facility was also specially geared to handle slow speed vehicles such as yard trucks where 200 hp at 15 mph is common. Electric chassis dynamometers are designed to accurately perform transient test cycles to quantify in-use real world emission. For more information on test cycles and specifications see Appendix A.

Figure 74: UCR's Heavy Duty Chassis Eddy Current Transient Dynamometer

Truck shown is not the test item but included for illustrative purposes.

Source: Gas Technology Institute

Test Article

Test Vehicle

The ISL G 320 engine was installed in a 2009 model year Peterbilt Class 8 drayage truck with a GVW of 50,000 lb, VIN 1NP-VD29X-7-AD112870. The truck is equipped with an Allison manual transmission. The engine is rated to 320 hp and is certified to the 0.2 g/bhp-hr NOx standard (Table 15). At the time of vehicle chassis testing, the natural gas truck had a mileage of 159,248 miles.

Table 15: The HD Truck Engine Parameters

Mfg	Model	Year	Eng. Family	Rated Power (hp @ rpm)	Disp. (liters)	Adv NOx Std g/bhp-h [1]	PM Std. g/bhp-h
CWI	ISL G 8.9	2009	9CEXH0540LBE	320 @ 2100	8.9	0.2	0.01

Source: Gas Technology Institute

Test Cycles

The hybrid natural gas HD vehicle selected for this demonstration program uses the ISL-G 8.9L natural gas engine that is widely used in California for: 1) transit buses, 2) refuse haulers, and 3) goods movement. For this project UCR selected four test cycles. First, the EPA Urban Dynamometer Driving Schedule (UDDS) that was developed for chassis dynamometer testing of heavy-duty vehicles [40 CFR 86, App.I]. The UDDS driving schedule was the basis for the development of the EPA HD FTP transient engine dynamometer cycle that was used when the ISL-G engine was on the engine dynamometer in the earlier section. Although there is not an exact match of emission values between the UDDS and FTP cycles, there is similarity in key measured parameters, thus providing an independent check of typical engine operation. In addition to the UDDS cycle, UCR found three chassis cycles related to port and freight movement operations as helpful in understanding emission from driving in: 1) severely congested traffic, 2) stop and go urban driving and 3) freeway or inter-city driving. These three cycles are representative of: Near Dock, Local, and Regional operations (Table 16).

Table 16: Summary of Statistics for the Proposed Driving Cycles

Cycle	Distance (miles)	Average Speed (mph)	Duration (sec)
Near Dock	5.61	6.6	3046
Local	8.71	9.3	3362
Regional	27.3	23.2	3661
UDDS	5.55	18.8	1061

Source: Gas Technology Institute

Test Weight

The representative test weight for Class 8 trucks moving freight in California is 69,500 lb[2]. The small displacement (8.9 liter) natural gas engine is not powerful enough to operate safely at these high loads in conventional mode, but could operate in the hybrid mode with an electric motor assist. Because of the low power from the 8.9L engine, the testing was carried out at two test weights; one test weight was based on a suitable Class 7 operation at 29,600 lb and the other was at 69,500 lb suitable for a Class 8 HDT. The 69,500 lb test weight has been used by UC Riverside and WVU for other research projects with natural gas, all electric, and diesel trucks. In summary, UCR used a testing weight of 29,600 lb for all test cycles (UDDS and port cycles) in conventional mode and both 29,600 lb and 69,500 lb in hybrid mode. In addition, the UDDS was performed at 69,500 lb in conventional mode to consider performance benefits on the hybrid system compared to the conventional system.

Test Fuel

Laboratory fuel properties were measured during a previous testing campaign. California pipeline liquefied natural gas fuel was used for the vehicle testing. Vehicle re-fueling was performed at the LNG station at Agua Mansa, Riverside, California.

Work Calculation

The reported emission factors presented in the main report are presented on a g/bhp-hr (for engine testing). The engine work is calculated utilizing actual torque, friction torque, and reference torque from broadcast J1939 ECM signals. The following two formulas show the calculation used to determine engine brake horsepower (bhp) and work (bhp-hr) for the tested vehicle. Distance is measured by the product of the circumference of the chassis dynamometer rolls and the total RPM that is broadcast by J1939.

$$Hp_{\_i} = \frac{RPM_{\_i}\left(Torque_{actual\_i} - Torque_{friction\_i}\right)}{5252} * Torque_{reference}$$

Where:

- Hp_i instantaneous power from the engine. Negative values set to zero
- RPM_i instantaneous engine speed as reported by the ECM (J1939)
- Torque_actual_i instantaneous engine actual torque (percent): ECM (J1939)
- Torque_friction_i instantaneous engine friction torque (percent): ECM (J1939)
- Torque_reference reference torque (ft-lb) as reported by the ECM (J1939)

$$Work = \sum_{i=0}^{n} \frac{Hp_{\_i}}{3600}$$

Added Measurements

To understand the benefit of natural gas fuel over conventional fuels one should also consider the pollutants that impact climate change categorized as short and long term. An example of a short-lived climate pollutant emission common for mobile sources is black carbon. To facilitate

[2] Wayne Miller, Kent C. Johnson, Thomas Durbin, and Ms. Poornima Dixit 2014, In-Use Emissions Testing and Demonstration of Retrofit Technology, Final Report Contract #11612 to SCAQMD September 2014.

the analysis of black carbon emission, UCR added black carbon measurements using the AVL micro-soot sensor (MSS) (Figure 75). The MSS system measures the equivalent black carbon and is denoted in the literature with an eBC. When the MSS is coupled with a gravimetric filter, the approach can also provide real time total mass measurements.

Figure 75: Setup of UCR's Black Carbon Measurement System (MSS 483)

Source: Gas Technology Institute

Vehicle GWP includes carbon dioxide (CO2), methane (CH4), and nitrous oxide (N2O). N20 emission were estimated from previous tests on this same engine on similar cycles. CH4 and CO2 levels were measured with the MEL.

Setup

Engine Inspection

Prior to testing, the test vehicle was inspected following a checklist to ensure proper tire inflation and tread, vehicle condition, vehicle securing, and the absence of any engine code emission faults. The vehicle met UCR's specifications. A minor check engine fault was identified and fixed. All tests were performed meeting all specifications and without any engine code faults. Thus, the results presented in this project are representative of a properly operating vehicle, engine, and aftertreatment system.

The vehicles setup on UCRs chassis dyno and emission laboratory is shown in Figure 76. The left figure shows the LNG fuel tank and the right figure shows the electric battery storage system.

Figure 76: Hybrid Truck Setup on UCR's Chassis Dynamometer

Source: Gas Technology Institute

Phase 1: Baseline Testing

Phase 1A: The baseline condition represents tests of the truck, as-delivered, which can only be tested safely at Class 7 weights. Tests with Class 7 weights were carried out twice; first, as received condition, and second, after installing an updated calibration for the engine and installing new switching oxygen sensors (Figure 77). Phase 2 testing involved testing the hybrid Class 8 HDT at 69,500lbs with the engine, battery, and electric motor operating.

Phase 1B: For re-flashing the engine calibration, UCR worked with Cummins-Westport, Inc. to install the latest approved calibration for this engine. The calibration provided was AQ90014.37.zip. The file was flashed into the ECM by a Cummins CalPacific service technician as shown in Figure 77, Figure 78, and Figure 79. The overall process included:

1. Replacement of the aged O2 sensors with new switching sensors as recommended by CWI.
2. Updating the calibration in the ECM.
3. The vehicle was operated for a while following the installation of a new calibration so adaptive learn algorithms can learn the sensor package on the engine.

Figure 77: New Oxygen Sensors in the Box (Left) and Prior to Installation (right)

Source: Gas Technology Institute

Figure 78: New Oxygen Sensors Installed Before (left) and After Catalyst (right)

Source: Gas Technology Institute

Figure 79: Calibration Flash Status at the Start (Left) and End (Right)

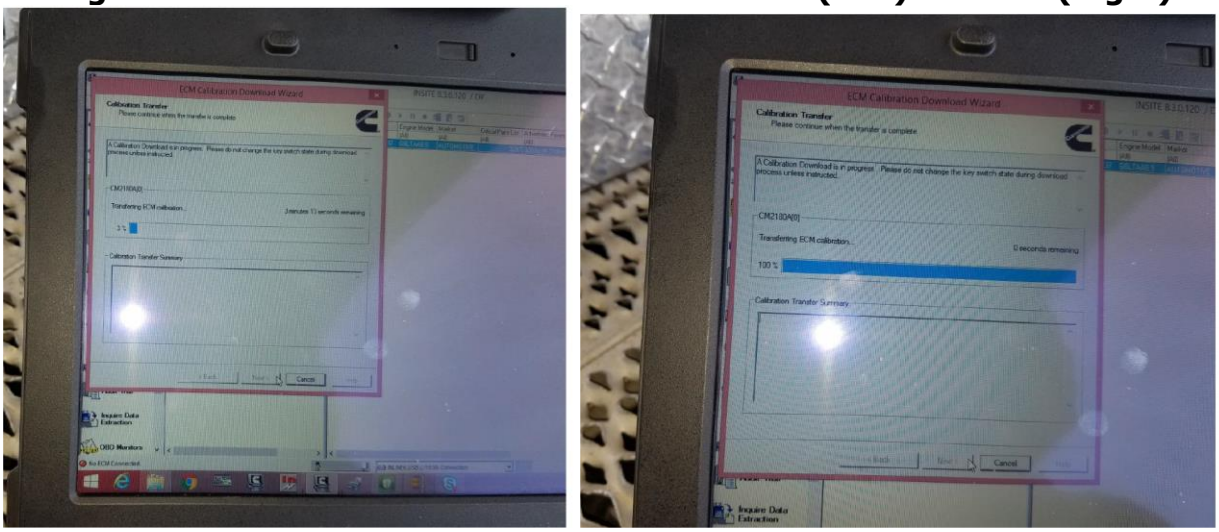

Source: Gas Technology Institute

Phase 2: Hybrid Truck - Class 8 Power

For Phase 2 testing, the team used the hybrid demonstration truck with three power sources: the CWI ISL-G engine rated at 320hp; an electric motor rated at 240 kW and 80 kWh of Li-ion batteries for reducing emission during cold start operation and for absorbing power while applying brakes to the vehicle. At this power level, the demonstration hybrid truck can be safely operated and tested at the full 69,500 pounds required for moving freight. Figure 80 shows the integrated power scheme.

Figure 80: Integrated Power Scheme for the Hybrid Natural Gas Port Truck

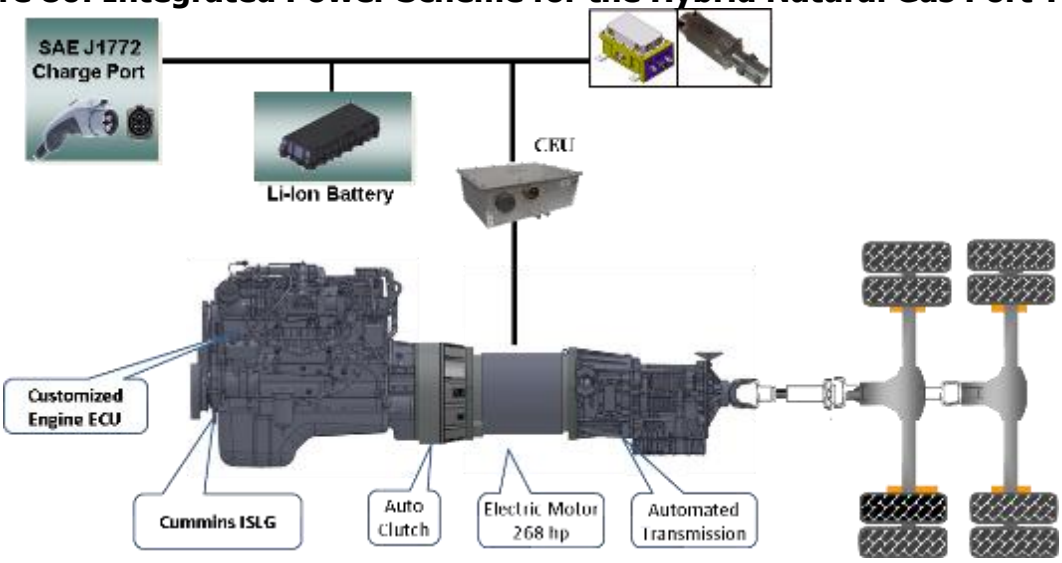

Source: Gas Technology Institute

Phase 2: Hioki Power Measurement

To understand and quantify the state of charge of the electric drive system, both the vehicle state of charge (SOC) and a direct power measurement were utilized. The vehicle SOC was measured utilizing the on-vehicle dashboard indictor and was recorded for each test segment. In addition, UCR installed an independent state-of-the art power measurement device called a Hioki power meter for an independent measure of vehicle power in and out of the battery (Figure 81 and Figure 82). This Hioki power system is commonly used for verification of electric power on hybrid and all-electric vehicles. The power meter includes current and voltage measurement in addition to sophisticated power, direction, and phase calculations. The electric power results reported for this truck are based on the Hioki measurement.

Figure 81: Electric Power Systems and Independent Measurements

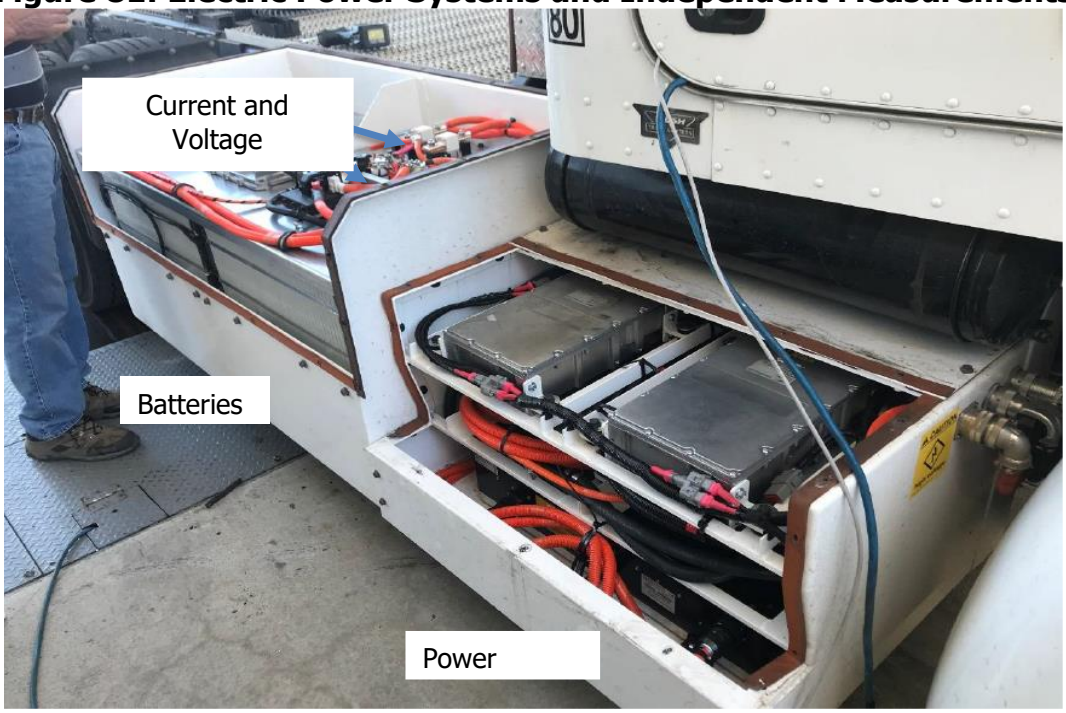

Source: Gas Technology Institute

Figure 82: Installation of Hioki Power Meter

Source: Gas Technology Institute

Results

The results are organized by Phase 1 and Phase 2 test conditions. Phase 1 represents the conventional non-hybrid condition and Phase 3 represents the hybrid condition. For Phase 1 there was a baseline (as received engine) denoted Phase 1A and then the upgraded engine calibration called re-flashed denoted Phase 1B.

Phase 1A, 1B, and 2: Work Comparison

The Phase 1 (Phase 1A and 1B) and Phase 2 tests on the chassis dynamometer involved comparing the changes caused by installing the new calibration codes, the new switching oxygen sensors, and the hybrid system. Each truck configuration was run over five different cycles as included the cold-start UDDS cycle in this project. Comparative results for the work and power are shown in Figure 83 and Figure 84. While operating as a Class 7 HDT, the results for the two operating modes are quite comparable, indicating that the re-flash upgrade did not result in much change. Furthermore, the values for power and work were as expected based on UCR's past test experience. The hybrid configuration shows less power and work consumed which is typical for a battery regeneration system.

Figure 83: Work from the Various Chassis Tests

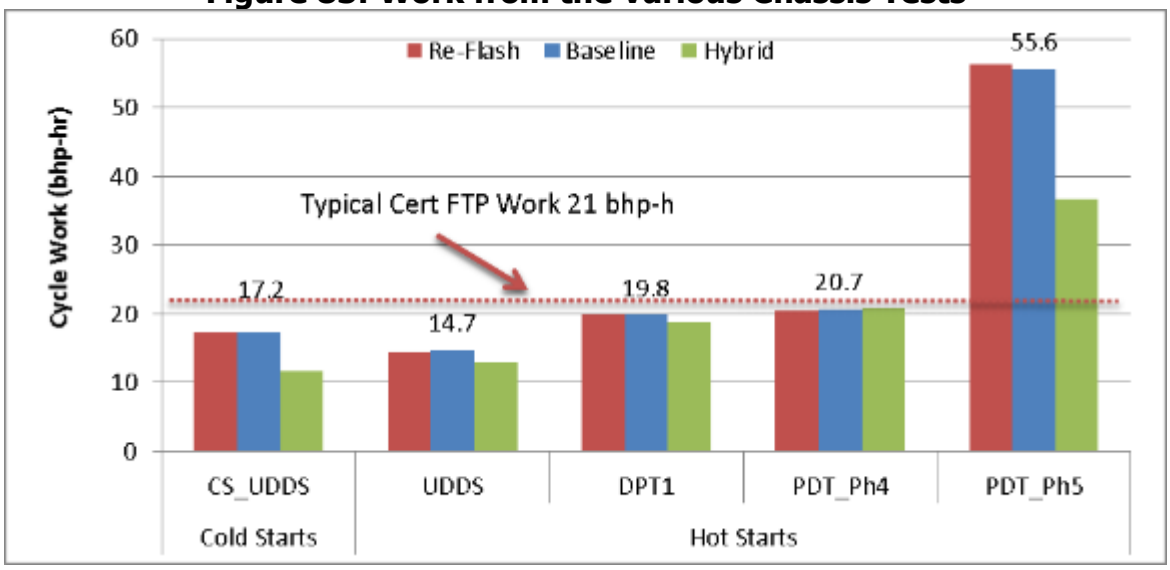

Source: Gas Technology Institute

Figure 84: Power from the Various Chassis Tests

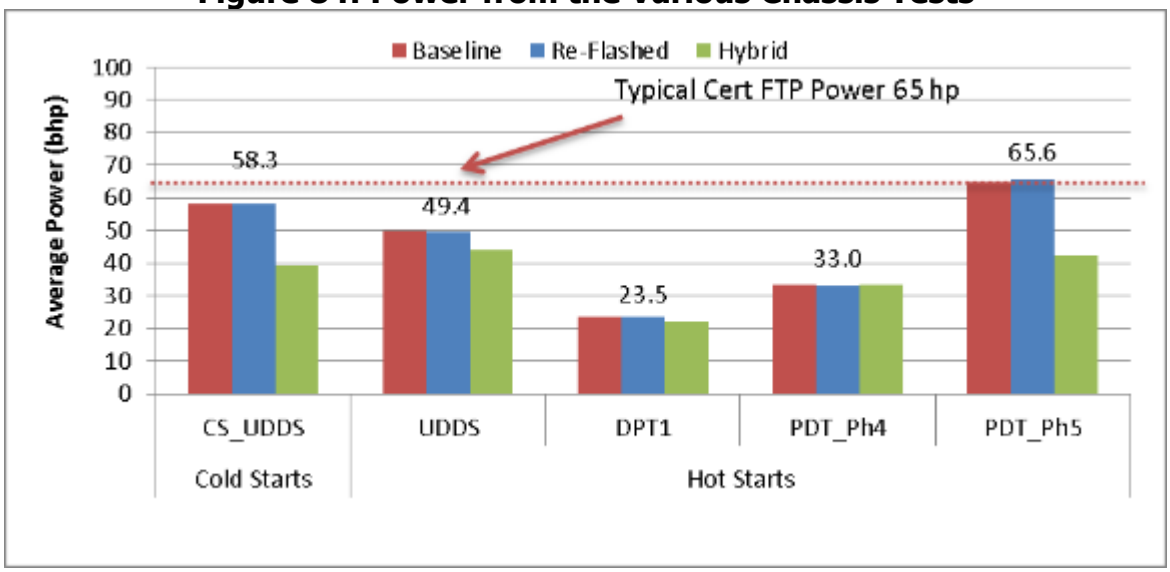

Source: Gas Technology Institute

Phase 1A: Baseline Emission Results

As described, the tests in Phase 1 were designed for a Class 7 vehicle moving 29,500 lb of load. Five different test cycles were run; first in Phase 1A for the truck in the as-delivered mode, and second in Phase 1B, after the new calibration and oxygen sensors were installed. In a subsequent phase of testing (Phase 2), the modified vehicle was powered with three energy sources and tested at the full Class-8 load of 69,500 lbs. Phase 1A results for engine work and for modal emissions are presented in Table 17 and Table 18. Results are presented in two output units: g/bhp-hr and in g/mile. Notice the NOx modal emission for the UDDS cycle is 0.131 g/bhp-hr and below the 0.2 g/bhp-hr standard. Other values for the UDDS look reasonable as well.

Table 17: Summary of Emission for the Baseline Condition (g/bhp-hr)

				Engine		Ave Modal Emission Factor (g/bhp-hr)							PM (mg/bhp-hr)			Conc. ppm
Trace	Case	Weight	sec	bhp	bhp-hr	THC	CH4	NMHC	CO	NOx	CO2	NH3	PM mg	eBC	cor_eBC	NH3
CS_UDDS	baseline	29,600	1061	58.3	17	3.36	2.94	0.42	11.1	0.676	597	0.5	2.39	0.1	0.0	150.2
UDDS	baseline	29,600	1061	49.9	15	2.35	2.08	0.27	10.1	0.131	620	0.3	0.67	0.2	0.1	80.0
DPT1	baseline	29,600	3049	23.4	20	3.64	3.25	0.39	12.6	0.172	744	0.4	3.70	1.4	1.2	67.9
PDT_Ph4	baseline	29,600	2231	33.4	21	2.59	2.30	0.29	11.9	0.083	666	0.7	2.83	1.0	0.9	115.0
PDT_Ph5	baseline	29,600	3096	64.7	56	2.80	2.50	0.30	15.1	0.291	608	0.4	0.66	0.2	0.1	89.6

Source: Gas Technology Institute

Table 18: Summary of Emission for the Baseline Condition (g/mi)

				Vehicle		Ave Modal Emission Factor (g/mi)							PM (mg/mi)			FE
Trace	Case	Weight	sec	bhp	mi	THC	CH4	NMHC	CO	NOx	CO2	NH3	PM mg	eBC	cor_eBC	MPG
CS_UDDS	baseline	29,600	1061	58.3	5.7	10.04	8.81	1.25	33.2	2.02	1786	1.6	7.14	0.36	0.02	4.20
UDDS	baseline	29,600	1061	49.9	5.7	6.09	5.39	0.71	26.2	0.34	1605	0.7	1.74	0.62	0.30	4.72
DPT1	baseline	29,600	3049	23.4	7.8	9.25	8.26	1.00	31.9	0.44	1889	1.1	9.40	3.49	2.97	3.99
PDT_Ph4	baseline	29,600	2231	33.4	8.3	6.43	5.71	0.72	29.6	0.21	1652	1.7	7.03	2.49	2.11	4.57
PDT_Ph5	baseline	29,600	3096	64.7	27.2	5.73	5.11	0.62	30.9	0.59	1243	0.7	1.34	0.47	0.26	6.00

Source: Gas Technology Institute

Phase 1B: Re-flash and New Oxygen Sensor Emissions

Phase 1B results for engine work and for modal emission are in Table 19 and Table 20. Results are presented in two output units: g/bhp-hr and in g/mile as different audiences prefer different units. Notice the NOx modal emission for the UDDS cycle shown in Figure 85 is 0.106, a value about 50 percent below the 0.2 standard and about 20 percent less than the baseline trial with the original calibration and oxygen sensors. Clearly the changes to the TWC system and engine operation, significantly improved the emission control system for NOx. Phase 1A and 1B values for PM mass and CO2 remained about the same, so there were no noticeable benefits from the upgrade. Additional emission trends are shown in Figure 86 to Figure 88.

Table 19: Summary of Emission for the Re-Flashed Condition (g/bhp-hr)

				Engine		Ave Modal Emission Factor (g/bhp-hr)							PM (mg/bhp-hr)			Conc. ppm
Trace	Case	Weight	sec	bhp	bhp-hr	THC	CH4	NMHC	CO	NOx	CO2	NH3	PM mg	eBC	cor_eBC	NH3
CS_UDDS	re-flash	29,600	1061	58.3	17.2	3.43	3.09	0.34	13.3	0.828	587	0.1	7.50	0.4	0.3	39.3
UDDS	re-flash	29,600	1061	49.4	14.5	2.87	2.56	0.31	11.7	0.106	610	0.3	0.53	0.2	0.0	76.4
DPT1	re-flash	29,600	3049	23.5	19.9	3.46	3.08	0.38	9.6	0.321	719	0.3	3.05	1.2	0.9	64.0
PDT_Ph4	re-flash	29,600	2231	33.0	20.4	2.98	2.63	0.35	11.1	0.155	647	0.5	0.18	0.1	0.0	81.5
PDT_Ph5	re-flash	29,600	3096	65.6	56.4	2.69	2.39	0.31	14.5	0.181	587	0.4	0.36	0.1	0.0	108.8

Source: Gas Technology Institute

Table 20: Summary of Emission for the Re-Flashed Condition (g/mi)

				Vehicle		Ave Modal Emission Factor (g/mi)							PM (mg/mi)			FE
Trace	Case	Weight	sec	bhp	mi	THC	CH4	NMHC	CO	NOx	CO2	NH3	PM mg	eBC	cor_eBC	MPG
CS_UDDS	re-flash	29,600	1061	58.3	5.7	10.38	9.36	1.04	40.3	2.51	1779	0.4	22.71	1.30	0.86	4.19
UDDS	re-flash	29,600	1061	49.4	5.7	7.34	6.54	0.80	29.8	0.27	1561	0.7	1.37	0.54	0.10	4.82
DPT1	re-flash	29,600	3049	23.5	7.8	8.79	7.82	0.97	24.5	0.81	1826	0.8	7.74	3.00	2.18	4.15
PDT_Ph4	re-flash	29,600	2231	33.0	8.2	7.41	6.55	0.87	27.7	0.39	1609	1.1	0.45	0.17	0.15	4.69
PDT_Ph5	re-flash	29,600	3096	65.6	27.1	5.61	4.98	0.64	30.1	0.38	1222	0.8	0.75	0.30	0.01	6.11

Source: Gas Technology Institute

Figure 85: NOx Emission Trends for the Re-flashed Condition (g/bhp-hr)

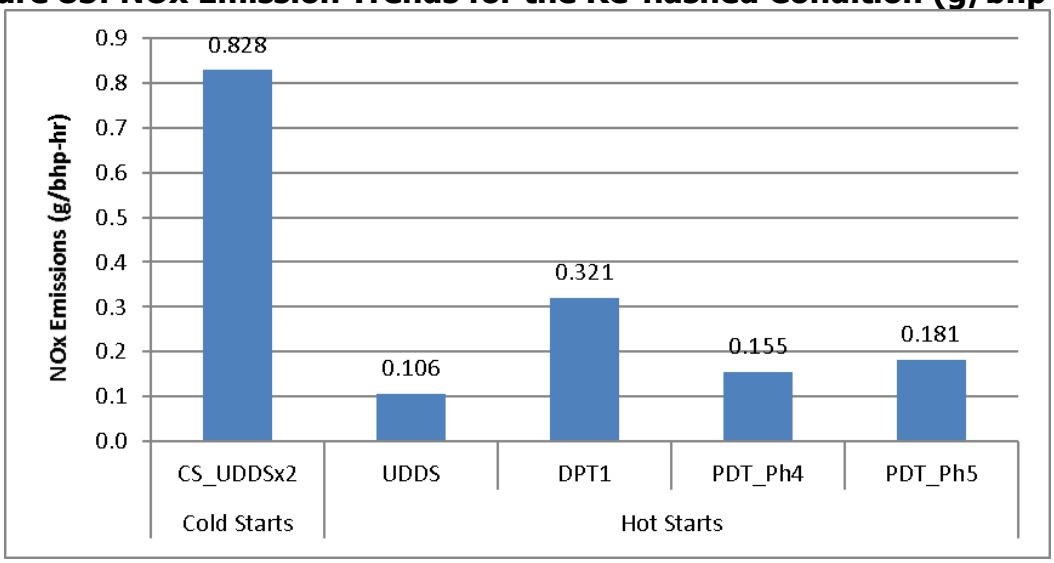

Source: Gas Technology Institute

Figure 86: HC Emission Trends for the Re-flashed Condition (g/bhp-hr)

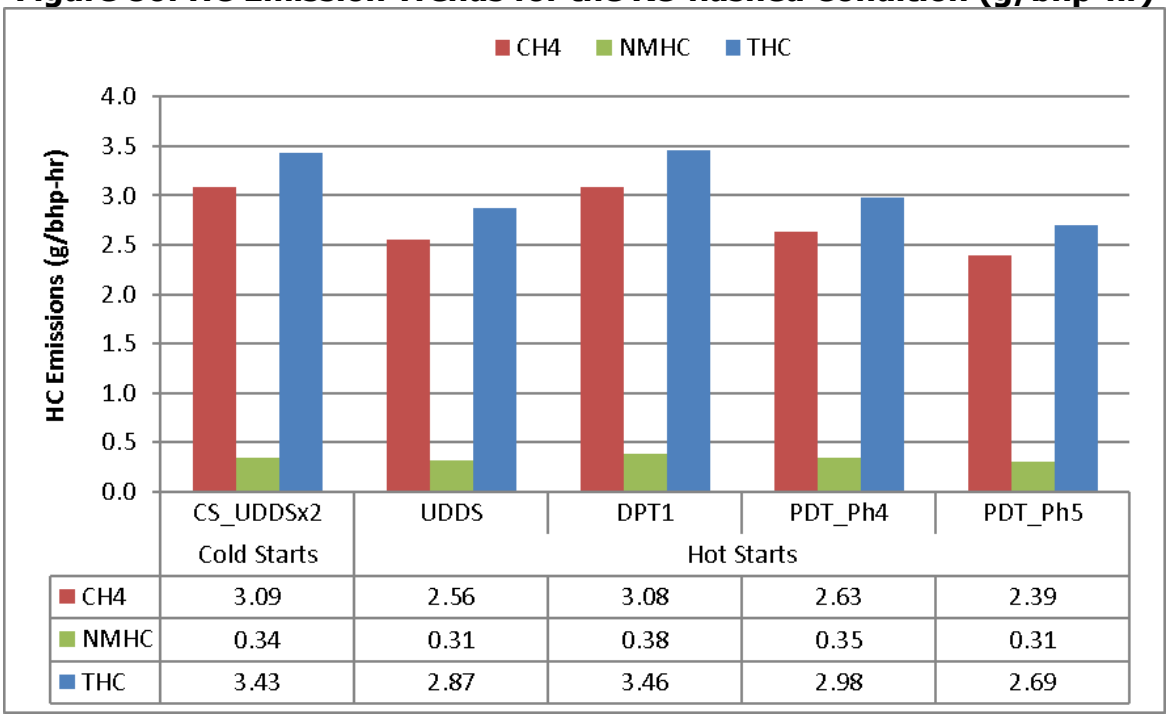

Source: Gas Technology Institute

Figure 87: PM Emission Trends for the Re-flashed Condition (g/bhp-hr)

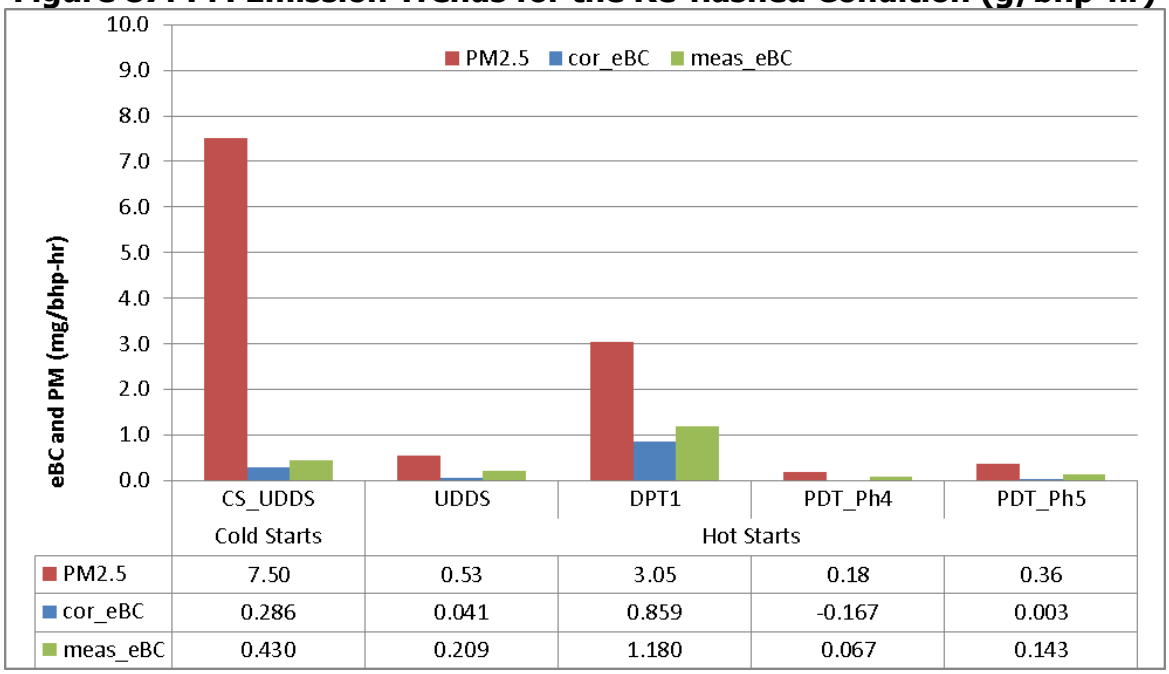

	CS_UDDS (Cold Starts)	UDDS (Hot Starts)	DPT1 (Hot Starts)	PDT_Ph4 (Hot Starts)	PDT_Ph5 (Hot Starts)
PM2.5	7.50	0.53	3.05	0.18	0.36
cor_eBC	0.286	0.041	0.859	-0.167	0.003
meas_eBC	0.430	0.209	1.180	0.067	0.143

Source: Gas Technology Institute

Phase 2: Hybrid

Two configurations were tested for the hybrid system, 1) light and 2) heavy. Light represents a comparison to the baseline vehicle configured for 29,600 lb and the heavy represents a fully loaded goods movement vehicle of 69,500 lb.

Hybrid – Light

The emission (light) from the hybrid configuration are shown in the next three tables in g/bhp-hr basis and the other table is on a g/mi basis. The work presented in Table 21 to Table 23 is based on the measured ECM power and work. The SOC percent is the net change over the test cycle. The SOC ranged from -16 percent (lower power state at the end of the test) to +2 percent. The hot UDDS showed almost less than 2 percent SOC change. The actual cycle average work includes the total work over the cycle, ECM plus electric power. The total cycle work is presented in the last table in this section.

Table 21: Summary of Emission for the Hybrid Condition in (g/bhp-hr): ECM Power

				Engine		Ave Modal Emission Factor (g/bhp-hr)							PM (mg/bhp-hr)			Conc. ppm	
Trace	Case	Weight	sec	bhp	bhp-hr	THC	CH4	NMHC	CO	NOx	CO2	NH3	PM mg	eBC	cor_eBC	NH3	SOC
CS_UDDS	hybrid, re-flash	29,600	1061	39.3	11.6	3.98	3.44	0.55	18.24	1.007	755	0.6	1.97	0.11	-0.06	114.8	-4.0
UDDS	hybrid, re-flash	29,600	1061	44.1	13.0	2.33	2.10	0.23	11.86	0.057	656	0.7	0.66	0.25	0.11	125.7	-1.0
DPT1	hybrid, re-flash	29,600	3049	22.1	18.7	2.65	2.38	0.28	6.83	0.131	793	0.4	5.17	1.84	1.62	20.6	-2.0
PDT_Ph4	hybrid, re-flash	29,600	2231	33.5	20.8	2.26	2.02	0.24	10.90	0.035	756	0.0	0.83	0.30	0.13	0.0	2.0
PDT_Ph5	hybrid, re-flash	29,600	3096	42.6	36.6	2.46	2.20	0.26	14.24	0.052	782	0.5	0.43	0.16	0.00	81.1	-16.0

Source: Gas Technology Institute

Table 22: Summary of Emission for the Hybrid Condition in (g/mi)

				Vehicle		Ave Modal Emission Factor (g/mi)							PM (mg/mi)			FE
Trace	Case	Weight	sec	bhp	mi	THC	CH4	NMHC	CO	NOx	CO2	NH3	PM mg	eBC	cor_eBC	MPG
CS_UDDS	hybrid, re-flash	29,600	1061	39.3	5.6	8.22	7.10	1.13	37.7	2.08	1559	1.3	4.07	0.22	-0.13	4.78
UDDS	hybrid, re-flash	29,600	1061	44.1	5.6	5.37	4.85	0.53	27.3	0.13	1512	1.7	1.53	0.58	0.26	5.00
DPT1	hybrid, re-flash	29,600	3049	22.1	7.8	6.38	5.73	0.66	16.4	0.32	1906	1.1	12.42	4.42	3.89	4.03
PDT_Ph4	hybrid, re-flash	29,600	2231	33.5	8.3	5.66	5.06	0.60	27.3	0.09	1893	0.0	2.07	0.75	0.32	4.02
PDT_Ph5	hybrid, re-flash	29,600	3096	42.6	27.1	3.33	2.98	0.36	19.3	0.07	1057	0.7	0.58	0.22	0.00	7.16

Source: Gas Technology Institute

Table 23: Summary of Emission for the Hybrid Condition in (g/bhp-hr): Total Power

				Engine		Ave Modal Emission Factor (g/bhp-hr)							PM (mg/bhp-hr)			Conc. ppm
Trace	Case	Weight	sec	bhp	bhp-hr	THC	CH4	NMHC	CO	NOx	CO2	NH3	PM mg	eBC	cor_eBC	NH3
CS_UDDS	hybrid, re-flash	29,600	1061	58.3	17.2	2.68	2.32	0.37	12.30	0.679	509	0.4	1.33	0.07	-0.04	114.8
UDDS	hybrid, re-flash	29,600	1061	49.4	14.5	2.08	1.88	0.20	10.61	0.051	586	0.6	0.59	0.23	0.10	125.7
DPT1	hybrid, re-flash	29,600	3049	23.5	19.9	2.49	2.24	0.26	6.42	0.123	745	0.4	4.86	1.73	1.52	20.6
PDT_Ph4	hybrid, re-flash	29,600	2231	33.0	20.4	2.29	2.05	0.24	11.07	0.036	768	0.0	0.84	0.30	0.13	0.0
PDT_Ph5	hybrid, re-flash	29,600	3096	65.6	56.4	1.60	1.43	0.17	9.25	0.033	507	0.3	0.28	0.10	0.00	81.1

Source: Gas Technology Institute

Hybrid – Heavy

The hybrid configuration can provide power up to 580 hp which is representative of a typical 15-liter engine for a Class 8 truck. As such, additional testing was performed at 69,500 lb. However, the baseline conventional vehicle is limited in power. To make comparisons with the baseline conventional vehicle at 69,500 lb, the UDDS test cycles were operated at baseline conditions.

The conventional vehicle (heavy configuration) emission are shown in Table 24 through Table 27. The hybrid emission (heavy configuration) are shown in tables after the baseline ones. The first table is in g/bhp-hr basis and the other table is on a g/mi basis.

Table 24: Summary of Emission for the Heavy Re-Flashed Condition in (g/bhp-hr)

				Engine		Ave Modal Emission Factor (g/bhp-hr)							PM (mg/bhp-hr)			Conc. ppm
Trace	Case	Weight	sec	bhp	bhp-hr	THC	CH4	NMHC	CO	NOx	CO2	NH3	PM mg	eBC	cor_eBC	NH3
UDDS	re-flash	69,500	1061	74.6	22.0	2.10	1.97	0.13	10.24	0.082	561	0.1	0.95	0.2	0.0	62.4

Source: Gas Technology Institute

Table 25: Summary of Emission for the Heavy Re-Flashed Condition in (g/mi)

				Vehicle		Ave Modal Emission Factor (g/mi)							PM (mg/mi)			FE
Trace	Case	Weight	sec	bhp	mi	THC	CH4	NMHC	CO	NOx	CO2	NH3	PM mg	eBC	cor_eBC	MPG
UDDS	re-flash	69,500	1061	74.6	5.6	8.18	7.68	0.50	39.9	0.32	2185	0.6	1.65	0.66	0.18	3.46

Source: Gas Technology Institute

Table 26: Summary of Emission for the Heavy Hybrid Condition in (g/bhp-hr): ECM power

				Engine		Ave Modal Emission Factor (g/bhp-hr)							PM (mg/bhp-hr)			Conc. ppm	
Trace	Case	Weight	sec	bhp	bhp-hr	THC	CH4	NMHC	CO	NOx	CO2	NH3	PM mg	eBC	cor_eBC	NH3	SOC
CS_UDDS	hybrid, re-flash	69,500	1061	74.8	22.1	2.18	1.91	0.27	13.10	0.595	524	0.5	2.19	0.12	0.02	134.4	-2.0
UDDS	hybrid, re-flash	69,500	1061	71.9	21.2	1.90	1.72	0.19	11.84	0.041	571	0.6	0.42	0.15	0.03	136.4	-3.0
DPT1	hybrid, re-flash	69,500	3049	44.5	37.7	1.47	1.35	0.13	9.94	0.028	646	0.7	1.02	0.38	0.22	81.9	13.0
PDT_Ph4	hybrid, re-flash	69,500	2231	43.6	27.0	1.94	1.75	0.19	12.51	0.025	718	0.7	0.66	0.25	0.09	126.8	2.0
PDT_Ph5	hybrid, re-flash	69,500	3096	84.8	72.9	2.26	2.05	0.21	13.96	0.214	594	0.3	0.32	0.12	0.02	88.9	0.0

Source: Gas Technology Institute

Table 27: Summary of Emission for the Heavy Hybrid Condition in (g/mi)

				Vehicle		Ave Modal Emission Factor (g/mi)							PM (mg/mi)			FE
Trace	Case	Weight	sec	bhp	mi	THC	CH4	NMHC	CO	NOx	CO2	NH3	PM mg	eBC	cor_eBC	MPG
CS_UDDS	hybrid, re-flash	69,500	1061	74.8	5.7	8.46	7.44	1.03	50.9	2.31	2038	2.0	8.52	0.48	0.08	3.67
UDDS	hybrid, re-flash	69,500	1061	71.9	5.6	6.74	6.08	0.66	41.8	0.14	2024	1.9	1.33	0.48	0.06	3.72
DPT1	hybrid, re-flash	69,500	3049	44.5	7.8	7.10	6.48	0.63	47.9	0.13	3112	3.2	4.89	1.83	1.06	2.45
PDT_Ph4	hybrid, re-flash	69,500	2231	43.6	8.2	6.43	5.81	0.62	41.5	0.08	2381	2.2	2.19	0.82	0.30	3.19
PDT_Ph5	hybrid, re-flash	69,500	3096	84.8	27.2	6.06	5.50	0.57	37.4	0.57	1590	0.9	0.85	0.33	0.06	4.71

Source: Gas Technology Institute

Fuel Economy: Phase 1 and 2

The fuel economy of a vehicles is evaluated by the carbon balance method which is a direct calculation of the CO2 emission. The higher the CO2 emission the higher the fuel consumption. CO2 emission are regulated by EPA using the engine dyno FTP and SET test cycles. The FTP is most comparable to the UDDS test cycle.

Conventional

The UDDS CO2 emission were above the 555 g/bhp-hr FTP standard (2017 FTP engine standard for HHDTs) for the cold start and hot start tests. The CO2 emission varied slightly between cycles and configuration where only the near dock cycle (DPT1) showed a statistically higher CO2 emission rate. The average CO2 for all the cycles was 584 g/bhp-hr, and 565 g/bhp-hr with the PDT1 cycle removed. The CO2 standard is 555 g/bhp-hr for this displacement engine. It is suggested the higher in-use CO2 value (in the chassis vs on a test stand) could be a result of additional losses in the chassis where the certification test occurs with the engine on a test stand.

The ISL G MPG on a diesel gallon equivalent (MPGde) basis (assuming 2863 g natural gas/gallon diesel (14)) ranges from 4.15 MPGde for the near dock port cycle (DPT1) to 6.1 MPGde for the regional cruise port cycle (PDT_Ph5).

Hybrid - Light

The hybrid vehicle fuel economy was about the same for some cycles and improved for others. The fuel economy ranged from 4 MPGde for DPT1 to 7.16 MPGde for the regional port cycle DPT_Ph5. Note there was a change in 16 percent for the SOC so the benefit is reduced by the need to recover the energy of the batteries.

Hybrid - Heavy

The hybrid-heavy vehicle fuel economy ranged from 2.4 MPGde for DPT1 to 4.7 MPGde for the regional port cycle DPT_Ph5. The SOC had a net change of +13 percent for the DPT1 cycle suggesting some additional energy loss should be applied.

Global Warming Potential

The global warming potential is presented in the next several tables for the baseline, re-flashed, and hybrid condition. The GWP and BC emission are lowest for the hybrid system.

Conventional

The conventional GWP and BC are presented in Table 28 through Table 31. Table 28 and Table 29 show the baseline and re-flashed conditions on a g/bhp-hr basis and Table 30and Table 31 show the same thing, but on a g/mi basis. There is no significant change in the GWP between Phase 1A and 1B.

Table 28: Summary of GWP Results for the Baseline Condition (g/bhp-hr)

Trace	Case	Weight	CO_2	CH_4	est N_2O	GWP ($CO_{2\ eq}$)	CO2/GWP	eBC mg	eBC/$PM_{2.5}$
CS_UDDSx2	baseline	29,000	597.1	2.94	0.047	872.3	0.68	0.007	1.9%
UDDS	baseline	29,000	620.4	2.08	0.047	711.4	0.87	0.116	14.8%
DPT1	baseline	29,000	743.8	3.25	0.047	830.1	0.90	1.170	18.0%
PDT_Ph4	baseline	29,000	665.6	2.30	0.047	728.2	0.91	0.851	17.8%
PDT_Ph5	baseline	29,000	608.0	2.50	0.047	675.6	0.90	0.125	14.8%

[1] N_2O was not measured but was estimated (est N_2O) from previous testing on a similar TWC 8.9 liter natural gas engine by UCR. This is needed to estimate the total GHG potential.

Source: Gas Technology Institute

Table 29: Summary of GWP Results for the Re-flashed Condition (g/bhp-hr)

Trace	Case	Weight	CO2	CH4	est N2O	GWP (CO2 eq)	CO2/GWP	eBC mg	eBC/PM2.5
CS_UDDSx2	re-flash	29,000	587.4	3.09	0.047	669.7	0.88	0.286	14.5%
UDDS	re-flash	29,000	610.0	2.56	0.047	678.9	0.90	0.041	5.4%
DPT1	re-flash	29,000	718.8	3.08	0.047	800.8	0.90	0.859	19.6%
PDT_Ph4	re-flash	29,000	647.1	2.63	0.047	717.9	0.90	0.010	4.3%
PDT_Ph5	re-flash	29,000	586.6	2.39	0.047	651.3	0.90	0.003	0.7%

[1] N_2O was not measured but was estimated (est N_2O) from previous testing on a similar TWC 8.9 liter natural gas engine by UCR. This is needed to estimate the total GHG potential.

Source: Gas Technology Institute

Table 30: Summary of GWP Results for the Baseline Condition (g/mi)

Trace			CO_2	CH_4	est N_2O	GWP ($CO_{2\ eq}$)	CO2/GWP	eBC	eBC/$PM_{2.5}$
CS_UDDSx2	baseline	29000	1786	8.81	0.209	2608	0.68	0.022	1.9%
UDDS	baseline	29000	1605	5.39	0.209	1841	0.87	0.300	14.8%
DPT1	baseline	29000	1889	8.26	0.209	2100	0.90	2.971	18.0%
PDT_Ph4	baseline	29000	1652	5.71	0.209	1799	0.92	2.112	17.8%
PDT_Ph5	baseline	29000	1243	5.11	0.209	1375	0.90	0.256	14.8%

[1] N_2O was not measured but was estimated (est N_2O) from previous testing on a similar TWC 8.9 liter natural gas engine by UCR. This is needed to estimate the total GHG potential.

Source: Gas Technology Institute

Table 31: Summary of GWP Results for the Re-flashed Condition (g/mi)

Trace			CO_2	CH_4	est N_2O	GWP ($CO_{2\ eq}$)	CO2/GWP	eBC	eBC/$PM_{2.5}$
CS_UDDSx2	re-flash	29000	1779	9.36	0.209	2018	0.88	0.865	14.5%
UDDS	re-flash	29000	1561	6.54	0.209	1730	0.90	0.105	5.4%
DPT1	re-flash	29000	1826	7.82	0.209	2026	0.90	2.183	19.6%
PDT_Ph4	re-flash	29000	1609	6.55	0.209	1778	0.91	0.150	25.9%
PDT_Ph5	re-flash	29000	1222	4.98	0.209	1352	0.90	0.007	0.7%

[1] N_2O was not measured but was estimated (est N_2O) from previous testing on a similar TWC 8.9 liter natural gas engine by UCR. This is needed to estimate the total GHG potential.

Source: Gas Technology Institute

Hybrid - Light

Table 32: Summary of GWP Results for the Hybrid Condition (g/bhp-hr)

Trace	Case	Weight	CO2	CH4	est N2O	GWP (CO2 eq)	CO2/GWP	eBC mg	eBC/PM2.5
CS_UDDS	hybrid, re-flash	29,600	755.1	3.44	0.047	846.0	0.89	-0.062	-3.1%
UDDS	hybrid, re-flash	29,600	655.6	2.10	0.047	713.2	0.92	0.112	16.9%
DPT1	hybrid, re-flash	29,600	792.8	2.38	0.047	857.4	0.92	1.619	31.3%
PDT_Ph4	hybrid, re-flash	29,600	755.8	2.02	0.047	811.3	0.93	0.128	15.5%
PDT_Ph5	hybrid, re-flash	29,600	781.5	2.20	0.047	841.6	0.93	0.002	0.5%

[1] N_2O was not measured but was estimated (est N_2O) from previous testing on a similar TWC 8.9 liter natural gas engine by UCR. This is needed to estimate the total GHG potential.

Source: Gas Technology Institute

Table 33: Summary of GWP Results for the Hybrid Condition (g/mi)

Trace			CO_2	CH_4	est N_2O	GWP ($CO_{2\ eq}$)	CO2/GWP	eBC	eBC/$PM_{2.5}$
CS_UDDS	hybrid, re-flash	29600	1559	7.10	0.209	1741	0.90	-0.128	-3.1%
UDDS	hybrid, re-flash	29600	1512	4.85	0.209	1638	0.92	0.259	16.9%
DPT1	hybrid, re-flash	29600	1906	5.73	0.209	2054	0.93	3.891	31.3%
PDT_Ph4	hybrid, re-flash	29600	1893	5.06	0.209	2024	0.93	0.322	15.5%
PDT_Ph5	hybrid, re-flash	29600	1057	2.98	0.209	1137	0.93	0.003	0.5%

[1] N_2O was not measured but was estimated (est N_2O) from previous testing on a similar TWC 8.9 liter natural gas engine by UCR. This is needed to estimate the total GHG potential.

Source: Gas Technology Institute

Hybrid - Heavy

Table 34: Summary of GWP Results for the Hybrid Condition (g/bhp-hr)

Trace	Case	Weight	CO2	CH4	est N2O	GWP (CO2 eq)	CO2/GWP	eBC mg	eBC/PM2.5
CS_UDDS	hybrid, re-flash	69,500	524.1	1.91	0.047	576.9	0.91	0.021	1.0%
UDDS	hybrid, re-flash	69,500	570.6	1.72	0.047	618.5	0.92	0.035	8.2%
DPT1	hybrid, re-flash	69,500	646.0	1.35	0.047	684.7	0.94	0.220	21.7%
PDT_Ph4	hybrid, re-flash	69,500	718.0	1.75	0.047	766.8	0.94	0.089	13.5%
PDT_Ph5	hybrid, re-flash	69,500	593.9	2.05	0.047	650.3	0.91	0.021	6.6%

[1] N_2O was not measured but was estimated (est N_2O) from previous testing on a similar TWC 8.9 liter natural gas engine by UCR. This is needed to estimate the total GHG potential.

Source: Gas Technology Institute

Table 35: Summary of GWP Results for the Hybrid Condition (g/mi)

Trace			CO_2	CH_4	est N_2O	GWP ($CO_{2\ eq}$)	CO2/GWP	eBC	eBC/$PM_{2.5}$
CS_UDDS	hybrid, re-flash	69500	2038	7.44	0.209	2229	0.91	0.081	1.0%
UDDS	hybrid, re-flash	69500	2024	6.08	0.209	2181	0.93	0.060	4.5%
DPT1	hybrid, re-flash	69500	3112	6.48	0.209	3279	0.95	1.059	21.7%
PDT_Ph4	hybrid, re-flash	69500	2381	5.81	0.209	2531	0.94	0.295	13.5%
PDT_Ph5	hybrid, re-flash	69500	1590	5.50	0.209	1732	0.92	0.056	6.6%

[1] N_2O was not measured but was estimated (est N_2O) from previous testing on a similar TWC 8.9 liter natural gas engine by UCR. This is needed to estimate the total GHG potential.

Source: Gas Technology Institute

Benefits Comparison

This section presents the emission, fuel economy and performance differences between the phase 1 (non-hybrid) conditions, the hybrid conditions, and the heavy vs light hybrid conditions.

Phase 1: Emissions

The re-flash approach resulted in NOx emission that were reduced for some cycles and increased for others (Figure 88). Significant NOx benefits were achieved for the hybridized system as explained later. NH3 emission reductions were also mixed as shown in Figure 89.

Figure 88: NOx Emission Trends for the Baseline and Re-flashed Condition (g/bhp-hr)

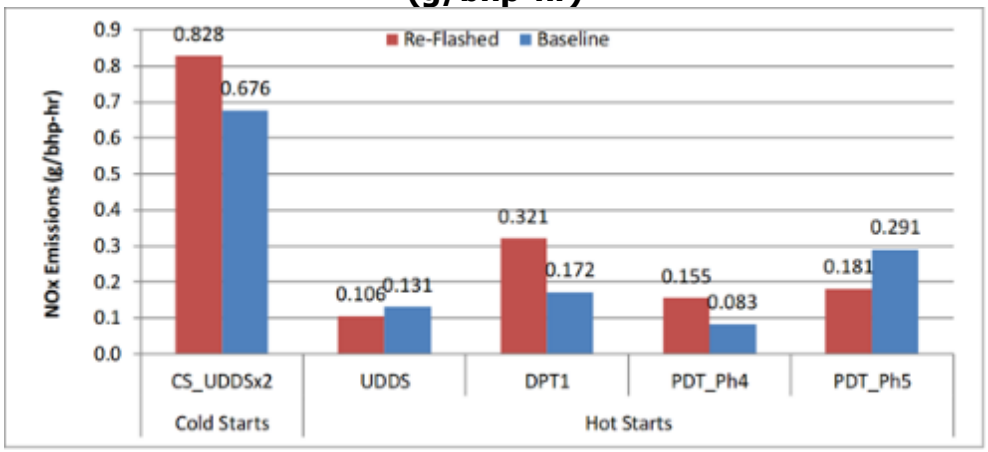

Source: Gas Technology Institute

Figure 89: NH_3 Emission Trends for the Baseline and Re-flashed Condition (g/bhp-hr)

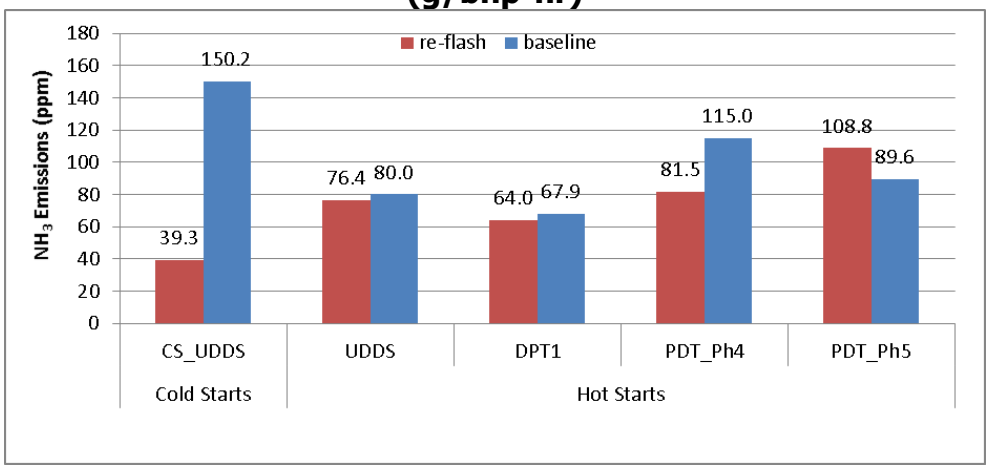

Source: Gas Technology Institute

Phase 1: Fuel Economy

The fuel economy did not significantly improve for the re-flashed ECM configuration as shown in Figure 90.

Figure 90: CO2 Emission Trends for the Baseline and Re-flashed Condition (g/bhp-hr)

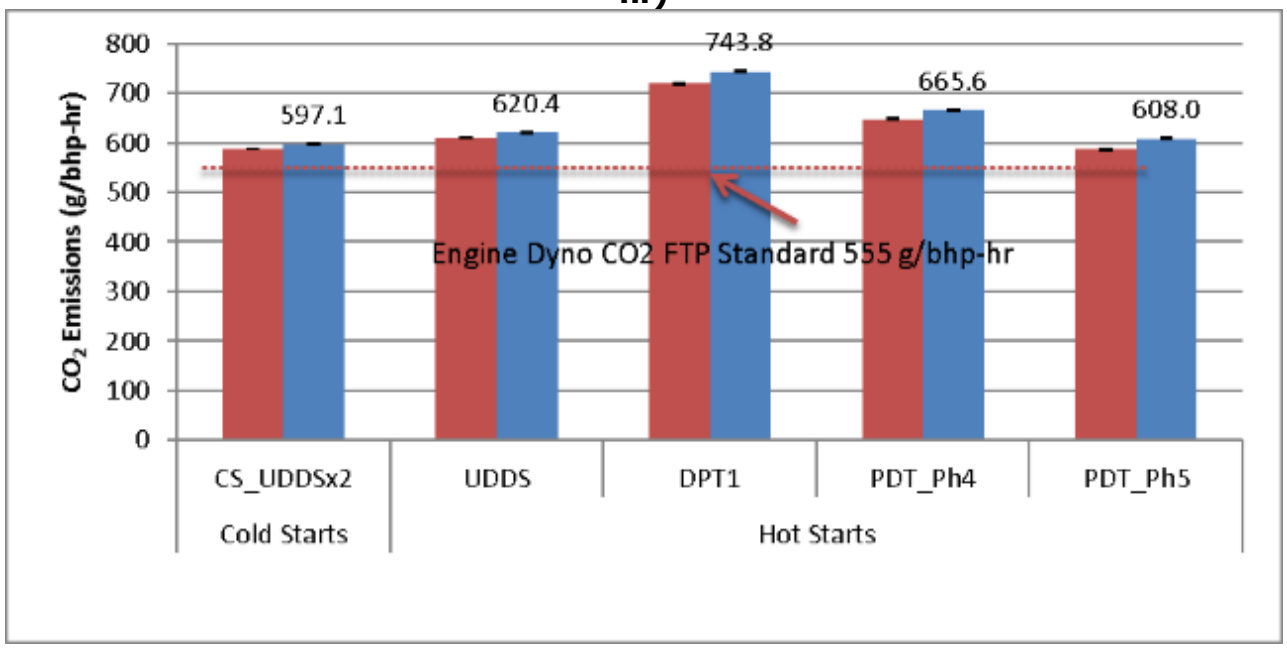

Source: Gas Technology Institute

Phase 1: Real Time Emissions

This section presents a discussion about the cause for the NOx emission, which were primarily a result of cold start operation and accelerations.

Cold Start Emissions

Colds starts are significant and represent about 80 percent of the total emission. Warm start emissions were much lower and not much different than running emissions.

In addition, the near-zero product has eliminated the cold start emission spike with better fuel management as can be seen in Chapter 7, which discusses the comparisons to the new near-zero engine (Figure 91 to Figure 93).

Figure 91: Hot and Cold NOx Real Time Mass Accumulation, Baseline Configuration

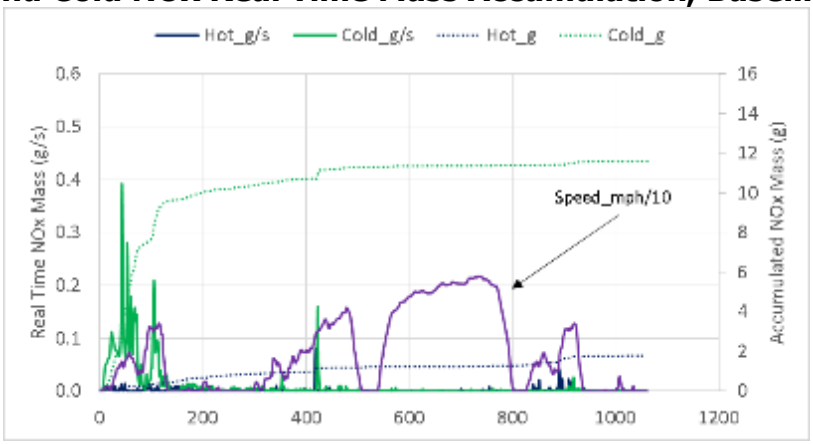

Source: Gas Technology Institute

Figure 92: Hot and Cold NOx Real Time Mass Accumulation, Re-Flash Configuration

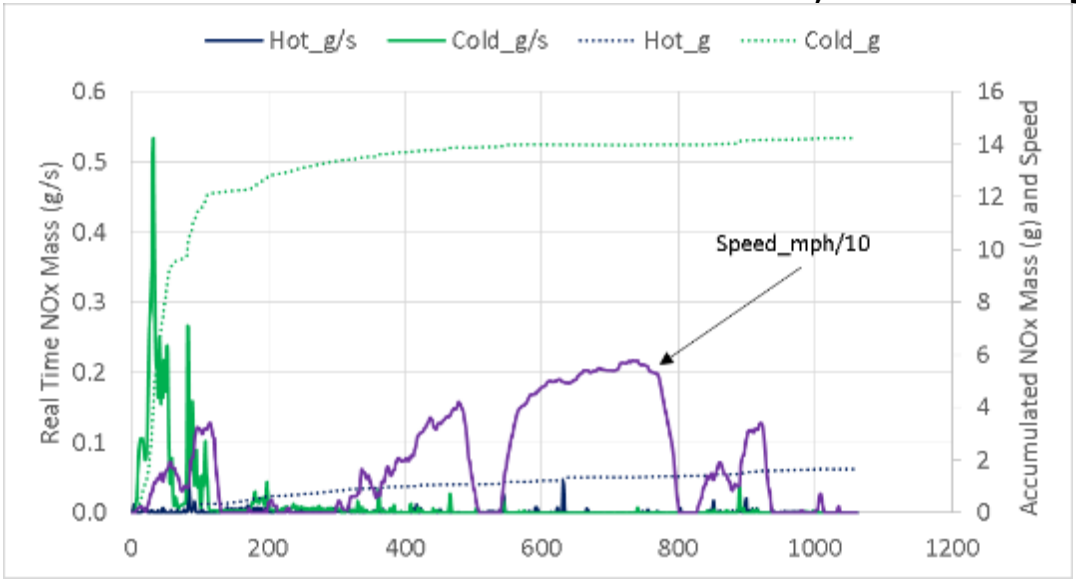

Source: Gas Technology Institute

Figure 93: Hot and Cold Start NOx Accumulation Mass and Exhaust Temperature

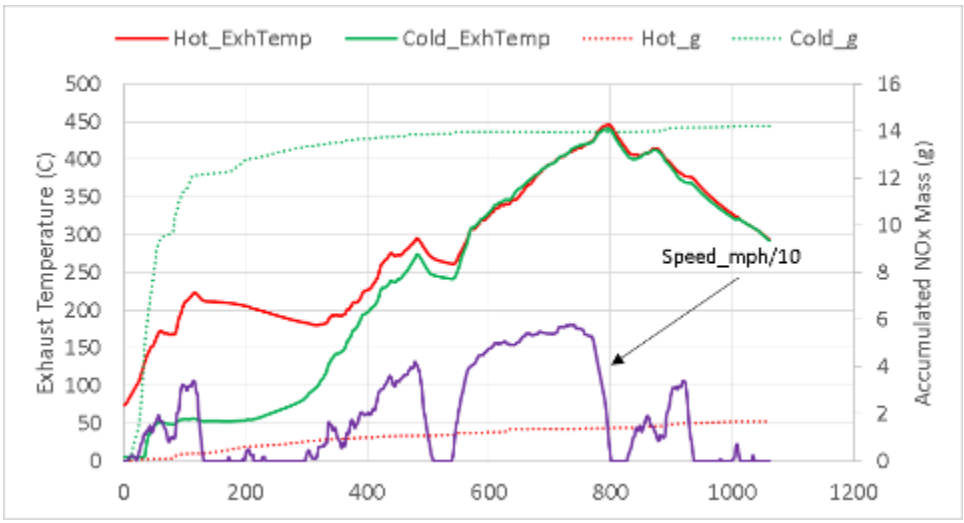

Source: Gas Technology Institute

Hot Transients

There was no change between baseline and re-flashed conditions for transient operation as seen in Figure 94 and Figure 95. When comparisons were made to the near-zero project, there was a significant difference between this engine and the near-zero engine.

Figure 94: Configuration

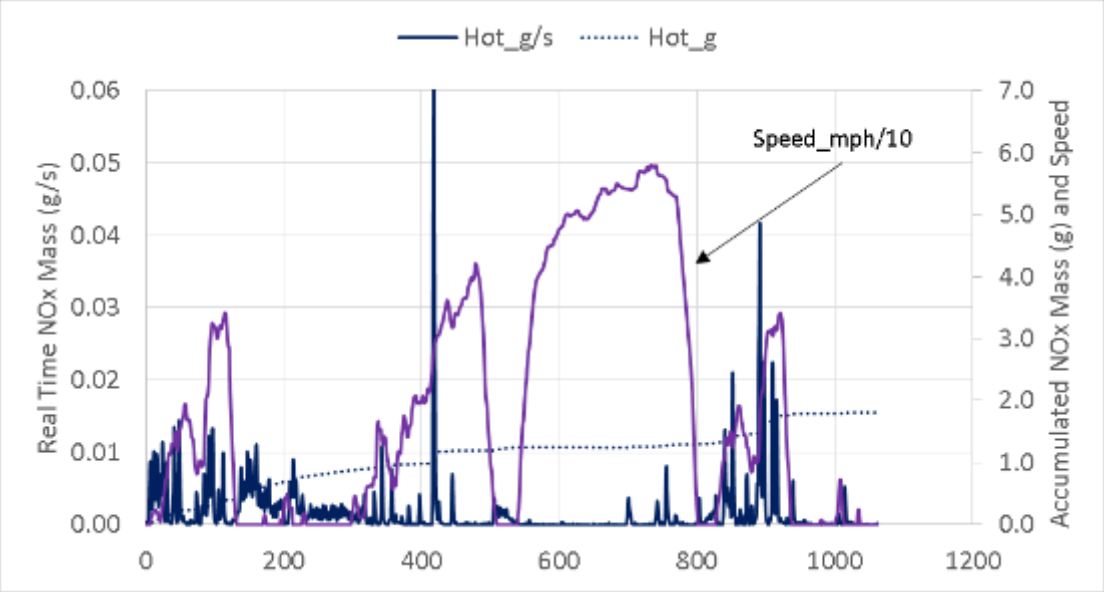

Source: Gas Technology Institute

Figure 95: Hot NOx Real Time Mass and Accumulation, Conventional Re-flash Configuration

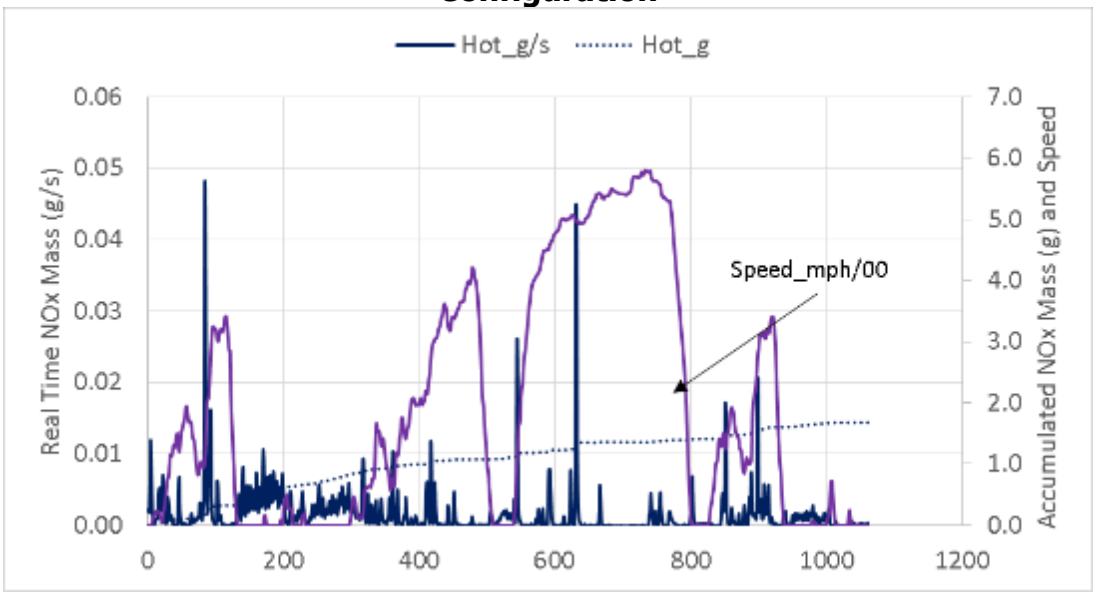

Source: Gas Technology Institute

Phase 2: Emissions

Since the hybrid uses less engine power, the work specific emission must be considered based on total cycle power instead of engine power. As such, the overall NOx emission benefit for the hybrid configuration over the improved conventional configuration is 64 percent for NOx, 1 percent for CO2, and 1 percent for fuel economy (based on total cycle power). If the cold start emissions are included, the benefit reduces to 32 percent, 4 percent, and 4 percent respectively (Figure 96).

Figure 96: CO_2 Emission Trends for the Re-flashed and Hybrid Condition (g/bhp-hr): total power

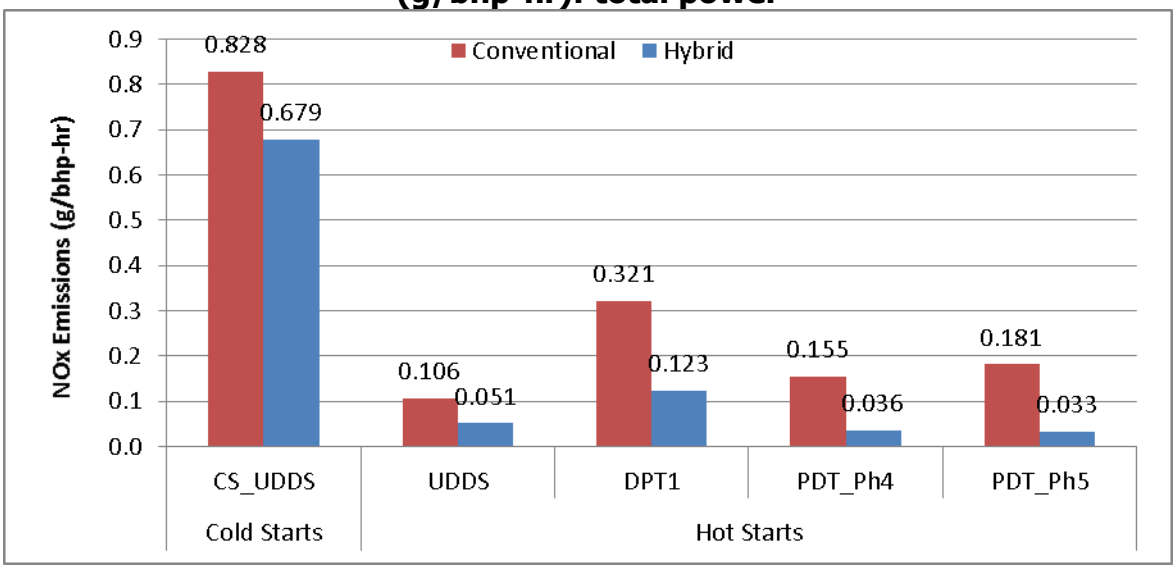

Source: Gas Technology Institute

Phase 2: Fuel Economy

The fuel economy comparison between the conventional (phase 1b) and the hybrid (light) is provided in Figure 97. The hybrid showed lower fuel consumption benefit for the UDDS and Ph5 of the port cycle, but higher fuel consumption for the DPT1 and Ph4 port cycle. The higher fuel consumption was a result of the light load and low duty cycle and the engine running as a charging system for more of the cycle. SOC for all the cycles was mostly the same for all the cycles. The CO2 emission of the hybrid system in Figure 99 show lower fuel consumption than a diesel equivalent where a diesel equivalent shows on average 800 g/bhp-hr but the hybrid was around 745 g/bhp-hr with equivalent power. The hybrid system shows the highest benefits at full load. The hybrid-heavy bsCO2 was the lowest and much lower than the diesel equivalent.

Figure 97: CO2 Emission for the Conventional and Hybrid Condition (g/bhp-hr)

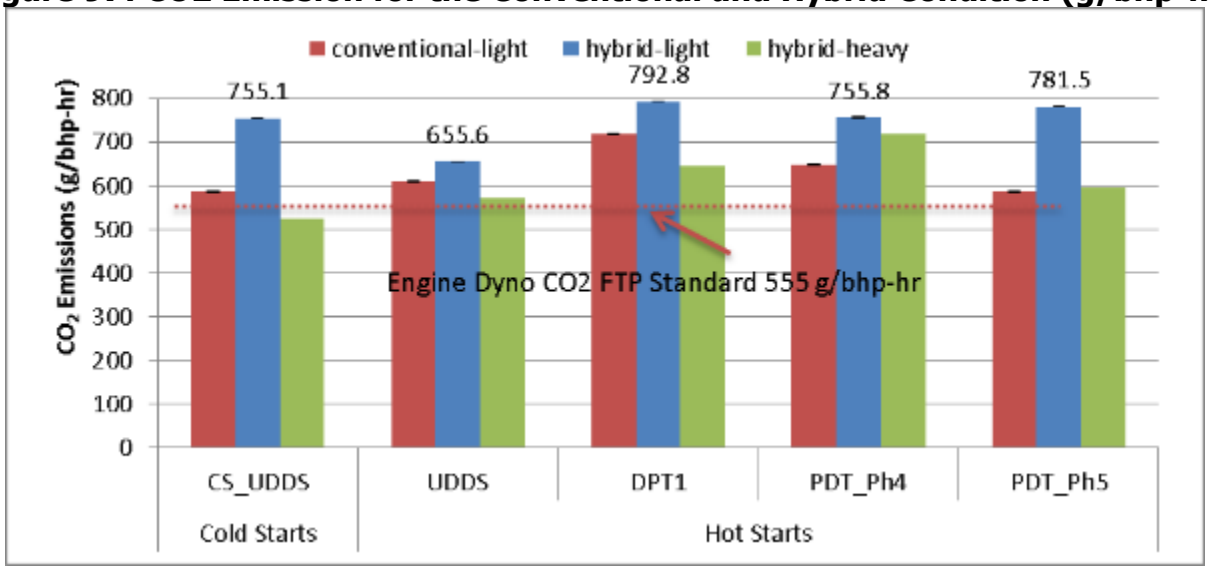

Source: Gas Technology Institute

Phase 2: Real Time Emissions

The real time emission show where the emissions are formed and what more can be done to minimize their contribution. Figure 98 shows that the hybrid configuration accumulated NOx emission less continuously than the conventional. All the benefit is from lower throttle response. This shows the benefit of hybridizing natural gas engines equipped with TWC and air-to-fuel ratio control.

Figure 98: NOx Emission Trends for the Re-flashed and Hybrid Condition (g/bhp-hr)

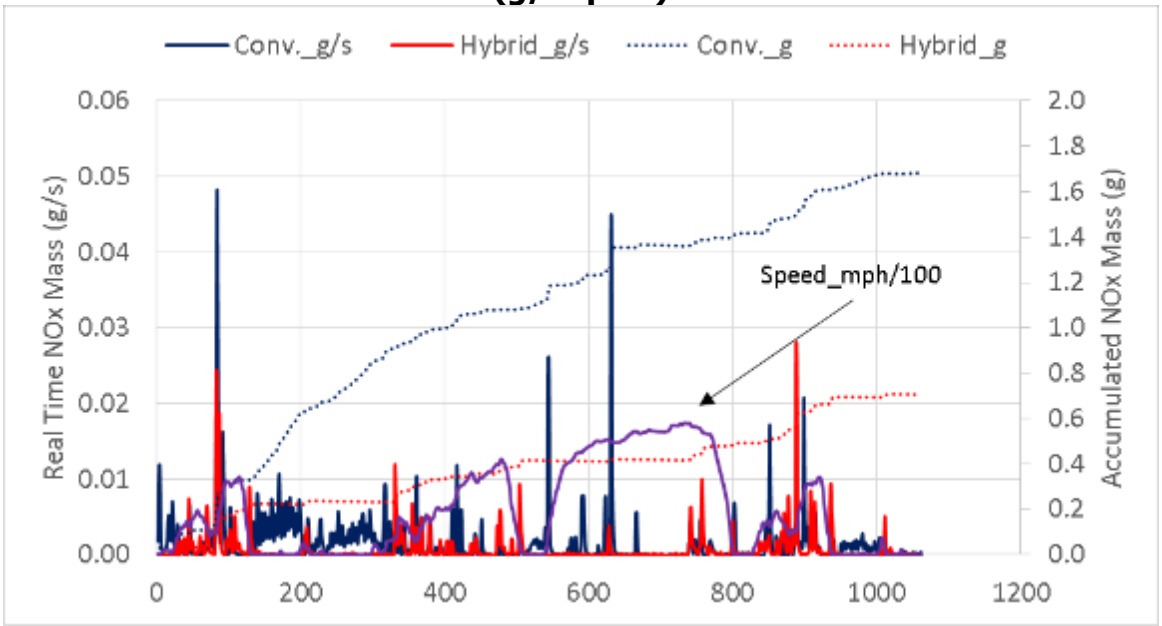

Source: Gas Technology Institute

Phase 2: Performance - Heavy

Figure 99 through Figure 101 show the velocity profile of the conventional and hybrid system and the associated power consumed by the hybrid for the engine and electric systems. The hybrid accelerated 11 seconds faster from 0-40 mph and showed an acceleration rate of 1.4 mph/sec compared to a 1 mph/sec rate for the conventional vehicle. The total engine power ranged from 0 hp to 280 hp where the electric ranged from -50 (charging) to + 100 hp (accelerating the vehicle). During the UDDS test cycle the total engine power peaked at 380 hp.

Figure 99: Real-Time Performance Conventional vs Hybrid – Heavy Condition

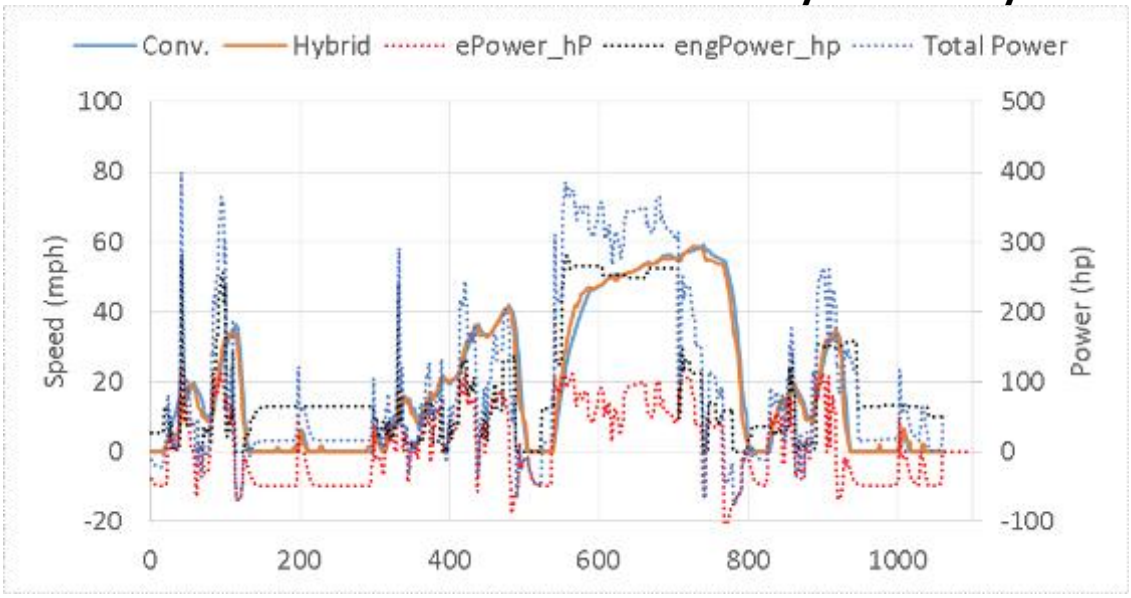

Source: Gas Technology Institute

Figure 100: Real-time Performance Conventional vs Hybrid – Heavy Condition: Detail 1

Source: Gas Technology Institute

Figure 101: Real-Time Performance Conventional vs Hybrid – Heavy Condition: Detail 2

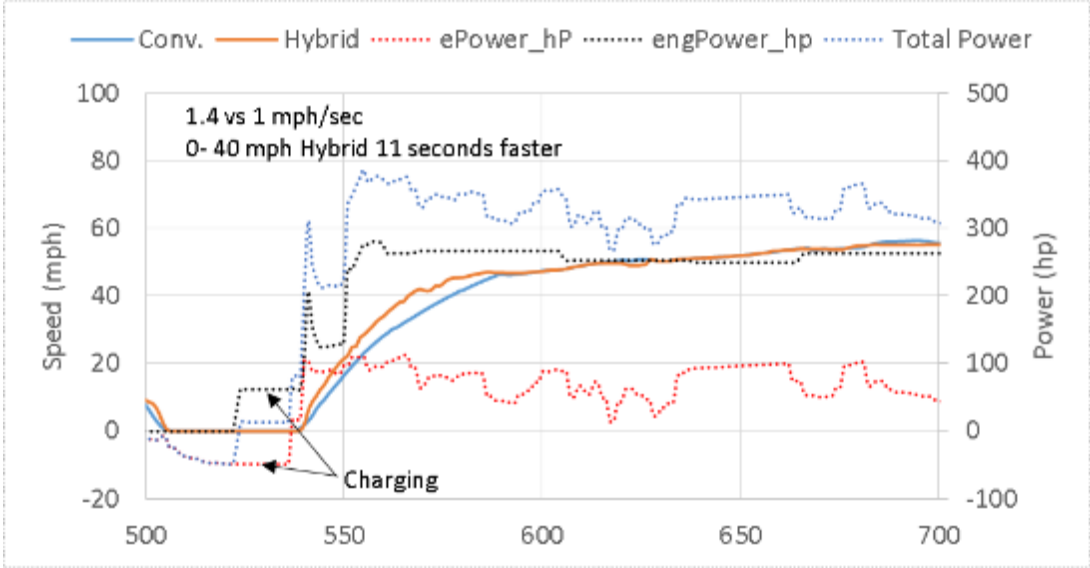

Source: Gas Technology Institute

Comparison to Near-Zero Technology

During the development of this project, CWI released their 8.9 liter near-zero engine. This engine is optimized for low NOx emission, 90 percent lower than the model utilized in this study. UCR was part of the team that evaluated the near-zero engine. This section provides comparisons between the near-zero engine and the hybrid optimized 2010-certified engine for cold start, hot transient, and fuel consumption conditions. Figure 102 through Figure 104 summarize the highlights of the comparison:

- Hot transient: The first and second figures shows more than 90 percent of the near-zero engine NOx emission resulted from a single spike at 100 seconds. The near-zero engine NOx emission were higher than the 2010 certified hybrid engine from 0 to 400 seconds. The near-zero engine showed no additional NOx accumulation for the rest of the cycle. The hot transients NOx emission for a hybridized near-zero engine may be almost eliminated where NOx emission could be reduced even lower than reported by UCR which ranged from 0.001 to 0.014 g/bhp-hr.
- Cold start: The near-zero cold start emission are 90 percent lower than the emission from the 2010-certified model, see Figure 7-3. This shows that electrical heating technology may not be needed to meet the 0.02 g/bhp-hr.
- Fuel economy: The near-zero engine showed a bsCO2 certification value of 465 g/bhp-hr and only slightly higher during UCRs test, but lower than the 2010 model tested in this study. The near-zero engine will be a better integration platform than the one demonstrated in this study. Hybridizing the near-zero engine with stop/start control technology could further enhance the fuel economy improvements desired.

Figure 102: Comparison for Transient Benefit of the Near-Zero Design Over the ISL G Engine

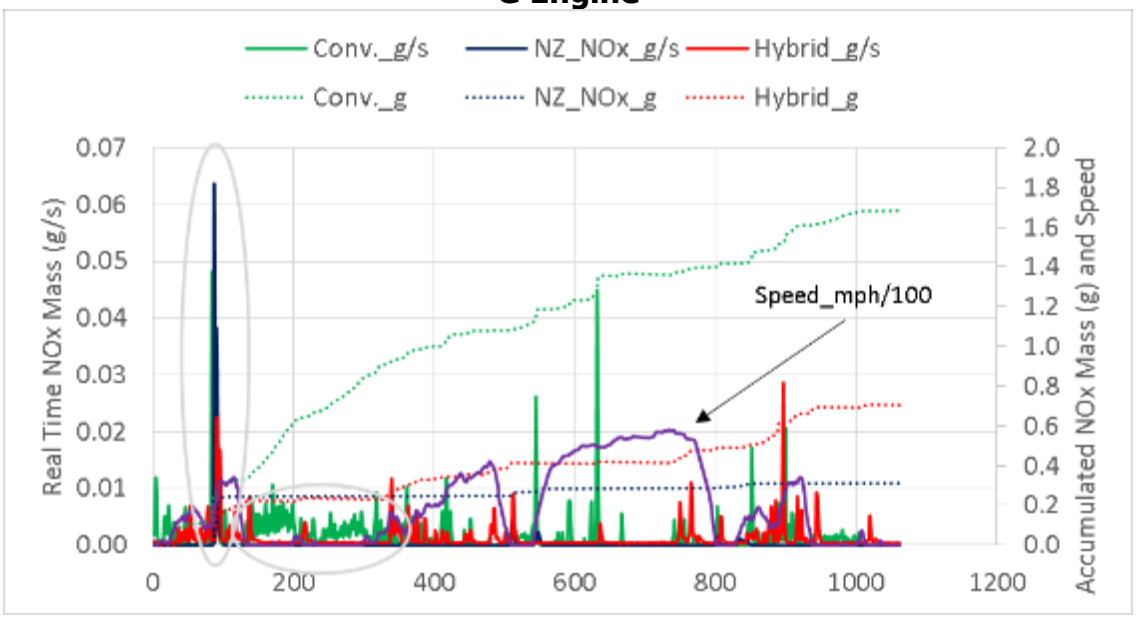

Source: Gas Technology Institute

Figure 103: Comparison for Transient Benefit of the Near-Zero Design Over the ISL G Engine

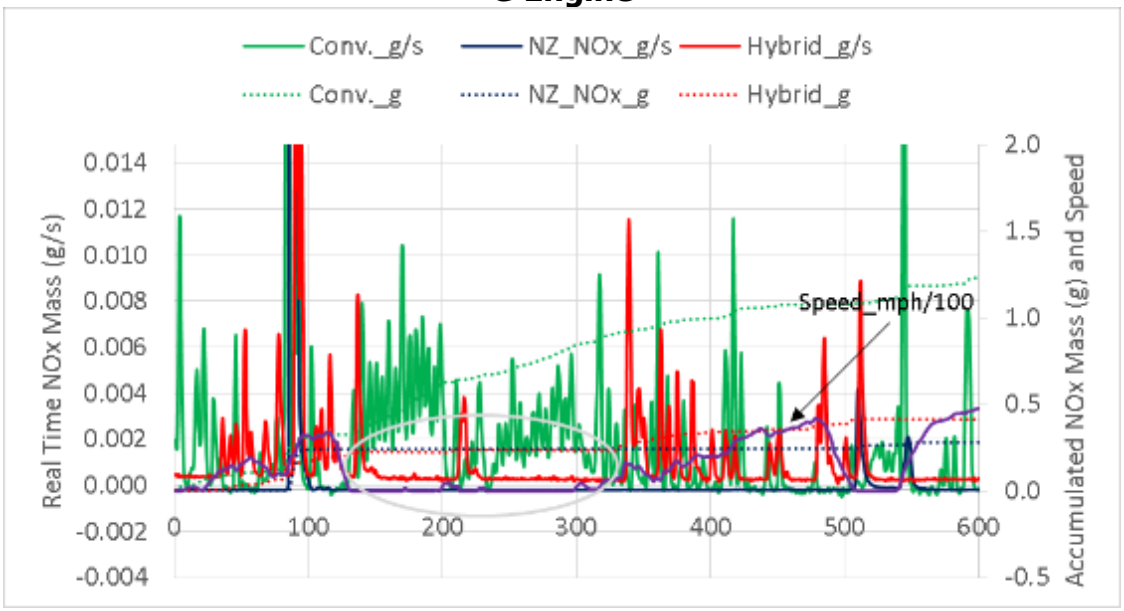

Source: Gas Technology Institute

Figure 104: Comparison for Cold Start Benefit of the Near-Zero Design Over the ISL G Engine

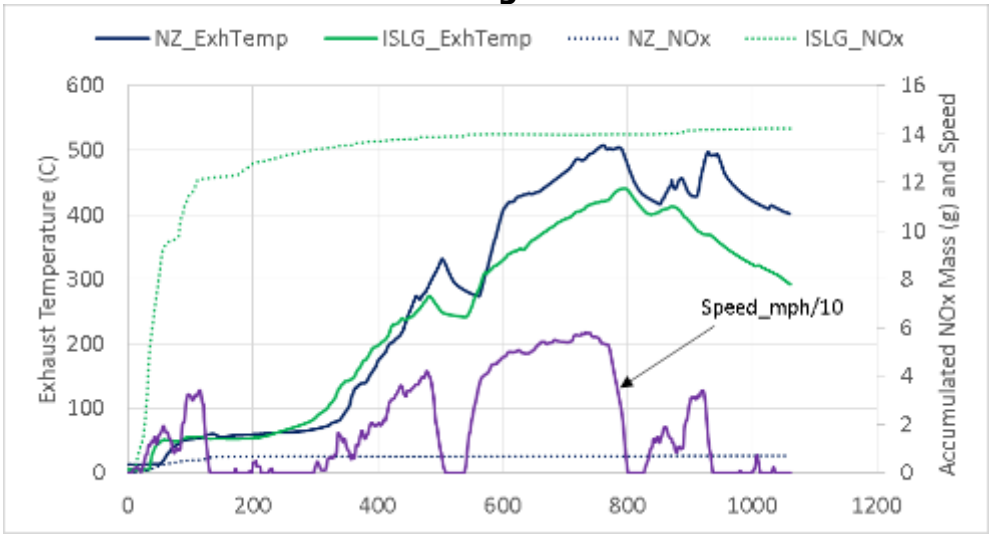

Source: Gas Technology Institute

Future deployment of hybrid technology should take advantage of the latest in engineering progress. This includes the commercial CWI near-zero natural gas engines which are superior to what was developed in this research project. It is recommended to develop a hybrid demonstration with the advanced ISL G 8.9 near-zero engine utilizing the same chassis platform. This platform would demonstrate best available technology for hybrid integration in goods movement.

CHAPTER 7:
Technology and Knowledge Transfer Activities

Impact on the Public

What follows is an explanation of how the knowledge gained from the project will be made available to the public. In this case, knowledge gained during this project will be embodied in the vehicles that eventually will be equipped with the optimization technology that was researched, including the targeted market sector and potential outreach to end users, utilities, regulatory agencies, and others.

The target market sector for the technology developed during execution of this agreement includes terminal operators, private companies, port tenants, and logistics companies operating in and out of California ports that use at least one diesel- or gasoline- powered drayage truck. This group represents the most immediate target market for the results of the project. Currently, US Hybrid considers its market for this type of technology to be its local area, which includes the Port of Long Beach. Branching out from Long Beach, US Hybrid also hopes to make in-roads into the larger market represented by California' s many ports and intermodal rail yards, where is it estimated that there are approximately 19,519 drayage trucks currently in operation. All of these trucks are subject to the California Air Resources Board's (CARB) Drayage Truck Regulations, which require all drayage trucks to meet or exceed 2007 model year California or federal emission standards, and now requires all trucks to have 2010 model year engines or equivalent no later than 2023. Thus, virtually all these trucks within California represent ideal targets for replacement with an electric or hybrid-electric counterpart or- depending on where they are in their useful lifetimes- retrofit upgrades to electric or hybrid modes of operation.

Intended Use

Drayage trucks are used to transfer cargo containers from/to ports in a warehouse or logistic yard. For port facilities in the South Coast Air Basin, as well as virtually all other ports, drayage trucks often queue for long periods, inching along at slow speeds while waiting for loading and unloading. During this process, the trucks are essentially idle. In this mode, engines continuously run and produce harmful emission. The PHET will operate in electric mode (EV mode) around 45 percent of time (30 miles, operating between ports and TTSI facility) in charge depletion mode, and then, once the battery energy is reduced to low State Of Charge "SOC" level, the vehicle will operate in LNG hybrid mode as charge sustaining. As such, there is no limitation of the range and usage of the PHET. In this mode of operation, the PHET will have higher operating hours with LNG fuel in comparison to when operating with diesel.

One unique aspect to operation in US Hybrid's target market, the Port of Los Angeles/Long Beach is the Vincent Thomas Bridge. This bridge has a steep approach grade so it is important to verify that new vehicle technologies can cross the bridge with a full load (GVW = 80,000 lb). The bridge is the 4th longest suspension bridge in the world at 6,060 feet long and is relatively high mid span (365 ft) to clear vessels in the navigation channel. The maximum grade of the bridge is estimated at 7 percent. High speed and low speed approaches are common when traveling across the bridge depending on traffic conditions. The VCT bridge is

unique in that it is preceded by traffic stops – lights/signs – as well as frequent traffic, which varies from other well-known routes such as the grapevine, which covers a larger elevation gain, but is much longer.

During sustained grade test cycles, US Hybrid's vehicles have proved that they can maintain performance while crossing the bridge and in the associated stop and go traffic that surrounds the bridge and the Port area. This testing was carried out with funding outside of this project. One test simulated approaching the bridge at 50 mph and increasing load (i.e. simulated grade) and another test simulated approaching the bridge at 0 mph (standstill traffic) and accelerating under full load conditions with the simulated grade. The vehicle was able to sustain maximum speed of 40 mph, but the added power of the hybrid resulted in a 50 mph speed for both tests. The sustained power of 350 HP at the wheels did not result in any system overheating or other issues, demonstrating that the vehicle is suitable for port operations. The higher power of the hybrid LNG HDV shows the added benefit of the hybridization over the conventional vehicles where power concerns for bridge or grade events are common.

In addition, an acceleration test was performed on the hybrid vehicle with a simulated load of 70,000 lb. (Again, this testing was carried out with funding outside of this project) Multiple acceleration tests demonstrated average time from 0-60 mph was under 80 seconds. The peak wheel power was 400 hp where the measured peak electrical power was 200 hp. Similar all-electric heavy-duty vehicles were also tested with this same acceleration profile where the 0-60 mph was 100 seconds (also with 70,000 lb simulation load). The hybrid vehicle showed a 25 percent faster 0-60 acceleration rate compared to the similar all-electric option.

These performance characteristics demonstrate US Hybrid's continuing commitment to provide a viable market option for their intended end user. The eventual result of this project, after follow on efforts to integrate existing ultra-low NOx emission engines, will provide a new option in the marketplace, especially in Southern California's ports, that has the potential to offer competitive performance characteristics with improved fuel economy and emission benefits.

Public Outreach

The progress made on this project was shared with the public at Department of Energy's Natural Gas Vehicle Technology Forum in October 2016. The technology forum has been led by the National Renewable Energy Laboratory (NREL) in partnership with the US Department of Energy (DOE) and the California Energy Commission (CEC). The forum unites a diverse group of stakeholders to share information and resources; identify natural gas engine, vehicle, and infrastructure technology targets; and facilitate government-industry research, development, demonstration, and deployment (RDD&D) to achieve targets. It also exists in order to communicate high-priority needs of natural gas vehicle end-users to natural gas equipment and vehicle manufacturers and enable fleets and large purchasers to aggregate demand for natural gas vehicles and equipment.

Examples of NGVTF stakeholders include:

- Original equipment manufacturers
- Vehicle and infrastructure packagers
- National laboratories

- Federal, state, and local government agencies
- Industry and trade associations
- Industry research groups and consultants
- Utilities and fuel distributors
- Fleet operators
- Equipment suppliers
- Nonprofit organizations

One of the US Hybrid vehicles demonstrated under agreement ARV-11-029 was showcased at the technology forum so that the stakeholders in attendance could learn more about the vehicle and see it in person. Soon after, the vehicle was delivered to TTSI and put into regular drayage service. This agreement improved upon the design of that vehicle, and the progress of those improvements to date was presented by GTI and US Hybrid.

Production Readiness Plan

Vehicle Production Process

The LNG-PHETs incorporate an advanced, low-cost hybrid motor design that is integrated with the transmission and employs an optimized hybrid vehicle control system to minimize NOx and fuel usage. The Plug-in Hybrid Electric LNG Truck (PHET) for this project incorporates the original Cummins ISL-G 8.9 liter engine and Allison Transmission with a drive motor/generator in-line between the engine and transmission. The drive motor/generator was equipped with the Auto Clutch, in addition to fully-electric air, hydraulic and HVAC systems. These systems were integrated with 12V and 24V batteries, DC-DC converter powering the auxiliary systems, and a high voltage Lithium-ion battery.

The existing Cummins ISL-G engine, which has been converted to run on LNG, is still in the vehicle and provides propulsion when needed. A 240 kW electric motor has been installed between the engine and the existing Allison automatic transmission. An electronically controlled pneumatic driven clutch allows the electric motor to be decoupled from the engine and permits electric only operation. All electric auxiliary systems, power steering, air compressor, and air conditioning, have been installed in parallel with the engine driven systems. This gives the vehicle all the capabilities of the original when in electric-only mode.

Two major enclosures have been added to the vehicle to permit electric and hybrid operation. The behind the cab enclosure houses the air compressor, the 12V batteries, and an additional twelve fuses and relays. The passenger side enclosure houses the battery, high voltage distribution, drive motor inverters, DC/DC converters, auxiliary motor drive, and the battery charger. They have all been integrated into one unit with two distinct sections that separate the battery and high voltage distribution from the rest of the electronics.

An additional coolant system has been added to support the cooling of the electronics and drive motor. A radiator and two pumps have been added to the middle section of the vehicle, just behind the 5th wheel connection. One coolant pump circulates water to the electrons, such as the two drive inverters, the DC-DC converter, the auxiliary motor inverter, and the battery charger. To control and monitor the hybrid drive system and execute the user's commands, a CAN data bus interconnects all the electronic equipment and displays the status on a dash mounted LCD user display touch screen.

Transitioning between pure electric mode and hybrid mode is an automated transparent function that is controlled by the vehicle control unit and requires no input from the driver. The vehicle Hybrid Controller Unit (HCU) can sense when there is a heavy load on the vehicle and will automatically start the LNG engine to accommodate. The engine may also turn on if the high voltage battery has reached its minimum charge level and needs to be recharged by the drive motor acting as a generator. The vehicle is equipped with an onboard charger that allows it to be plugged in when not in service, providing a full battery at the beginning of every shift.

In the future, integration of Cummins-Westport's 8.9 liter ISL-G will not provide customers with the ultra-low NOx performance of newer 8.9 liter L9N engines from Cummins Westport, which conform to modern onboard diagnostic requirements. Future development work will seek to advance hybridization optimization and include the advantages provided by lower baseline emission from the newest engines available.

Estimated Cost of Production

The cost of a new, baseline 8.9-liter LNG truck is $195,000. The cost of a repowered truck is $330,000 per unit. The cost of boosting the power of the existing, underpowered ISL-G 8.9-liter engine by adding an electric drivetrain is actually less than the cost of replacing the engine with a new, larger Cummins ISX15 or ISX12 running on diesel in the near future (2020). The incremental capital cost of the conversion—which will deliver double the fuel economy and an expected 50-percent reduction in GHG emission for virtually identical performance to its diesel counterpart—is $0 in comparison with the 12- or 15-liter ISX15, which would provide sufficient power, but at the cost of half the fuel economy of the existing, underpowered trucks and double the GHG emission.

By 2020, US Hybrid anticipates that its hybrid drivetrain will be installed by vehicle OEMs, bringing the cost of a new LNG-PHET in line with that of a larger conventional diesel engine, such as the Cummins ISX15, employing idle control technologies. These cost improvements will come from a combination of improved scale and synergistic use of assembly facilities.

The gross combined weight rating (GCWR) of the baseline LNG truck is 80,000 lbs. The GCWR of the LNG-PHET is roughly 750 kg heavier than the baseline LNG truck; most of which is directly related to the weight of the battery. In comparison with a new or repowered diesel truck utilizing the Cummins ISX15 and idle control technologies, however, the net added weight is zero.

Forward Integration and Diversification

The integration of electrical components relies on a key competency of the US Hybrid organization. The manufacture of a vehicle represents a forward integration of the already existing production process that produces numerous US Hybrid products, including:

- Isolated and non-isolated, directional and uni-directional DC-DC Converters
- Electric drive units (EDU) - High Torque / Power Density Induction Motor Drive Systems in 200 and 240 kW sizes
- Auxiliary Power Units with permanent magnet motor for specialty vehicles
- Electric Auxiliary Drives from 8-18 kW
- Three-phase DC-AC inverters for power export (6-30 kW)

From US Hybrid's standpoint as a manufacturer and supplier of these electrical components in the automotive space, scaling up this type of forward integration activity neutralizes some aspects of buyer power. If one of US Hybrid's customers feels the threat that US Hybrid may begin manufacturing a vehicle subsystem or a whole vehicle that would compete with their own subsystem or, they may be motivated to leave US Hybrid with a larger amount of supplier surplus. This type of threat protects US Hybrid's core business.

However, this benefit is only in the short term, as US Hybrid expects that its hybrid drivetrain will eventually be installed by truck OEMs. In the long run, the component supplier-integrator relationship that US Hybrid expects with truck OEMs will allow US Hybrid to take advantage of OEM's economies of scale and customer channels to bring consumers a lower-cost product. This type of component supplier-OEM model is closer to the dominant model in the industry.

US Hybrid's core business is also protected in that his vehicle architecture is a suitable substitute for other heavy haul vehicles. The most direct substitutes include traditional gasoline drayage trucks, electric drayage trucks, hydrogen fuel cell drayage trucks. This vehicle platform is designed specifically for the needs of port drayage haulers. The developed vehicle architecture and the vehicle subsystems are a less direct substitute for electric and hydrogen fuel cell cargo trucks, hydrogen fuel cell passenger busses, and hydrogen fuel cell street sweepers and the subsystems that are integrated into those vehicles.

This diversification of US Hybrid products opens up new customer segments, new funding, and new partners that will be beneficial to US Hybrid's existing business activity. The benefits of short-term forward integration and diversification give US Hybrid sufficient motivation to evaluate investments in order to scale up production processes and streamline sub-system assembly and integration.

CHAPTER 8:
Conclusions and Recommendations

Project Results

This demonstration project used a commercially available, 2010 certified, dedicated natural gas, Cummins Westport Inc. (CWI) ISL G 8.9L engine and enhanced the system to make it representative of an engine meeting CARB's optional low NOx "near-zero" standard. The commercially-available, 2010 certified, CWI ISL G 8.9 and the newly certified near-zero engine technologies were reviewed and evaluated at UCR to provide an in-depth characterization of emission formation and fuel consumption results. The UCR emission test laboratory was upgraded in order to quantify such low emission factors where ambient concentrations represent more than 50 percent of the diluted sample concentration. Two primary observations were identified during the review: 1) up to 90 percent of the emission are the results of either rapid engine speed transients (i.e. hot start tests) or cold starts emission and 2) the impact of transient and cold start emission is more critical at the lower near-zero emission standard (0.02 g/bhp-hr) when compared to the 2010 certified, ISL G standard. This suggests emission differences may be significant between drivers, vocations, and vehicle configuration (automatic transmissions vs manual transmissions).

The optimized design approach is based on the dedicated natural gas, 2010 certified, ISL G 8.9 liter engine platform. This engine is configured in a vehicle equipped with a liquid natural gas fuel delivery system with a 100-diesel gallon equivalent fuel tank (400 mi range estimated), a stock three way catalyst (TWC), and a throttle body fuel injection system. To minimize the NOx emission spikes during transients throttle tip-ins, a model based air-to-fuel ratio (AFR) model and controller were designed and evaluated. A simulation of the model based AFR control was shown to have a similar response to that found on the ISL G near-zero 8.9 liter engine during throttle tip-in, (simulated rapid throttle control resulted in a short open loop time of 3 seconds).

Transient open loop conditions were minimized by limiting transient engine speed differentials to 300 rpm/second with the hybrid system. This can be seen by the results in Figure 105 where the hybrid accumulated NOx emission were 56 percent below that of the conventional configuration. Analysis revealed the main difference in total NOx emission was a result of lower and fewer NOx spikes from the engine's throttle control system. The reduced throttle control did not minimize engine performance as can be seen by the 11 second faster acceleration rate (0-40 mph) where the total power was 380 hp resulting from a combination of 280 hp from the engine and 100 hp from the electric motor. The 380 hp of total power was only needed for 300 seconds to accelerate up to cruising conditions where 6.2 kWhr of the battery energy was used which was then quickly recharged during cruise, idle, and decelerations for a net zero change by the end of the cycle. The short acceleration and high energy usage suggest heavy-duty hybrid applications can have advantages over all-electric where range can be compromised.

Figure 105: Accumulated NOx for the Conventional and Hybrid Systems

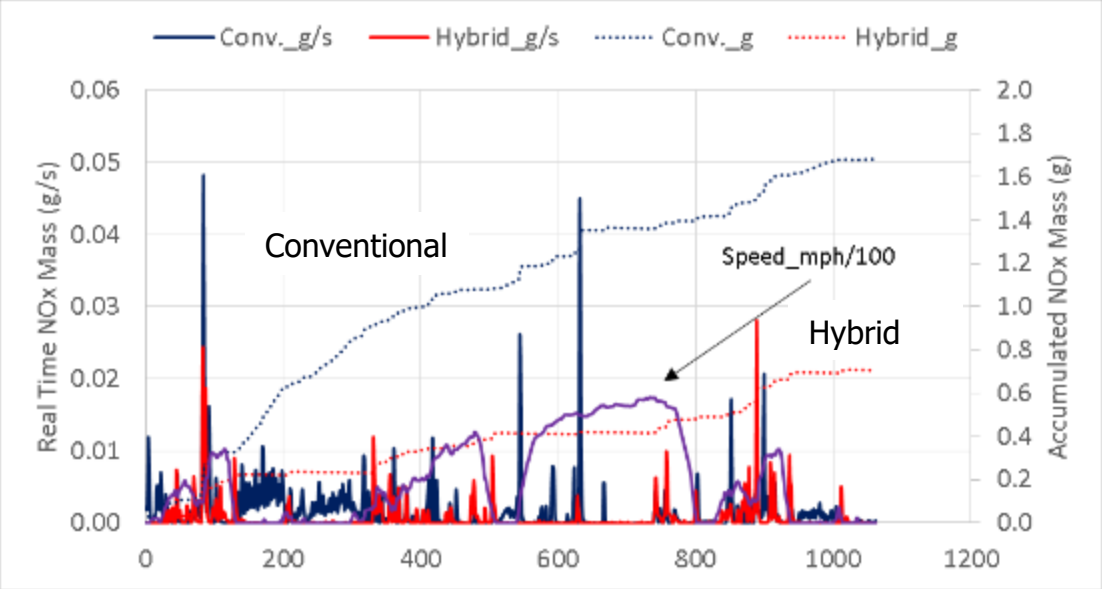

Source: Gas Technology Institute

Cold start emission and electric stop start technologies were considered for this project, but due to the sustained low emission at idle and complexities in integrating the electrically heated catalyst section, these approaches were not fully implemented, but modeled for their estimated benefit. Additionally, the success of the CWI near-zero 8.9L engine may suggest heated catalyst are not needed since the near-zero approach reduced cold start emission by 90 percent compared to the 2010 certified engine used in this study. The CWI near-zero improvements were primarily based on engine calibration which is more robust and lower cost compared to electrically heated catalyst approaches.

In general, the hybrid equipped natural gas engine showed hot transient NOx emission of 0.057 g/bhp-hr (70 percent lower than the 0.2 g/bhp-hr standard) and overall cold start weighted NOx emission of 0.19 g/bhp-hr. The fuel economy of the hybrid system was slightly improved (5 percent) from the baseline system over the cycles tested (Figure 106). Additional benefits could be obtained from a charge depletion mode strategy where plug in charging is used. Such an approach is realistic if a geofenced zero emission regulation adopted near ports. Such a strategy could maximize the potential of hybrids and 25 percent fuel economy benefits observed, but at the added cost of a dual power (engine plus electric) system.

Figure 106: Acceleration Comparisons for the Conventional and Hybrid Systems

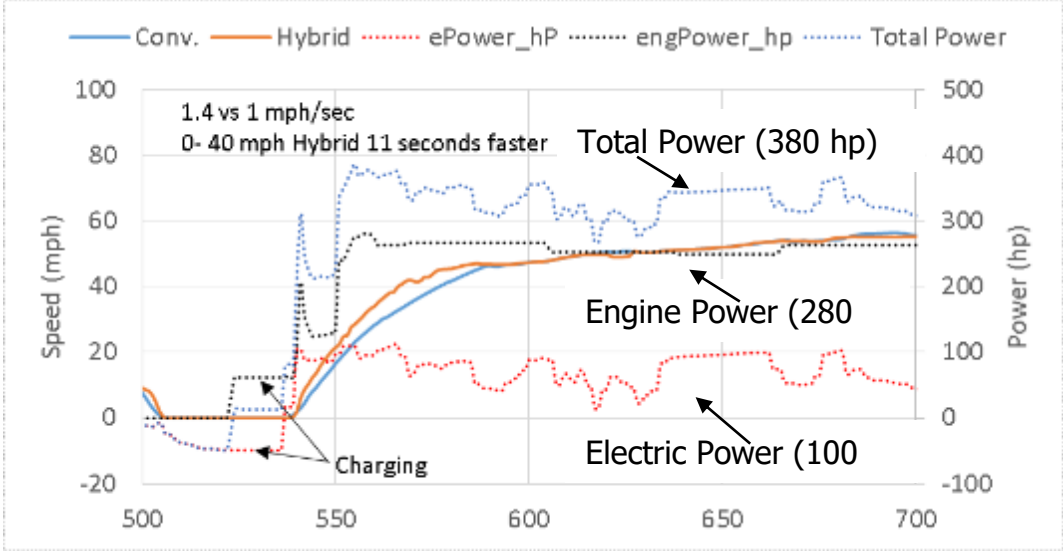

Source: Gas Technology Institute

Project Benefits

This demonstration project used a commercially available, 2010 certified, ISL G engine and enhanced the system to make it close to the optional low NOx standard with an NOx emission of around 0.05 g/bhp-hr with some (5 percent) increase in fuel economy. The commercial benefit of this project is in repowering goods movement fleets (Class 8 tractors with 15-liter engines) with hybrid systems in order to achieve significantly higher fuel economy while meeting near-zero emission standards. Additional NOx and fuel consumption reductions are possible by integrating cutting edge Intelligent Traffic Systems (ITS) research conducted at UC Riverside with this fully integrated heavy-duty chassis demonstration project and open source engine/hybrid controller. Future hybrid demonstrations projects should consider the new advanced Cummins Westport natural gas engine, which has shown an in-use emission as low as 0.001 g/bhp-hr NOx emission (more than 99 percent below the 2010 standard).

LIST OF ACRONYMS

Term	Definition
AFR	Air-To-Fuel Ratio
ARB	Air Resources Board
bs	Brake Specific
CEC	California Energy Commission
CE-CERT	College of Engineering-Center for Environmental Research and Technology (University of California, Riverside)
CFI	Central Fuel Injection
CFR	Code of Federal Regulations
CNG	Compressed Natural Gas
CO	Carbon Monoxide
CO2	Carbon Dioxide
CWI	Cummins Westport Inc.
EGO	Exhaust Gas Oxygen
EGR	Exhaust Gas Recirculation
FE	Fuel Economy
FID	Flame Ionization Detector
g/bhp-hr	Grams Per Brake Horsepower-Hour
GDE	Gallons Diesel Equivalent
GHG	Greenhouse Gas
HC	Hydrocarbon
ITS	Intelligent Traffic Systems
LNG	Liquid Natural Gas
lpm	Liters Per Minute
MAF	Mass Air Flow
MEL	Mobile Emission Laboratory
MPI	multi-port fuel injection
N2O	Nitrous Oxides
NG	Natural Gas
NGHEV	Natural Gas Hybrid Electric Vehicle

Term	Definition
NH3	Ammonia
NOx	Nitrogen Oxides
NZ	Near Zero
OEM	Original Equipment Manufacturer
Term	Definition
PID	Proportional-Integral Derivative [Control]
PM	Particulate Matter
PON	Program Opportunity Notification
PPM	Parts Per Million
PSD	Particle Size Distribution
RD&D	Research and Development Division
RPM	Revolutions Per Minute
scfm	Standard Cubic Feet Per Minute
SCR	Selective Catalytic Reduction
THC	Total Hydrocarbons
TWC	Three Way Catalyst
UCR	University of California- Riverside
USH	US Hybrid

REFERENCES

1. AQMD 2 October 2015 see: http://www.aqmd.gov/docs/default-source/Agendas/aqmp/white-paper-working-groups/wp-blueprint-revdf.pdf?sfvrsn=2
2. Wayne Miller, Kent C. Johnson, Thomas Durbin, and Ms. Poornima Dixit 2013, In-Use Emission Testing and Demonstration of Retrofit Technology, Final Report Contract #11612 to SCAQMD December 2013
3. Hesterberg T., Lapin C., Bunn A., Navistar, Inc. 4201 Winfield Road, P.O. Box 1488, Warrenville, Illinois 60555, VOL. 42, NO. 17, 2008 / ENVIRONMENTAL SCIENCE & TECHNOLOGY 9 6437
4. Thirubvengadam A., Besch M., Pradhan S., Carder D., and Emission Rates of Regulated Pollutants from Current Technology Heavy-Duty Diesel and Natural Gas Goods Movement Vehicles. ENVIRONMENTAL SCIENCE & TECHNOLOGY 2015, 49, 5236−5244
5. Patrick Couch, John Leonard, TIAX Development of a Drayage Truck Chassis Dynamometer Test Cycle, Port of Long Beach/ Contract HD-7188, 2011.
6. Results from UC Riverside's Chassis Dyno while testing an 8.9 liter heavy duty vehicle at transient and state operating modes.
7. Chatterjee, D., Deutschmann, O., and Warnatz, J., Detailed surface reaction mechanism in a three-way catalyst, Faraday Discussions, 119, pg 371-384 (2001).
8. Cocker III, D. R., Shah, S. D., Johnson, K. C., Zhu, X., Miller, J. W., Norbeck, J. M., Development and Application of a Mobile Laboratory for Measuring Emission from Diesel Engines. 2. Sampling for Toxics and Particulate Matter, Environ. Sci. Technol. 2004, 38, 6809-6816.
9. Cocker III, D. R, Shah, S. D., Johnson, K. C., Miller, J. W., Norbeck, J. M., Measurement Allowance Project – On-Road Validation. Final Report to the Measurement Allowance steering Committee.
10. Johnson, K., C., Durbin, T., Khan, Y., M., Jung, H., Cocker, D., (2010). Validation Testing for the PM-PEMS Measurement Allowance Program. California Air Resources Board, November 2010, Contract No. 07-620, http://eprints.cert.ucr.edu/505/
11. Johnson, K.C., Durbin, T.D., Cocker, III, D.R., Miller, W.J., Bishnu, D.K., Maldonado, H., Moynahan, N., Ensfield, C., Laroo, C.A. (2009) On-road comparison of a portable emission measurement system with a mobile reference laboratory for a heavy-duty diesel vehicle, Atmospheric Environment 43 (2009) 2877–2883
12. Cocker III, D. R, Shah, S. D., Johnson, K. C., Miller, J. W., Norbeck, J. M., Development and Application of a Mobile Laboratory for Measuring Emission From Diesel Engines I. Regulated Gaseous Emission, Environmental Science and Technology. 2004, 38, 2182-2189.

13. Sei-Bum Choi: Design of a Robust Controller for Automotive Engines; Theory and Experiment. PhD Dissertation, 1993 Berkeley CA

14. E. Hendricks and S.C. Sorenson: SI engine controls and mean value engine modeling; SAE Paper 910258, 1991

15. John J. Moskwa, Automotive Engine Modeling for Real Time Control, Doctor of Philosophy in Mechanical Engineering, MIT 1988

16. D. Cho and J.K. Hedrick: An observer-based controller design method for automotive fuel injection systems; Proc. Automatic Controls Conference, 1993

17. Robert W. Weeks and John J. Moskwa, Automotive Engine Modeling for Real-Time Control Using MATLAB/SIMULINK, SAE Paper 950417, 1995, http//www.simcar.com

18. Rasoul Salehi1, Mahdi Shahbakhti and J. Karl Hedrick Real-Time Hybrid Switching Control of Automotive Cold Start Hydrocarbon Emission J. Dyn. Sys., Meas., Control 136(4), 041002 (Mar 13, 2014) (10 pages) Paper No: DS-12-1361; doi: 10.1115/1.4026534 History: Received November 05, 2012; Revised January 14, 2014

19. Johnson, K., C. (2010) PM Speciation and Analysis Evaluation on AVL's PM PEMS 494 Measurement System, Final Report to AVL North America, July 2010.

20. Johnson, K., AVL's MSS+GFM In-Use Comparison with UCR's MEL Over a Variety of Operating Conditions, Final Report to AVL North America July 2010

21. Durbin, T.D., Jung, H., Cocker, D.R., and Johnson, K. 2009. PM PEM's Pre-Measurement Allowance – On-Road Evaluation and Investigation. Final by UC Riverside to the Measurement Allowance Steering Committee, January.

22. Durbin, T.D., Jung, H., Cocker, D.R., Johnson, K., 2009. PM PEM's On-Road Investigation – With and Without DPF Equipped Engines. Final Report by UC Riverside to the Engine Manufacturers Association, July.

23. T.D. Durbin, K.C. Johnson, D.R. Cocker, J.W. Miller, "Evaluation and Comparison of Portable Emission Measurement Systems and Federal Reference Methods for Emission from a Back-up Generator and a Diesel Truck Operated on a Chassis Dynamometer," Environmental Science and Technology, 41, 17, 6199-6204, 2007.

24. Durbin, T., D., Miller, W., M., Welch, W., A., (2010) Evaluating Emission from Heavy-Duty Front-End Loaders, Final Report to California Department of Transportation (CalTrans) Division of Research and Innovation, February 2010

25. Miller, J.W., Durbin, T.D., Johnson, K.J., Cocker, D.R., III, (2006) Evaluation of Portable Emission Measurement Systems (PEMS) for Inventory Purposes and the Not-to-Exceed Heavy-Duty Diesel Engine Regulations; final Report for the California Air Resources Board, July.

26. Miller, J.W., Younglove, T., and Smith, M.R. (2003) Incidence of Malfunctions and Tampering in Heavy-Duty Diesel Vehicles – Phase 1 Final Report. for the California Air Resources Board under contract no. 01-340, March 2003.

27. JRC (2006) WNTE – A Regulatory Tool for the EU? Presentation at the GRPE Meeting of the Off-Cycle Emission Working Group, Geneva, June.

28. Environmental Protection Agency of the United State (2003) Draft Regulatory Impact Analysis for Control of Emission from Nonroad Diesel Engines. EPA Document No. EPA420-R-03-008, April.

29. Gautam, M., Carder, D.K., Clark, N.N., and Lyons, D.W. (2002) Testing of Exhaust Emission of Diesel Powered Off-Road Engines. Final Report under CARB contract No. 98-317, May.

30. Frey, H.C., Pang, H-S, Rasdorf, W. (2008) Vehicle Emission Modeling for 34 Off-Road Construction Vehicles Based upon Real-World On-Board Measurements. Proceedings of the 18th CRC On-Road Vehicle Emission Workshop, San Diego, CA, April.

31. Durbin, T. D., M. R. Smith, R. D. Wilson, T. Younglove, J. Jones, and M.P.H. Barnett. 2003. Off Highway/All-Terrain Vehicle Activity-Data Collection; and Personal Watercraft Activity-Data Collection; Test-Cycle Development and Emission Tests, California Air Resources Board, CE-CERT Technical Report No. 03-VE-18399-04-FR, June.

32. Durbin, T.D., Miller, J.W., Johnson, K.C, Hajbabaei, M., Kado, N.Y., Kobayashi, R., Liu, X., Vogel, C.F.A., Matsumura, F., Wong, P.S., 2011 "Assessment of Emission from Use of Biodiesel as a Motor Vehicle Fuel in California: Biodiesel Characterization and NOx Formation and Mitigation Study," Draft Final Report by UC Riverside to CARB, March.

33. Durbin, T.D., Miller, J.W., Johnson, K.C, and Hajbabaei, M., 2011 "Assessment of Emission from Use of California Air Resources Board Qualified Diesel in Comparison with Federal Diesel," Draft Final Report by UC Riverside to CARB, March.

34. Durbin, T. D., J. W. Miller, J. T. Pisano, C. Sauer, T. Younglove, S. H. Rhee, T. Huai, and G.I. MacKay. 2003. The Effect of Fuel Sulfur on NH_3 and Other Emission from 2000-2001 Model Year Vehicles. Final report for Coordinating Research Council, CRC Project No. E-60, CE-CERT Technical Report No. 02-VE-59971-E60-04, May.

35. Durbin, T. D., J. W. Miller, J. T. Pisano, C. Sauer, S. H. Rhee, and T. Huai. 2002. Impact of Engine Oil Properties on Emission. Coordinating Research Council, CRC Project No. E-61, CE-CERT Technical Report No. 02-VE-59971-02-DFR, August.

36. Durbin, T.D., J.W. Miller, T. Younglove, T. Huai, and K. Cocker. 2006. Effects of Ethanol and Volatility Parameters on Exhaust Emission: CRC Project No. E-67. Final report for Coordinating Research Council, CRC Project No. E-67, January.

37. Holden, B., J. Jack, J.W. Miller, T.D. Durbin. 2006. Effect of Biodiesel on Diesel Engine Nitrogen Oxide and Other Regulated Emission Project. Final Report to the Department of Defense under the Energy Security Technology Certification Program, Project No. WP-0308, Technical Report No. TR-2275-ENV, May.

38. Steppan, J., Henderson, B., Johnson K., Khan, M., Diller, T., Hall, M., 2011 Comparison of an On-Board, Real-Time Electronic PM Sensor with Laboratory Instruments Using a 2009 Heavy-Duty Diesel Vehicle. SAE Technical Paper. Vol. 2011-02-0627: 1 P1 – 15.

39. UCR unpublished fuels study in 2006, emission results for a DDC 1991 series 60 PM composition analysis from UCRs database archives.

40. Tanfeng Cao, Thomas D. Durbin, David R. Cocker III, Roland Wanker, Thomas Schimpl, Volker Pointner, Karl Oberguggenberger and Kent C. Johnson, 2015 "A Comprehensive Evaluation of a Gaseous Portable Emission Measurement System with a Mobile Reference Laboratory" in press Env. Science and Tech.

41. M. Yusuf Khan, Kent C. Johnson*, Thomas D. Durbin, Heejung Jung, David R. Cocker III, Dipak Bishnu, Robert Giannelli, Characterization of PM-PEMS for In-Use Measurements Conducted during Validation Testing for the PM-PEMS Measurement Allowance Program, Atmospheric Environment 55 (2012) 311e318.

APPENDICES

The following Appendices are available under separate cover (Publication Number CEC-500-2021-054-APA-D) by contacting Reynaldo Gonzalez at Reynaldo.Gonzalez@energy.ca.gov.

- Appendix A: Emission Technology Review
- Appendix B: Performance Specifications
- Appendix C: Emergency Response Team Manual
- Appendix D: User Manual